CHALMERS

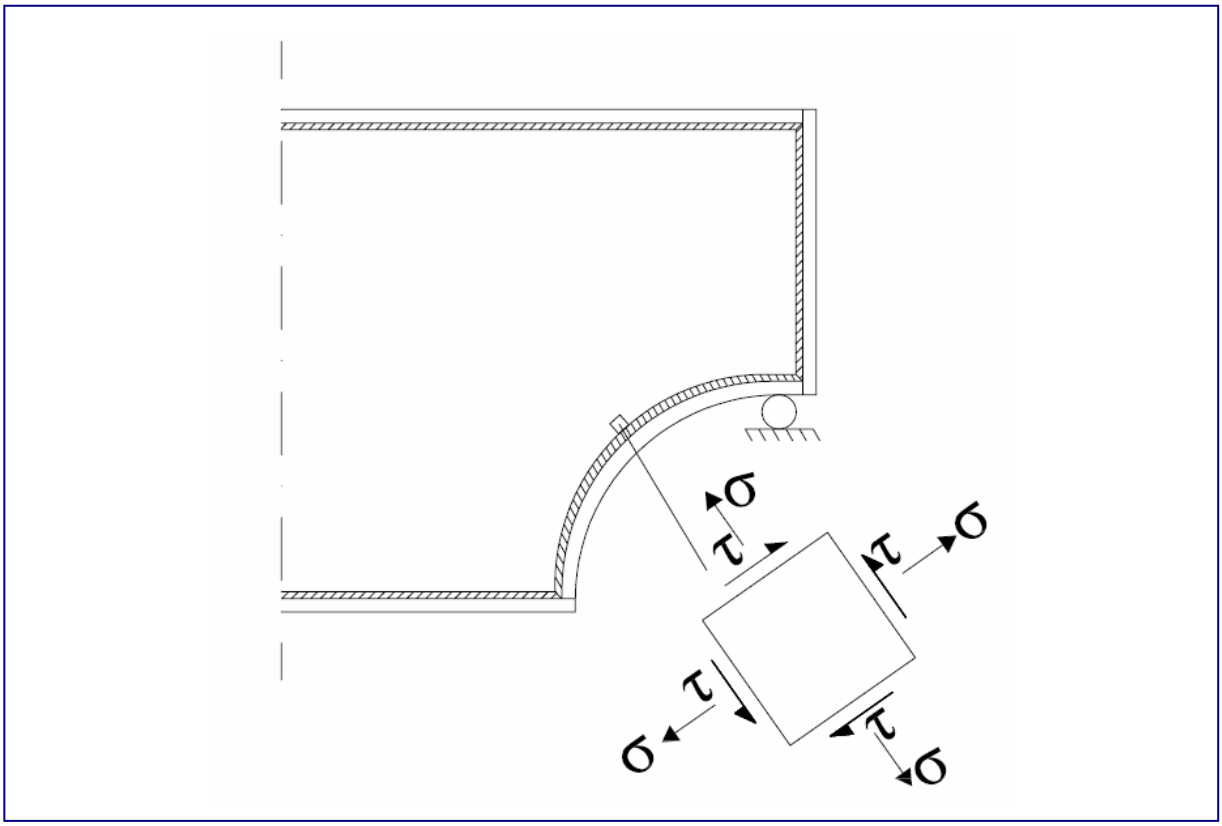

Multi-axial fatigue in welded details

-An investigation of existing design approaches

Master's Thesis in the Master Degree Programme Civil Engineering

JOHANNES GUSTAFSSON

JUHA SAARINEN

Department of Civil and Environmental Engineering
Division of Structural Engineering
Steel Structures
CHALMERS UNIVERSITY OF TECHNOLOGY
Göteborg, Sweden 2007
Master's Thesis 2007:64

MASTER'S THESIS 2007:64

Multi-axial fatigue in welded details

-An investigation of existing design approaches

Master's Thesis in the Master Degree Programme Civil Engineering

JOHANNES GUSTAFSSON

JUHA SAARINEN

Department of Civil and Environmental Engineering
Division of Structural Engineering
Steel Structures
CHALMERS UNIVERSITY OF TECHNOLOGY
Göteborg, Sweden 2007

Multi-axial fatigue in welded details
-An investigation of existing design approaches
Master's Thesis in the Master Degree Programme Civil Engineering

JOHANNES GUSTAFSSON

JUHA SAARINEN

Master's Thesis 2007:64
Department of Civil and Environmental Engineering
Division of Structural Engineering
Steel Structures
Chalmers University of Technology
SE-412 96 Göteborg
Sweden
Telephone: + 46 (0)31-772 1000

Cover:
Multaxial stresses due to geometry (Section 1.12.1)

Chalmers Reproservice / Department of Civil and Environmental Engineering
Göteborg, Sweden 2007

Multi-axial fatigue in welded details
-An investigation of existing design approaches
Master's Thesis in the Master Degree Programme Civil Engineering

JOHANNES GUSTAFSSON

JUHA SAARINEN

Department of Civil and Environmental Engineering
Division of Structural Engineering
Steel Structures
Chalmers University of Technology

ABSTRACT

Multiaxial fatigue is a stress state where two stress components act in a detail. These stresses may be dependent or independent of each other depending on the loading case and geometry of the loaded detail. The geometry it self may create multiaxial stress state which many designers ignore or are unaware of. The stresses may also be in or out-of-phase. Prediction of the fatigue damage under multi-axial loading conditions can be done by several methods. Eurocode 3 suggests two basic methods, by calculating the damage caused by each stress component and limiting the sum to a unity, or by using the principle stress in the detail as a design parameter. There are, however, poor guidelines in Eurocode 3 for how these recommended methods should be used. This seems also to be the common problem in most other design codes. The aim of this Master's thesis is to investigate different prediction models that can be employed to calculate the fatigue life of details under multi-axial loading. By investigating the literature in the field, test data has been collected and compared against predicted fatigue life according to various models. From such comparison, the differences between methods could be highlighted and also the accuracy of fatigue life prediction agrees with the test results could be investigated. The criterion for choosing the methods to be studied was to only include methods that can be used with simple hand calculation. Therefore methods, which require FEM analysis or other complex calculation, were excluded.

The methods investigated were those proposed in EC 3 and the recommendations from the International Institute of Welding (which is similar to that in EC 3 but with some modification regarding the allowed damage sum). The Modified Wöhler Curve method was another model that seems to be usable for prediction of the multiaxial fatigue life. This method showed best accuracy with test results. Most of the methods give conservative results, with exception for the principle stress method in the EC 3. This survey includes also a modified EC 3 method using the exponent 3 for damage calculations for normal stress and shear stress. The method showed a good correspondence between experiments and predictions for the chosen specimen.

Key words: Multiaxial fatigue, in-phase loading, out-of-phase loading, stress range, modified Wöhler curve, interaction methods, principal stress methods, S-N curves.

Fleraxlig utmattning i svetsade detaljer

-En utredning av befintliga dimensionerings metoder

Examensarbete inom Konstruktionsteknik

JOHANNES GUSTAFSSON
JUHA SAARINEN
Institutionen för bygg- och miljöteknik
Avdelningen för Konstruktionsteknik
Stål- och Träbyggnad
Chalmers tekniska högskola

SAMMANFATTNING

Fleraxlig utmattning är ett spänningstillstånd då två spänningskomponenter verkar på en detalj. Dessa spänningar kan vara beroende eller oberoende av varandra beroende på lastfall och geometri hos den belastade detaljen. Geometrin hos detaljen kan ge upphov till fleraxliga spänningar som konstruktörer bortser ifrån eller är omedvetande om. De verkande spänningarna kan vara i eller ur fas i förhållande till varandra. Uppskattning av utmattningsskador på detaljer påverkade av fleraxlig belastning kan utföras på flera sätt. Eurocode 3 föreslår två grundläggande metoder där den första utgår ifrån att skadan för varje spänningskomponent beräknas och att summan av delskadorna begränsas till ett värde. Den andra metoden utgår från användandet av jämförande spänning (huvudspänning) i detaljen som en dimensionerings parameter. Dessvärre finns det knappa anvisningar i Eurocode 3 om hur metoderna bör användas. Detta är också det genomgående problemet för de flesta andra dimensionering regler. Syftet med detta examensarbete är att undersöka olika beräkningsmodeller som kan användas vid uppskattning av utmattningslivslängden för detaljer utsatta för fleraxligt spänningstillstånd. Genom att utföra en litteraturstudie inom området har en del försöksdata erhållits och sedan jämförts med beräknade utmattningslivslängder erhållna från olika beräkningsmodeller. Från beräkningarna kunde skillnader mellan beräkningsmodellerna påvisas samt hur väl beräkningsmetoderna överrensstämmer med aktuella försöksresultat. Kriteriet för urval av beräkningsmetoder som har undersökts var att enbart studera metoder som medger enkel handräkning. Av denna anledning utesluts metoder som kräver finita element eller annan invecklad beräkningsanalys.

Undersökta beräkningsmodeller är de föreslag i EC 3 och rekommendationer givna av International Institute of Welding (som är snarlika med EC 3 men med viss modifikation gällande tillåten summa från delskador). Den Modifierade Wöhler Kurva metoden är en annan beräkningsmodell som verkar användbar för uppskattning av utmattningslivslängden för detaljer med fleraxligt spänningstillstånd. Denna metod visade bäst överrensstämmelse med försöksresultat. De flesta beräkningsmodeller ger underskattade beräkningsresultat med undantag för jämförande spännings metoden enligt EC 3. Denna studie innehåller också en modifierad metod från EC 3. I metoden används exponenten 3 vid delskadeberäkningar för normalspänningar och skjuvspänningar. Metoden visar god överrensstämmelse mellan försöksresultat och beräkningar för den valda försöksdetaljen.

Nyckelord: Fleraxlig utmattning, i fas belastning, ur fas belastning, spänningsvidd, modifierad Wöhler kurva, iterationsmetod, jämförande spännings metod, S-N kurvor:

Contents

Preface

Recently published research results indicate that the use of some current code recommendations for the fatigue design of welded details subjected to multiaxial fatigue might be excessively non-conservative. This has made the department of steel structures at Chalmers University of technology interested in an investigation considering this subject. Dr Mohammad Al Emrani also the supervisor for the master thesis is also a member in the reference group handling design code issues in fatigue for EC 3. The master thesis should try to bring clearness if possible in the subject.

The master thesis has been carried out from January 2007 to June 2007 at the division of Structural Engineering, Department of Civil and Environmental Engineering at Chalmers University of Technology.

We want to thank our supervisor Mohammad Al-Emrani at Chalmers University of technology. We also want to thank Professor Certin Morris Sonsino at Fraunhofer Institute for Structural Durability, Darmstadt, Germany for all support.

Göteborg June 2007

Johannes Gustafsson & Juha Saarinen

1 Background -fatigue the phenomenon

Fatigue is commonly referred to as a process in which damage is accumulated in a material undergoing fluctuating loading, eventually resulting in failure even if the maximum load is well below the elastic limit of the material [8]. Fatigue is a process of local strength reduction which occurs in different materials. The fatigue process develops slowly and accelerates quickly to the end. Fatigue is a weakest link process which depends on the local stress in a small area. Fatigue analysis is also divided into two major types, low and high cycle fatigue. Low cycle fatigue is characterized by plastic deformation. This means that peak stresses are above the tensile yield strength. As a result of loading the cycles to failure for low cycle fatigue is up to 50 000 cycles [31]. In opposite to low cycle the peak stresses in high cycle fatigue are considerably below the yield stress and causes crack initiation. The cycles to failure are in the range of several million cycles. This study will concentrate on the latter case because the phenomenon is more common in civil engineering. In welded structures it is rarely suitable to weight stresses together to a nominal stress when predicting fatigue life. The reason is that the welds react more negatively to stresses perpendicular to it than parallel [35]. The conclusion is that stresses perpendicular to weld has lager impact on the structure than stresses parallel. Two different stress types acting on a specimen has a multiaxial influence. Such stresses may appear due to several reasons and can also be independent of each other. Recently studies have shown that the impact on a specimen affected to multiaxial stresses may result in shorter real lifetime than predicted. The cause lays in designing methods and probably also in lack of skill by designers. Some design codes take multiaxial stress ranges in account by using interaction formulas [35]. Design codes like EC 3 even give choice of predicting method which also may affect the result. This paper will focus on multiaxial fatigue issues but include also necessary relations to uniaxial fatigue. Uniaxial fatigue is related to one applied stress acting on a specimen where the damage due to this is predicted. The main relation lays in the common use of S-N curves for details which are used for fatigue prediction for booth uni and multiaxial methods. As there has been mentioned earlier this paper focuses on multiaxial high cycle fatigue problems. Three major steps present the ordinary behaviour of high cycle fatigue. These steps are

1. Crack initiation
2. Crack propagation
3. Final failure

1.1 Aim

The aim of this Master's thesis is to investigate different prediction models that can be employed to calculate the fatigue life of details under multi-axial loading. By investigating the literature in the field, test data has been collected and compared against predicted fatigue life according to various models. From such comparison, the differences between methods could be highlighted and also the accuracy of fatigue life prediction agrees with the test results could be investigated.

1.2 Different cycle regimes

The fatigue strength of a detail depends on how many cycle the detail is subjected to and therefore it is common to divided the fatigue strength after how many cycles the part is exposed for. In [31] Sonsino and Dieterich make a partition depending on cycles to failure and they get 3 different groups, finite life, low- and high cycle. The low cycle fatigue is the region up to 50 000 cycles, the finite life is between 50 000 to 2 000 000 cycles and above 2 000 000 cycles is the region for high cycle fatigue. In some existing reports the finite life is mentioned as medium cycle fatigue. A variation of the limits for the different cycle regimes can also exist, for example the limitation for low cycle is about 100 000 cycle in some reports.

1.3 Crack initiation

The crack initiation phase is distinguished by crack birth. The crack starts to initiate in areas with stress concentrations (see also Section 1.7), welds and other changes in geometry (discontinuities), defections like notches are affected faster. Even smooth specimens without lacks of notches are affected. They usually have a longer initiation time. A notch in a smooth specimen gives a starting point to crack initiation. In most cases the initiation process is confined to a small area being the root or the toe for welded details, see Figure 1.1. The weld toe contains defects called undercuts. These undercuts work as notches lead to local stress raise. Stress raise is one main factor behind crack initiation and growth. The weld root is usually more difficult to inspect by the naked eye and can easily include weaknesses and defects. The welding process can result in adverse features affecting the fatigue life. Porosity caused by gas bubbles incorporated in the weld can act as local stress raisers and make the initiation of fatigue cracks easier (see also Section 1.6.4). When a crack has been initiated it starts to increase gradually in length and propagation phase will start.

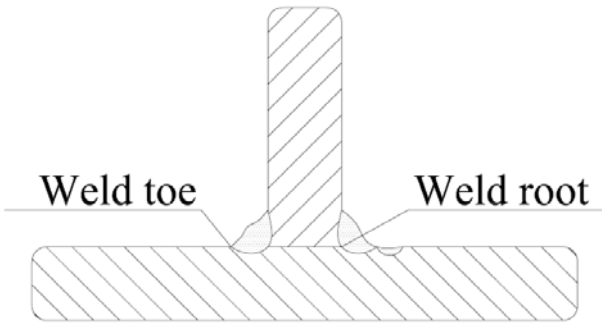

Figure 1.1 Picture of weld toe and weld root.

1.4 Crack propagation

A material with already existing defects like notches makes the initiation phase short for cracks and they can start to grow (propagate). Cracks propagate with each stress cycle and leads to shorter fatigue life. When propagation reached a critical stage the cracked detail or specimen goes to failure. When this happen the finial stage has been reached.

1.5 Residual stresses

Residual stresses are built in welded detail under manufacturing process of steel elements. The stresses can be built in by the manufacturing process or by welding. Other residual stress affecting performances are cutting processes and misalignment between connected members. Manufacturing residual stresses are created during the cooling process for hot rolled elements. Outer part of flanges and mid part of web becomes compressed while rest of the section are in tension, see Figure 1.2. Residual stresses due to welding are caused by stresses locked in when the weld metal contracts during cooling, see Figure 1.3 [8].

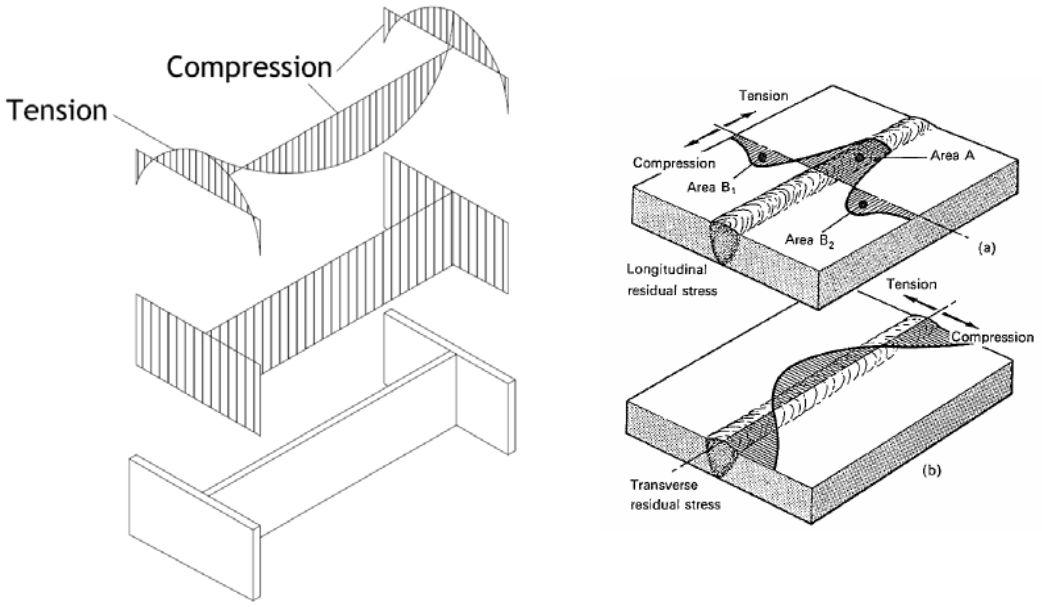

Figure 1.2-1.3 The residual stresses in a hot rolled element (left) and due to welding (right) [4].

The residual stresses might have yield stress magnitude close to the yield stress where compression and tension balance each other. High tensile welding stresses contribute to a poor fatigue performance of welded joints [8]. Residual stresses have similar influence on fatigue life as externally imposed mean stresses. A tensile stress reduces fatigue life while a compressive stress increases life. However one must remember that residual stress may relax with time, especially if there is peaks in the load spectrum that cause local yielding at stress concentrations. There are other methods also to reduce residual stresses. Stress relief by reheating is the most common procedure but not always possible to implement. Complete stress relief can rarely be achieved. As has been mentioned residual stresses can be positive for a structure but also of disadvantage. Design code [23] describes the origin to residual stresses but does not describe in what way they are considered in the models or not.

1.6 Weld defects

Welding is a method that requires good knowledge and workmanship to accomplish. There are a number of weld types, fillet and butt welds, see Figure 1.4, are the most common. A weld can contain many lacks some visible other more difficult to detect.

- Undercuts
- Incomplete penetration
- Lack of fusion
- Porosity
- Start & stop of weld

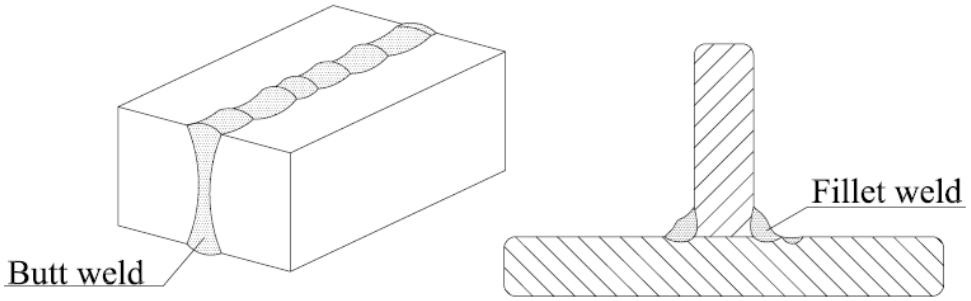

Figure 1.4 The difference between butt- and fillet weld.

1.6.1 Undercuts

Undercuts are created during the welding process when the parent metal has melted and forms a ditch at the weld toe see Figure 1.5. These undercuts (ditches) work as stress raisers due to the reduction in thickness in the parent metal. Undercuts work therefore as good starting points for crack initiation and propagation in structures subjected to fatigue. Actually undercuts can be seen as "pre cracks" where propagation continues and leads to failure. Design codes are aware of this phenomenon and regulate the theoretical lifetime. For example in [23] this is taken into account by detail categories regulating the reference fatigue strength.

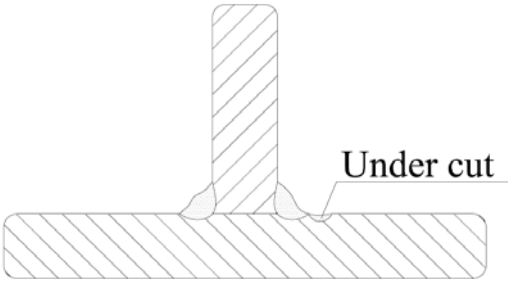

Figure 1.5 A undercut in the weld.

1.6.2 Incomplete penetration

When the throat thickness is smaller than the design thickness this is called incomplete penetration. The resistance of the joint might be insufficient. This can be the case when the weld has not penetrated deep enough to the parent metal. Inclusion can also reduce the penetration depth if the weld is built up by several runs. This might be a serious problem because it is not easy to determine the depth of penetration of the weld by visional inspection.

1.6.3 Lack of fusion

Lack of fusion is an area where weld material and parent material has insufficient bonding. Two usual causes is poorly prepared joints or incorrect adjusted weld equipment. For example with tight weld profiles, weld arc can attract one joint side more than the other which results in lack of fusion on the other. It is also important to have the correct adjustment of equipment and welding speed to prevent that the melted steel runs by forehand in to the joint and causes lack of fusion. Much of these aspects can be prevented by proper workmanship.

1.6.4 Porosity

Porosity is obtained when weld gases are trapped in to the weld metal during welding see Figure 1.6. Solution of weld gases in metal change with temperature and can create porosities in the weld under cooling. Some welding methods require protection gas which is added along the procedure. Disturbance of protection gas flow can generate pores in the weld.

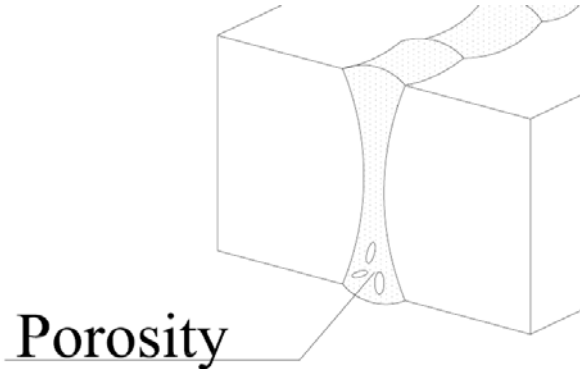

Figure 1.6 Porosity in a Butt-weld.

1.6.5 Start & stop

This type of defects is normally generated when the welder continues to weld from a spot where the weld ended earlier. Start- stop positions in longitudinal weld are points of stress concentration. This can lead to decreasing fatigue life because cracks can be initiated and propagated from these positions.

1.7 Stress concentration

Welds and welded details contain areas of stress concentration. The welds need to transfer the forces from one element to another which forces stresses to pass through the welds, see Figure 1.7. This change in direction and also change in contributed area results in stress concentrations. The geometry of the specimen itself can be done in ways that affects stress flow less when it's done with good design practice. Figure 1.7 – 1.8 shows examples on the subject.

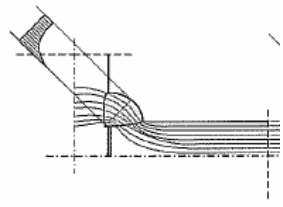

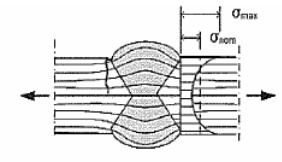

Figure 1.7-1.8 Stress concentration in a fillet weld (left) and in a butt weld (right) [8].

The fatigue life of any detail is directly related to the stress range experienced by the detail. It is well known that fatigue cracking always starts at locations of stress concentration or were localized stress raisers are present. Geometrical stress concentrations are generally obtained in locations where the stress flow in the element or the detail is disturbed due to change in geometry (in some cases in stiffness) [8]. Both parallel and perpendicular welds to the stress flow will be affected by the stress concentrations. Welds perpendicular to the direction of stress gets stress concentrations at the weld toe, see Figure 1.9. Welds parallel to stress flow are affected because these welds normally contains start & stop positions or weld ripples. In these start & stop positions stress concentration acts and results in cracking, see Figure 1.10 [8]. As a designer it is of great importance to minimize stress concentrations which leads to good design and longer fatigue life.

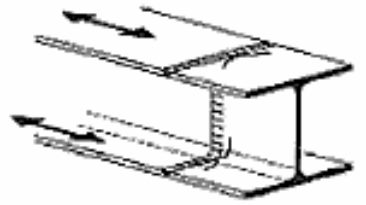

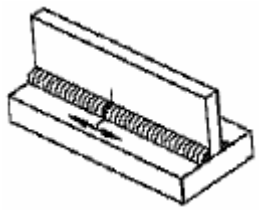

Figure 1.9-1.10 On side but Welds parallel to stress flow (left), start & stop in a longitudinal fillet weld (right) [8].

1.8 Mean stress

The simplest form of stress spectrum to which a structural element may be subjected is a sinusoidal or constant amplitude stress-time history with a constant mean load, see Figure 1.11 [8]. The following six parameters are used to define a constant amplitude stress cycle.

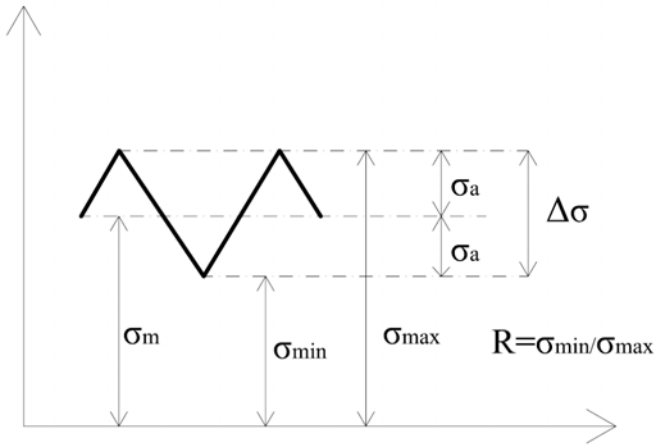

- σ_{max} = maximum stress in cycle
- σ_{min} = minimum stress in cycle
- σ_m = mean stress in cycle
- σ_a = stress amplitude
- $\Delta\sigma$ =stress range = (σ_{max} - σ_{min})
- R= stress ratio = σ_{min} / σ_{max}

Figure 1.11 The different terms for a loading curve.

The stress range is the primary parameter to influence the fatigue life, with mean stress as a secondary parameter. The stress ratio is often used as an indicator of the influence of mean loads, but the effect of a constant mean stress is not the same as for a constant mean ratio. S-N curves based on stress ratio gives a less good prediction in fatigue life than S-N curves based on mean stress, see Figure 1.12 a. When plotting results from tests curves based on ratio and curves based on mean stress, the S-N curves appear to differ from each other, see Figure 1.12 b. The curve based on ratio will overestimate lifetime compared to the one based on mean stress curve, see Figure 1.13 [8].

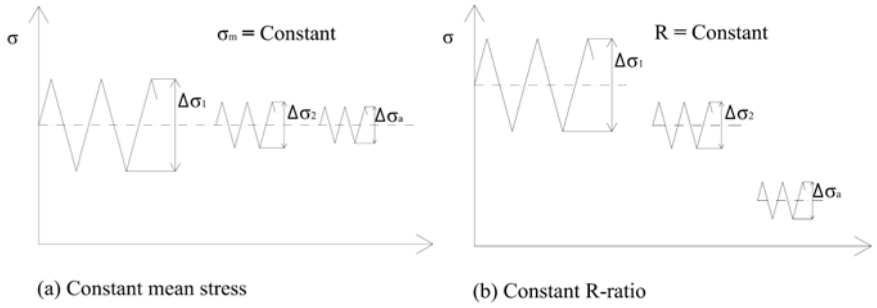

Figure 1.12 (a) Constant mean stress and (b) constant ratio.

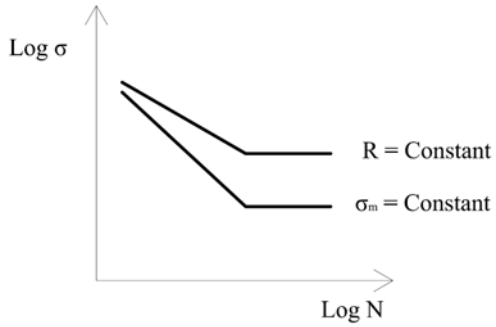

Figure 1.13 The two different S-N-curves with constant ratio and mean stress.

1.9 Stress ratio/ Stress range

The stress ratio (R) may vary for different details. These variations depend on the peak values itself but also their position regarding to zero level contributes. In the following there is a short simplified explanation on the subject. The stress ratio is defined as R= minimum stress / maximum stress, see Figure 1.14 [34]. The stress here is of arbitrary type which means that it can be normal stress, shear stress or principal stress. The message is just that the ratio presents the quota between the minimum and the maximum peak of the same stress. There should be mentioned that other reports for example contain ratio between shear stress and normal stress. Such ratio shall not be mixed up with the ratio of minimum and maximum stress of same type. All fatigue calculations are based on stress range which is similar to stress ratio. In stress range the maximum and minimum peak value is derived from the load history by fore example rain-flow method. The rain flow method is not discussed here because of the common use in the subject. However these values represent the extreme values in a stress cycle.

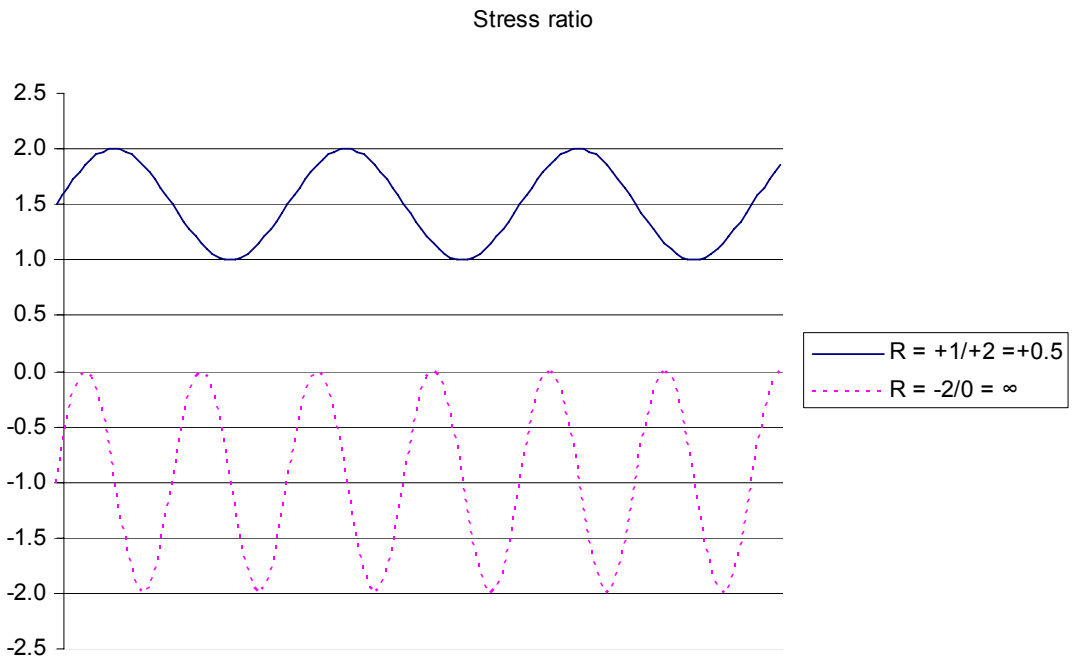

Figure 1.14 The stress ratio for two different loadings.

1.10 Fatigue design concepts

There are several methods how to predict fatigue life. Codes differ from each other and have different way of treating the subject.

1.10.1 Nominal stress method

Design code like Eurocode 3 uses the nominal stress method in prediction of fatigue life [23]. The general design rules in Eurocode 3 recommend the use of nominal stress range combined with detail categories when calculating fatigue lifetime. Nominal stresses in parent metals adjacent to potential crack location shall be calculated in accordance with simple elastic strength of materials theory. Stress concentration effects shall be excluded. In theory this means that for a steel beam the normal stress in flanges can be obtained by Naviers formula. By comparing detail categories with the present case the values for constant amplitude fatigue limit and cut-off limit can be received in EC 3. The designer then needs to compare if the nominal stress is in range according to EC 3. The damage in the detail can be calculated by comparison of the predicted number of cycles to failure and the actual number of cycles the detail has experienced [23]. The explained procedure comprises one stress, but in reality shear and normal stresses in combination may affect the detail. The number of cycles to failure regarding to shear can be calculated in a similar way as explained for normal stress. The cut of limit must be considered according to Eurocode 3. In cases where shear and normal stresses act on the same detail the damage shall be calculated as the sum of damage caused by normal and shear stress, see expression (1.1). This value shall be less than 1.0. Expression (1.1) is also called the Palmgren - Miner rule and is mentioned in many papers.

$$D_{d.\sigma} + D_{d.\tau} \leq 1 \qquad (1.1)$$

$D_{d.\sigma}$ = damage caused by normal stress

$D_{d.\tau}$ = damage caused by shear stress

The method is well established among designers using EC 3 and causes normally no problems.

1.10.2 Hot-spot method

EC 3 accepts also fatigue prediction by the hot-spot method. The hot-spot stress is also called geometric stress. One advantage of the hot-spot stress approach is the possibility of predicting fatigue life of many joint types using a single S-N curve [4]. The hot-spot stress needs to be verified for a welded joint. Normally this can be done by finite element analysis for the weld structure, or be obtained by stress concentration formulas or experimental model. The parametric formulas normally described as

$\sigma_{hotsp} = k_s \cdot \sigma_{nom.}$

σ_{hotsp} = maximum principal stress

σ_{nom} = Nominal stress

k_s = stress concentration factor

The factor k_s describe the stress concentration factor and σ_{nom} is calculated by ordinary elementary stress analysis [9]. The maximum principal stress is obtained at the hot-

spot which normally is at the weld toe or adjacent to it. It shall exclude local stress concentration effects due to the weld geometry and discontinuities at the weld toe. The calculation method is similar to the normal stress case described in Section 1.10.1, by replacing the normal stress with the hot-spot stress. The fatigue strength is determined by the design code [23]. The weld type regulates the type of curve and value to use. The number of cycles to failure is received in the same way as earlier. One of the disadvantages of the hot-spot approach is that only the surface stress is considered; no distinction is made between the effects of membrane and shell bending components on crack propagation life [4]. Figure 1.15 shows how hot-spot stress may appear in a detail. The hot-spot stress is located in the weld toe where a crack is expected to exceed [41].

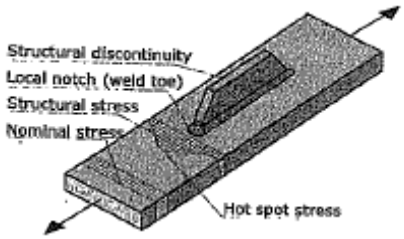

Figure 1.15 showing hot-spot stress [41].

When crack initiate from weld toe and it will be analysed by the hot-spot method this is denoted with the same name in this master thesis. Further on deeper analysis are made on promising methods where this will be used. There should also be mentioned that there can be found two types of hot-spots in welded structures. Type (a) hot-spots located along plate surface and type (b) hot-spots located on plate edge. Figure 1.16 shows type (a) and type (b) [41]. Type (b) have a numerous of variation.

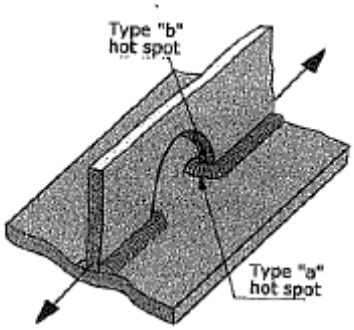

Figure 1.16 showing type (a) and (b) hot-spot [41].

1.10.3 S-N curves

The S letter in S-N stands for stress while N stands for number of cycles to failure. The curves are based on representative experimental investigations and include parameters for weld imperfections, local stress concentration, welding residual stresses, stress direction, metallurgical conditions, welding process, etc. One

important property for welded joints is the independence of tensile strength of the material [9]. The fatigue strength curve is identified by the characteristic fatigue strength of the detail at 2 million cycles. This value is also called the fatigue class (FAT). The curves differ from each other by the slope of the curve. For details assessed for shear the slope (m) = 5, while it is (m) = 3 for details affected by normal stresses. There is also a fatigue limit for constant amplitude where the curves planes out. This happens at 5 million cycles for normal stresses and 100 million cycles for shear stress. All S-N curves of details are limited by the material S-N curve which may vary due to different strengths of materials. In Figure 1.17 S-N curves for detail categories from 36 to 140 are presented. Figure 1.18 shows detail category 80 and 100 used to assess details subjected to shear stress [8].

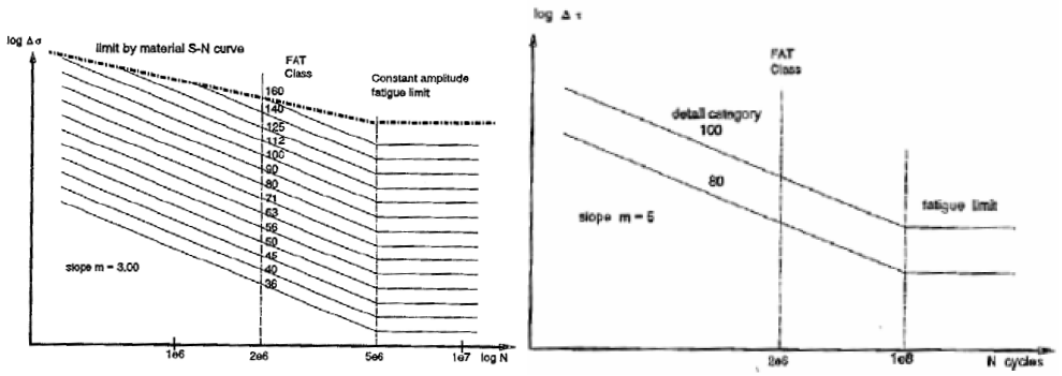

Figure 1.17-1.18 Fatigue strength curves for normal stress range in EC 3 (left), Fatigue strength curves in EC 3 for shear stress range (right) [23].

1.11 Detail classification

When predicting fatigue life with nominal stress method detail categories affect the fatigue life. In Eurocode 3 detail categories has been classified in a system with category numbers from 160 to 36, see Figures 1.19-1.21 for examples on categories. High category number is favourable and gives higher number of cycles to failure for a detail. The classified fatigue design curves adopted in Eurocode 3 are the same as proposed in "European Convention for Construction Steelwork Fatigue Recommendations" [8]. The ECCS Recommendations define a set of equally spaced S-N curves plotted on a log-log scale. Reference to these curves allows a detail category to be classified for a particular structural detail which corresponds to a notch effect or characteristic geometrical discontinuity. This classification has been determined by series of fatigue test results, from which a statistical and probabilistic evaluation is performed [8]. When the actual detail has been compared with different failure types given by the detail categories, prediction of life time against fatigue can be calculated by the method described in Section 1.10.1.

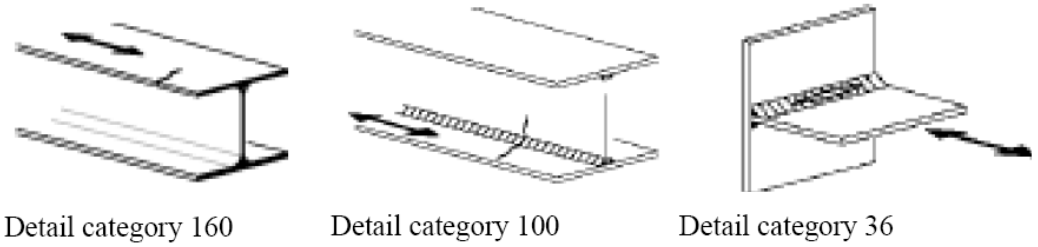

Figure 1.19-1.21 Shows examples of Figures representing different detail categories.

1.12 The problem of multiaxial fatigue in structural details

Several structural details exist in which the detail is subjected to a combined action of stresses (multiaxial stress). The stresses can be in- or out-of-phase which can have a big influence for the fatigue life. The geometry of the structural detail can cause multiaxial stresses in the welds or in the parent metal and is also important to consider in the design.

1.12.1 Examples of structural details exposed of multiaxial fatigue

In this Section some examples of details in structures exposed for multiaxial stress will be shown. These details can be divided into two groups, details exposed for multiaxial stresses caused by load case, called here primary stresses, and multiaxial stresses caused by the geometry of the detail, called secondary stresses. Multiaxial stresses caused by the geometry are often local issues, in the other parts of the detail no multiaxial stresses exist. In Figure 1.22 a simply supported member is loaded with a uniformly distributed load which causes shear and normal stress in the parent metal. The shear stress is a result from the shear force and the normal stress is from the acting bending moment.

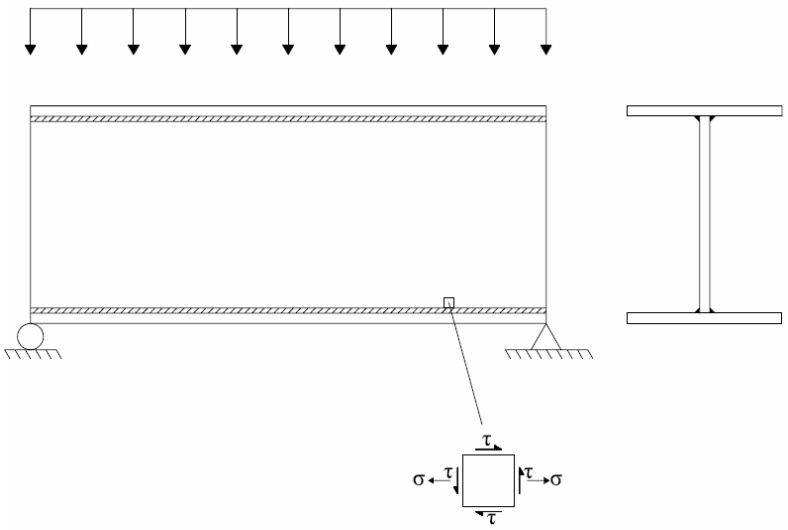

Figure 1.22 In plane multiaxial stresses in the weld and the parent metal caused by a apply load.

σ = Normal stress

τ = Shear stress

In Figures 1.23, 1.24 and 1.25 another case of in plane stresses are shown. The multiaxial stresses are a result of the geometry of the member and the multiaxial stresses in these members include both shear and normal stresses. Figure 1.23 is a part from a bridge girder with reduced height at the support. Change in cross-section gives rise to additional stress components in the web plate and in the welds [30]. Figure 1.24 shows a centric loaded plate which gives multiaxial stresses except in the center there only normal stress acts. The stress flow in those parts that have an inclination to the horizontal stress flow causes shear stresses and normal stresses in the weld. Here is a typical detail where booth uniaxial and multiaxial stresses act depending on which part is considered. This kind of detail has shear and normal stresses in-phase which is of great importance in designing. Figure 1.25 is from a hanger in an arc bridge and also here secondary stresses arise because of the geometry of the detail.

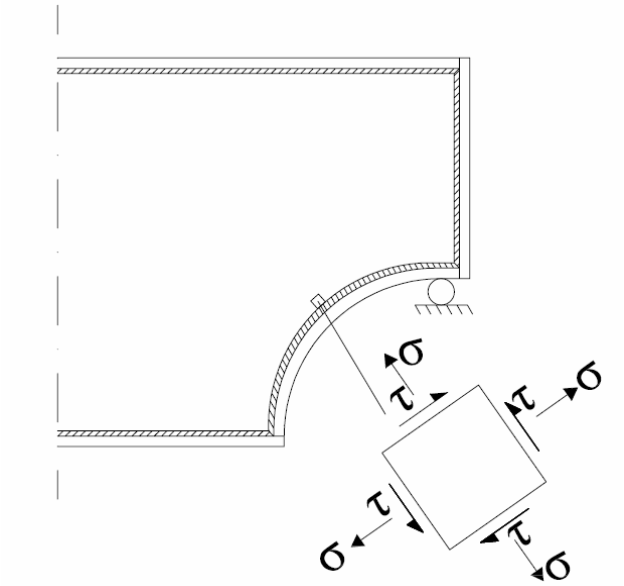

Figure 1.23 Because of the geometry of this member multiaxial stresses arise in the material.

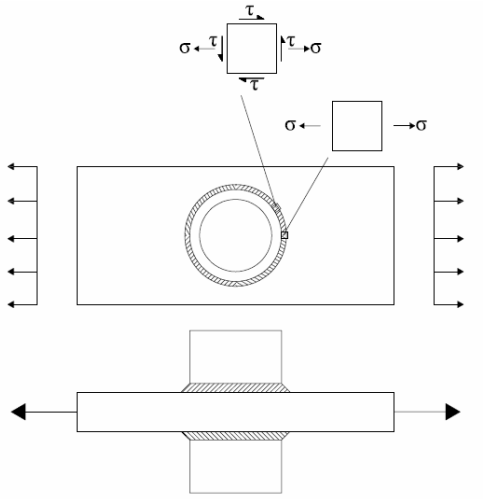

Figure 1.24 A centric loaded plate where the geometry causes multiaxial stresses.

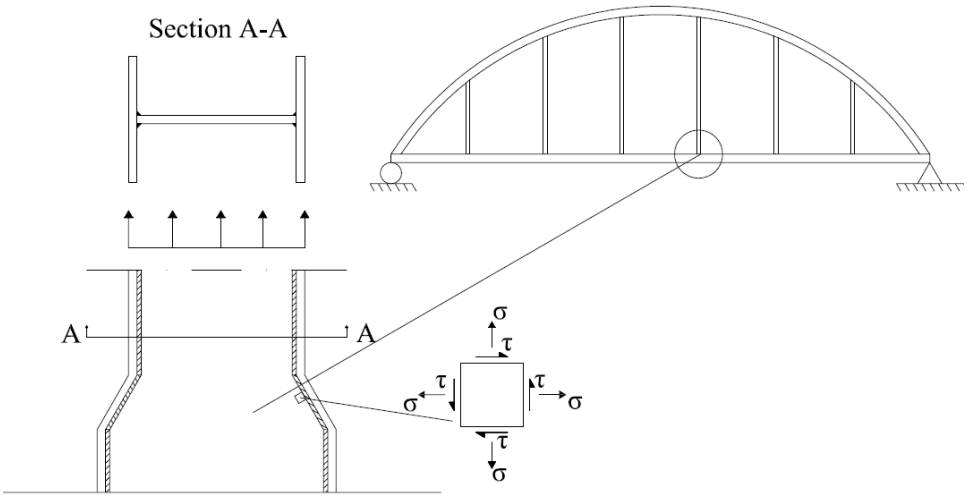

Figure 1.25 Detail from a steel part in tensile, the multiaxial stresses will arise in the sloped part.

In Figure 1.26 an orthotropic plate from a bridge is shown. An orthotropic plate consists of a thin steel plate which is stiffened by several longitudinal beams. The longitudinal beams are connected by welds to the floor-beams. A great advantage with this kind of bridges is that the self weight is very low. This type of construction is quite common in Europe and USA, in Sweden it is not so common but in some moveable and larger bridges it is used, for example the Högakustenbron and the new Svinesundsbron.

In orthotropic plates can some other type of stress come up just because of the longitudinal box beams under the bridge deck. This kind of multiaxial stresses will contains of shear, normal and bending stresses, for example, out of the plane of the floor-beam web.

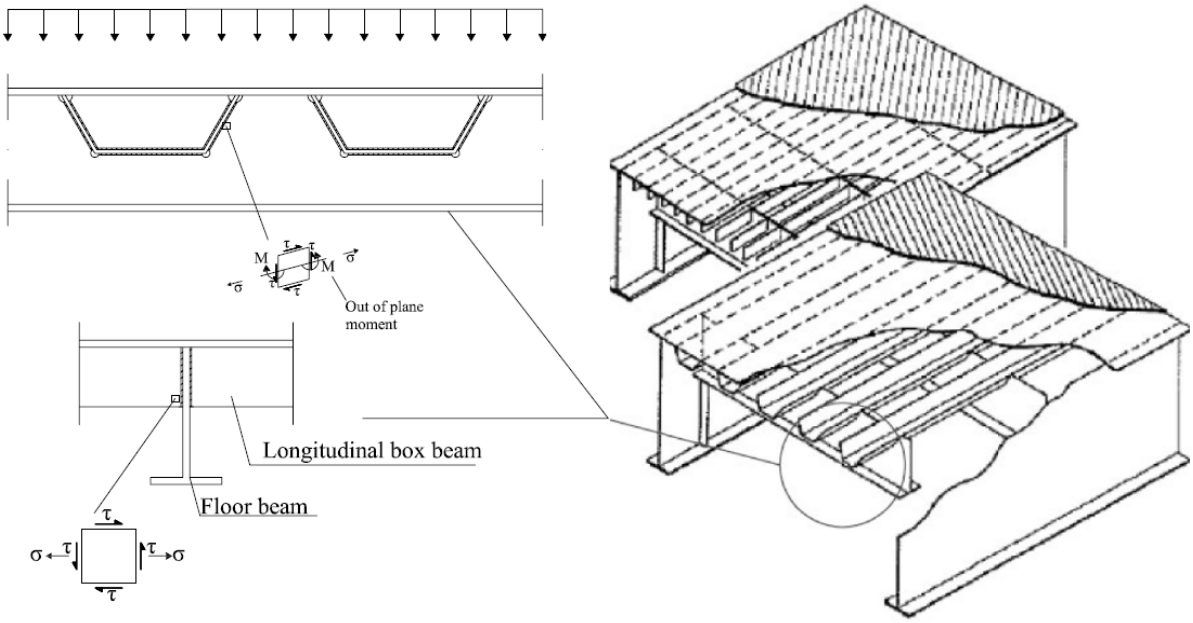

Figure 1.26 In a orthotropic plate in a bridge deck can some multiaxial stresses in the secondary box beams arise.

1.12.2 Loading in and out-of-phase

The different stress components in a multiaxial stress state can be either in-phase or out-of-phase depending on the loading condition and the geometry of the loaded element. To explain how the stresses can be in-phase an example with train with an overhead crane with load moving back and forward on a simply supported beam, see Figure 1.27. In the simply supported beam the shear force and the bending moment will have an influence line like the one shown in Figure 1.28.

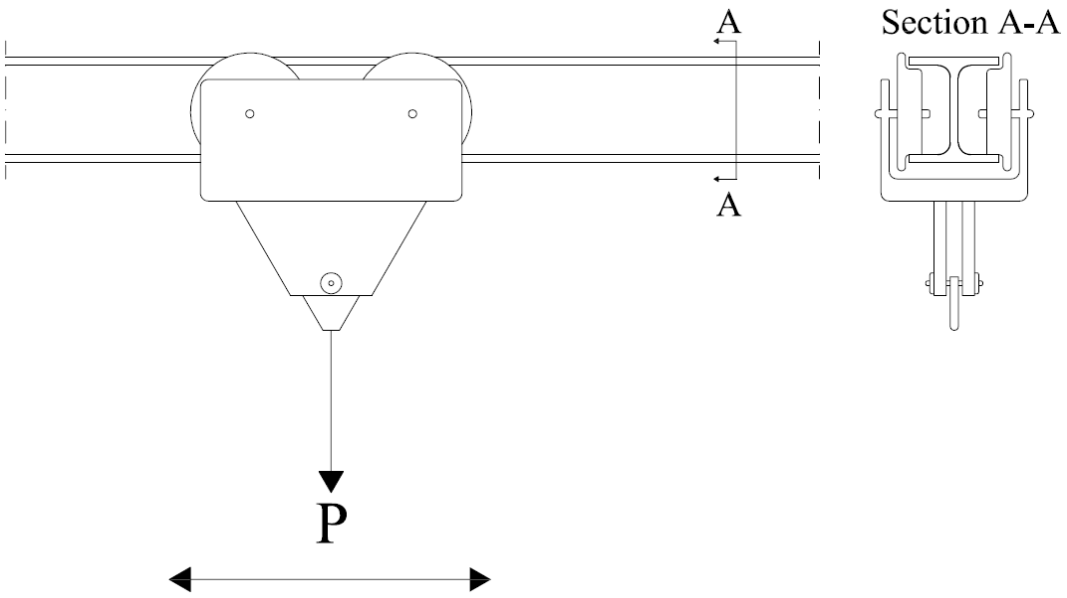

Figure 1.27 A overhead crane moves back and forward on a simply supported beam.

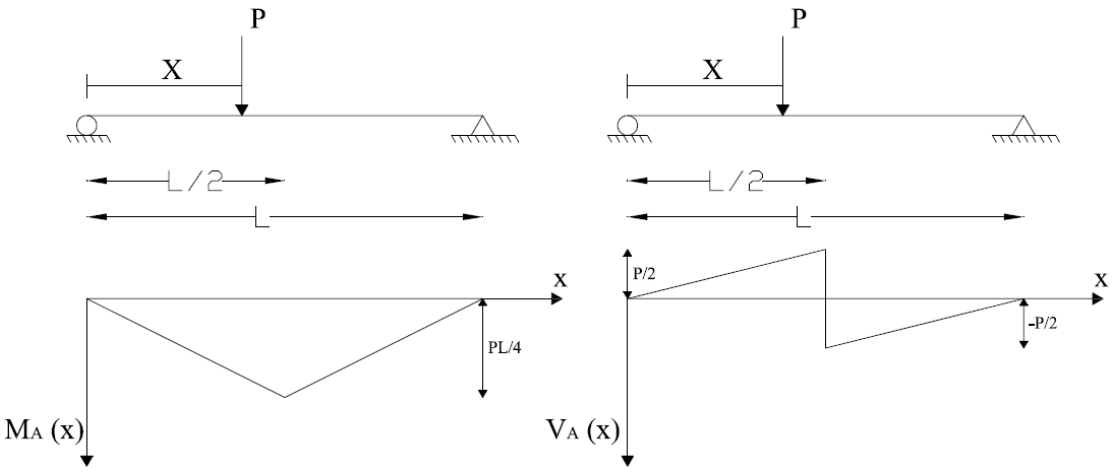

Figure 1.28 Influence line from the shear force and bending moment in the simply supported beam.

M_A = Moment

V_A = Shear force

To explain how shear stresses and normal stresses can be out-of-phase, one good and easy example about a train passage over a bridge will be shown. A train consists of a couple of wheel pairs with different distances, see Figure 1.29. These wheels are the moving point loads on the bridge and they cause shear stresses and normal stresses in the bridge girders. The bridge girder is a continuous beam on three supports, the spans are 10 meter wide. If the shear force and moment are calculated in a section one meter from the inner support, see Figure 1.30, the relationship between the forces is like Figure 1.31. The length of the curves depends on how many train vehicles it is in every train passage, but the shape of the curves will only be repeated for every new vehicle that pass the bridge.

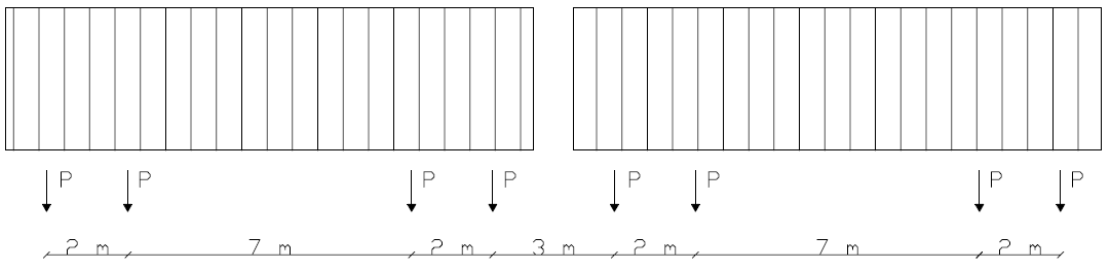

Figure 1.29 The spacing between the wheels in two train vehicles.

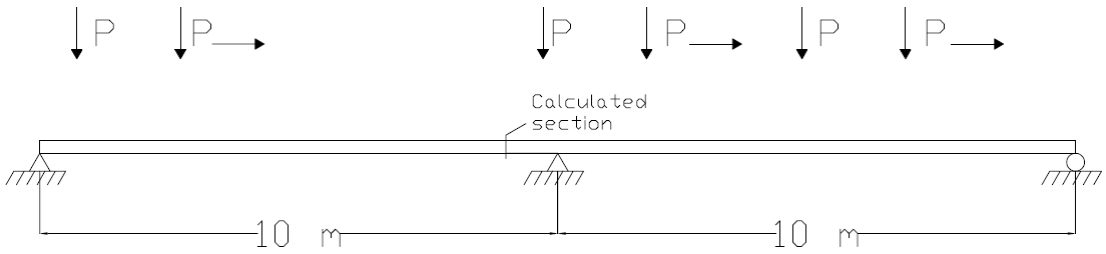

Figure 1.30 The continuous beam and the position of the calculated section.

P= Train axel load

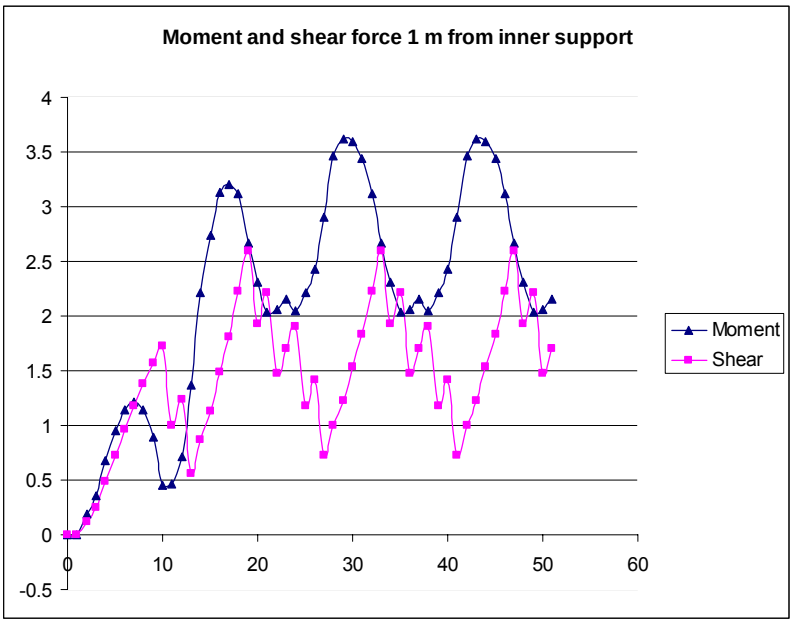

Figure 1.31 The relationship between the moment and shear force one meter from the inner support.

From Figure 1.31 it can be seen that the two forces are not in-phase, the turning points of shear force are not coincided with the turning points of the moment. The behaviour of the stresses in beams are very much affected of the arrangement of the beam, if the beam from the example above instead was a simply supported beam on two supports, the moment and shear will have another behaviour. This has also been calculated and the relationship between the moment and shear are showed in Figure 1.32, in Figure 1.33 the beam is showed. A section in the mid-span has been calculated and the difference with Figure 1.31 is obvious.

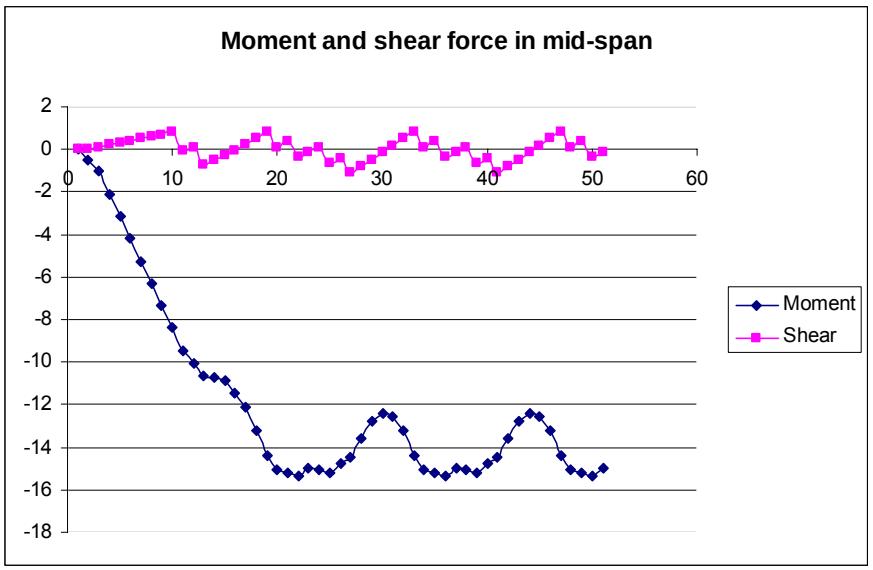

Figure 1.32 The relationship between the moment and shear in the mid-span of the beam.

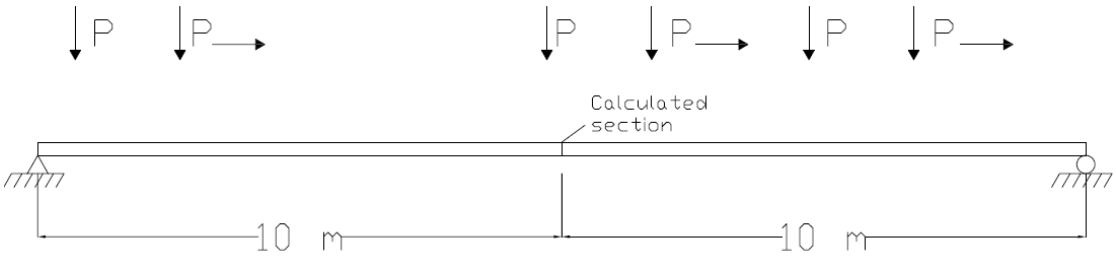

Figure 1.33 The beam on two supports and the position of the calculated section.

1.12.3 Problems due to multiaxial fatigue

There are several complications that can appear for designers working with details affected to multiaxial fatigue. The first problem is to evaluate the magnitude of the stresses acting on the weld or the parent metal. One other problem is that the most of the available standard codes classified different standard structural details and from these details the fatigue life is calculated by using the S-N curves. These S-N curves are often made from test done in uniaxial stresses and if these S-N curves are used for calculation of multiaxial fatigue life. The results might in some cases be not accurate.

2 Design against multiaxial fatigue

From several studies on the subject investigators agree that the multiaxial problem is complex and require more investigation. Different calculation methods were proposed to solve the multiaxial fatigue issue. Some methods are complex and require computer assistance while other approaches can be made by hand.

2.1 Historical review

The progress in fatigue awareness has developed with different speed for different professions. The mechanical industry has developed faster than the construction industry. The following summary is a review from the mechanical industry.

Wöhler was one of the most famous early fatigue researchers. During 1850 to 1875 experiments were conducted to establish a safe alternating stress below which failure would not occur. Full scale train axles as well as smaller laboratory specimens were employed to establish the endurance limit for fatigue design.

In 1903 Ewing and Humphrey published their classic paper *the fracture of metals under repeated alterations and stress*. They were motivated by the work of Wöhler and Bauschinger who developed a mirror extensometer, an instrument which was able to measure strain.

1923 Jenkins proposed the first spring-slider model for simulating stress-strain behaviour of metals. The importance of cyclic deformation was clearly established at that time, but largely ignored until 40 years later. In the 1920's Griffith showed by his work that the last cycle of growth was nothing more than brittle fracture, caused by cyclic growth of fatigue crack to an unstable length. Nothing was done on this problem until 40 years later by Paris.

The 1930's and 1940's were largely devoted to experimentally establishing the effects of the many factors influencing long-life fatigue strength.

In 1950 Coffin and Manson established quantitative relationships between plastic strain and fatigue life. They focused on problems related to metals at high temperatures.

1960 Significant contributions were made by many under this period. Paris quantified the relationships for fatigue crack propagation. Irwin and others developed a practical engineering tool in fatigue using fracture mechanics. Smooth specimen simulations of notches and cycle counting methods for variable loading were developed.

1970's fatigue analysis became an established engineering practice in many industrial applications. There were several studies made by communities which resulted in a large number of tests on various types of specimens. Some experiments were made to characterize the mechanical behaviour in order to account multiaxial response.

Nearly one hundred years of research has been performed to establish the effects of the variables that influence the fatigue strength of metals [21]. Designers have become more aware of the fatigue problem due to the accidents that appear to aeroplanes under 1950s. The awareness in bad detailing on structures causing decreased lifetime. Understanding has grown by knowledge that multiaxial stresses can act on a detail by load effects or by geometrical properties.

2.2 Different multiaxial fatigue models

Models treating the problem of multiaxial fatigue can be divided into the following main groups. For example in stress-based models some methods can be associated with critical plane analysis but still be a stress-based model which makes them more difficult to organize. Observe that all calculation methods put focus on fatigue life prediction.

- Stress-based models
- Strain-based models
- Energy-based models
- Fracture-mechanics models
- Methods for welded components

As mentioned earlier there are several methods included in each main group or category. In the following a short summary is given of the methods included in each main group.

2.3 Stress-based models

Stress-based models continue to be more widely used and are suitable for the large class of components that must operate near or below the fatigue threshold. Many of the stress based models can be used successfully in the finite life regime if the plastic strains are small [10]. It has been stated in [11] that stress based theory only deals with high cycle fatigue and can not be applied to other cases. Both stress and strain based models have the limitation that they don't reflect explicitly the effect of phase difference on fatigue strength.

The stress based approaches can be divided into four sub-groups:

- Empirical equivalent stress
- Stress invariants
- Average stress
- Critical plane stress

2.4 Empirical equivalent stress

The empirical equivalent stress approaches are often easy to calculate and convenient for engineering application. Popular formulas based on the empirical equivalent stress are Gough and Lee [3].

2.4.1 Gough

Gough was one of the earliest multiaxial fatigue researchers and he performed a lot of experiments. He tested different materials under different ratios between bending stress and torsion stress, and from the results he established a fatigue limit in combined loading. He plotted his test data as the ratio of bending stress to the bending fatigue limit, and he did similarly for the shear stress to the fatigue limit in torsion. From this he proposed a formulation, called the ellipse quadrant, see expression 2.1. This formulation is made for ductile materials, for brittle irons and/or notched specimens he proposed another formulation, the ellipse arc, see expression 2.2 [10]. In Figure 2.1 the Gough ellipse is plotted for different steel qualities, the bending stress is plotted versus the shear stress. The ellipse quadrant and ellipse arc have two limitations, first the criterion is based on one type of material and is therefore an empirical criterion; and second is that the criterion only can be applied for proportional loading conditions [3]. Further studies in [12] show that Gough's criterion does not fit in with test data under non-proportional loading. It can also be mentioned that the Gough's criterion only can be applied for parent metals, not for welded details.

$$\frac{f^2}{b^2}+\frac{q^2}{t^2}=1 \tag{2.1}$$

f = bending stress

b = bending fatigue limit

q = shear stress

t =fatigue limit in torsion

$$\frac{q^2}{t^2}+\frac{f^2}{b^2}\cdot\left(\frac{b}{t}-1\right)+\frac{f}{b}\cdot\left(2-\frac{b}{t}\right)=1 \tag{2.2}$$

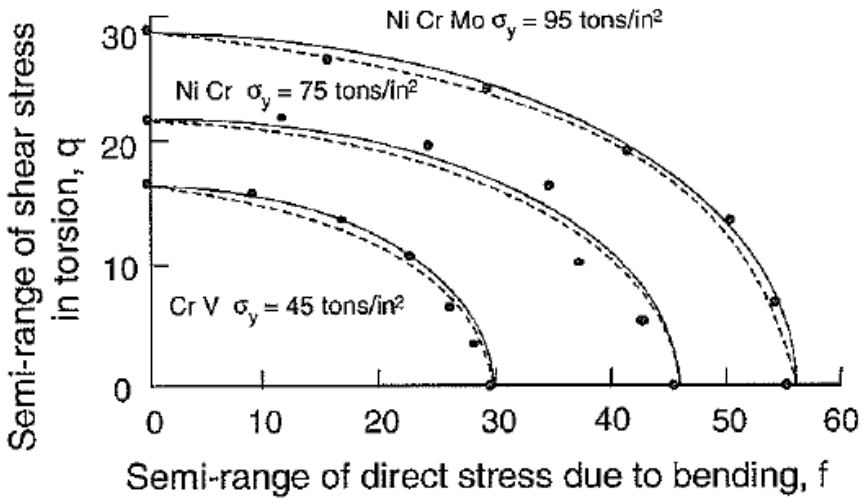

Figure 2.1 The Gough ellipse for different steel qualities [10].

2.4.2 Lee

Lee proposed a new equivalent stress criterion modified from the old Gough's ellipse quadrant and he ended up with the expression given in 2.3 that was validated by experimental data of tested material, such as the structural steel SM45C. The steel SM45C, have a tensile yield strength of 347 MPa and a ultimate tensile strength of 562 MPa, in Swedish standard steel can it be compared to S355.

$$\sigma_{eq} = \sigma_a \left[1 + \left(\frac{b\tau_a}{t\sigma_a} \right)^{\alpha} \right]^{\frac{1}{\alpha}} / \left(1 - (\sigma_m / \sigma_u)^n \right) \qquad (2.3)$$

σ_a =bending stress amplitude

b, t = bending and torsion fatigue strength

τ_a, σ_a = the torsion stress and bending stress amplitude

$2(1+\beta\sin\phi)$ = α

ϕ =the phase difference between bending and torsion

β = a material constant

σ_u =the tensile strength of the material

σ_m =the bending mean stress

n =an empirical constant between 1 and 2

Later Lee combined expression 2.3 with Findley's formula and reached up to a new formula to predict the multiaxial fatigue life, see expression 2.4. This life prediction

formula takes consideration of both out-of-phase loading and phase difference between bending and torsion. Lee's formula includes a material constant, β, and this put some limitations for the use of the method, because it requires more information or experimental work to find this constant [3], [13]. Like Gough's criterion can this method only be applied for parent metal and not for welded details.

$$\left(\frac{\sigma_a}{b}\right)^{b(1+\gamma\sin\phi)/t} + \left(\frac{\tau_a}{t}\right)^{2(1+\gamma\sin\phi)} = 1 \qquad (2.4)$$

γ = material constant

2.5 Stress invariants

The basic idea in the stress invariants (constant stress) approach is to directly relate the fatigue strength with the second invariant of the stress deviator and first invariant of the stress (3 times the hydrostatic stress). Sines's criterion is one example on a stress invariant approach. Some disadvantages with the stress invariants approaches is that the orientation of the initial crack cannot be predicted and that obtained results can be no conservative [14] and [13].

2.5.1 Sines

Sines considered the experimental data of Gough for combined bending and torsion loading. After studying several failure criteria including both maximum shear stress and octahedral shear stress, he proposed that the octahedral shear stress be used as damage criteria. The physical significance of the octahedral shear stress is that it expresses the average effects of slippage on different planes and in different directions of all crystals in the aggregate, with slip in any given grain caused by the critical resolved shear stress in that grain. Sines concluded that a torsional mean stress did not affect the fatigue life in bending until the torsional yield strength was exceeded by at least 50 % [10].

2.6 Average stress

The average stress approach uses an average of the stress components involving the critical point. The stress components are treated as an equivalent stress and correlated to the fatigue damage. Papadopoulos original criterion is one example on average stress approach.

2.6.1 Papadopoulos

Papadopoulos proposed a fatigue limit criterion which could be applied in the case of constant amplitude multiaxial proportional and non-proportional loading in the field of high-cycle fatigue. The fatigue limit criterion was written as $\tau_{a,cr} + k\sigma_{H,max} = \lambda$ [12]. In the report [15] Papadopoulos writes that the method is valid for ferritic steels but the methodology can be modified to derive models for other metallic materials. The fatigue limit criterion is of the critical plane type. The model defines so called generalised shear stress amplitude for each plane by the following method. At any point O of a body, a material plane Δ can be defined by its unit vector n. This vector n makes an angle θ with the z-axis of a Oxyz frame attached to the body, and its

projection on the xy plane makes an angle φ with axis x. For each plane Δ a new quantity is introduced called generalised shear stress amplitude and denoted as T_a, see Figure 2.2 [15]. Papadopoulos was the first to introduce this shear stress quantity later used by others.

m, r, l, n = Unit normal vector

T_a = Generalised shear stress amplitude

γ_∞, α_∞ = material parameters

Δ = Material plane

φ, θ = Defines the angle to actual axis

ξ = Arbitrary line

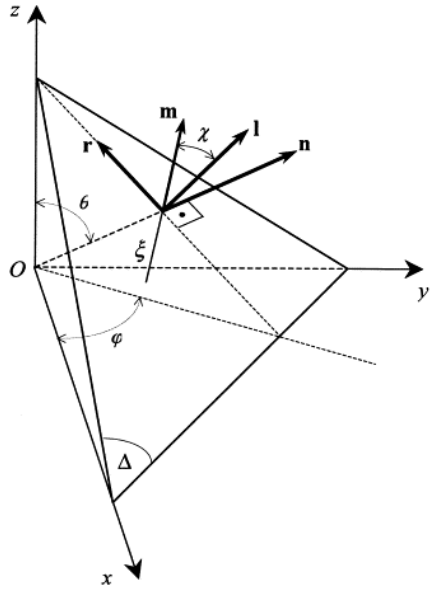

Figure 2.2 The material plane [15].

Papadopoulos method seems to be quite general and could be used in predicting fatigue life for specimens affected to multiaxial loading. But it is no simple method and requires advanced mathematic knowledge.

2.6.2 F Morel

In [11] Morel proposes a relevant method to predict fatigue life on specimens affected by any arbitrary uniaxial, multiaxial, constant or variable amplitude loading. This method is different from stress and strain based methods since it is derived from a model employing a plasticity analysis to assess cyclic micro plasticity. More precisely it is based on the approach introduced by Dang Van and further developed by Papadopoulos. The accumulated plastic strain computed at a mesoscopic scale is considered as the damage variable. Some explanations are required to bring understanding to the mesoscopic scale. Morel in [11] declares that to depict the fatigue crack initiation phenomenon in polycrystalline metallic materials two scales of description of a material will be distinguished, the usual macroscopic scale and the

mesoscopic one. The macroscopic scale is defined with the help of an elementary volume V determined at any point O that can be considered as homogenous. Engineers usually use stresses and strains measured or estimated at this scale. V contains a large number of crystals and the mesoscopic scale is defined as a small portion of this volume. In high cycle fatigue regime some crystals undergo local plastic strain while the rest behaves elastically. The overall plastic strain is negligible.

2.7 Critical plane stress

Critical plane models have been developed from observations of fatigue cracking behaviour on specimens which show that cracks initiate and propagate in preferential orientations [16]. Bäckström writes [16] that Findley (1959) was the first to develop a critical plane model which estimated fatigue damage. The critical plane approach can have lacks because its deals with the ratio between shear stress and maximum normal stress. This is normally measured and given in tables with a factor ρ which is defined as $\rho=\sigma_{n.max} / \tau_{A.}$ In the rapport [17] high ratios of ρ seems to be not suitable for describing fatigue situations. It is also mentioned that the critical plane can not be defined when the shear stress amplitude approaches zero or equals zero. From the same rapport critical plane approach seems to be successful in predicting the material fatigue limit up to an upper cut value of the ρ ratio. The critical plane approach has sense up to those situations for which the shear stress amplitude relative to the critical plane continues to play a fundamental role in damaging materials. Moreover it seems even logical to assume that this limiting value of ρ is different from material to material [17]. The critical plane approach was originally proposed based on observations that the fatigue crack nucleation occurs at the persistent slip bands, formed in some crystals of the materials. The planes are named critical plane and the stress components on it are used for fatigue analysis [18]. This assumption or basis makes it difficult to apply the model to materials with microstructures different with normally used metals. Also this assumption usually requires cracking analysis to distinguish the failure modes before the appropriate critical plane based model can be applied. Most of existing critical plane based models can only be applied to certain types of failure modes i.e. shear dominated or tensile dominated failure [18].

The critical plane approach is suitable to apply to the multiaxial fatigue problem. There are a lot of different models with different definitions of the critical plane but the methodology is the same. Methods based on the critical plane approach have been shown to have a good correlation with the experimental observations.

ρ = Ratio

$\sigma_{n.max}$ = Maximum normal stress

τ_A = Shear stress

2.7.1 Findley

Findley's method is based on stress analysis acting on a plane. In a biaxial stress field with shear and normal stress these can be calculated from Mohr's circle [19].

The Findley model suggested that normal stress (σ_n) on a shear plane might have linear influence on the allowable alternating shear stress ($\Delta\tau/2$) [16].

From [10] Findley concluded that a linear model was sufficient to describe experimental data. This model identifies the stress acting on a specific plane within the material. Findley identifies a critical plane for fatigue crack initiation and growth that is dependent on both alternating shear stress and maximum normal stress. The combined action of shear and normal stresses is responsible for fatigue damage. Failure is expected to occur on the plane that has the largest combination of $((\Delta\tau/2) + k \cdot \sigma_n)_{max.}$ [10]. This is also Bäckströms conclusion -Any combination of $\Delta\tau$ and σ_n resulting in the same effective shear range ($\Delta\tau$') gives the same fatigue life. Failure is expected to occur on the plane that has the largest ($\Delta\tau$') and not necessarily the plane of largest alternating shear stress [16]. The constant k in expression (2.5) represents a material sensitivity to normal stress on a shear plane [16]. The constant k can be determined experimentally by performing fatigue test involving two or more stress states. For ductile materials k typically varies between 0.2 and 0.3 [10]. The Findley method is accurate for stresses in-phase and out-of-phase.

$$\left(\left(\frac{\Delta\tau}{2}\right) + k \cdot \sigma_n\right)_{\max} = \left(\frac{\Delta\tau'}{2}\right) = f \qquad (2.5)$$

$\Delta\tau$ = Shear stress

σ_n = Normal stress

k = Material dependent coefficient normally 0.2-0.3

$\Delta\tau$'= Effective shear range

f = Fatigue damage on a certain plane

2.7.2 McDiarmid

1991 McDiarmid introduced another criterion for failure in high cycle multiaxial fatigue and he based the criteria on the critical plane approach where fatigue strength is a function of the shear stress amplitude and the maximum normal stress amplitude which act in the same plane as the shear stress, see expression 2.6. This criterion taking account the two different cases of shear cracks, case A and case B, illustrated in Figure 2.3. Case A appears from in-plane shear stress, the cracks propagate along the surface. Case B is a result of out of plane shear stress, the cracks propagate inwards from the surface. This two crack cases was proposed by Brown and Miller. McDiarmid's method is widely used and is implemented in much commercial fatigue software [10], [20].

$$\frac{\Delta\tau_{\max}}{2t_{A,B}} + \frac{\sigma_{n,\max}}{2\sigma_{uts}} = 1 \qquad (2.6)$$

$\Delta\tau_{\max}$ =Shear stress amplitude

σ_{uts} =Ultimate tensile strength

$\sigma_{n,\max}$ =Normal stress (acting on the same plane as $\Delta\tau_{\max}$)

$t_{A,B}$ = The shear fatigue strength there A, B are two different cases in cracking

This criterion only works in the region

$$0.5 \cdot t \le \tau_{\max} \le t \quad \text{and} \quad 0 \le \sigma_{n,\max} \le \sigma_{uts}$$

t =fatigue strength in torsion

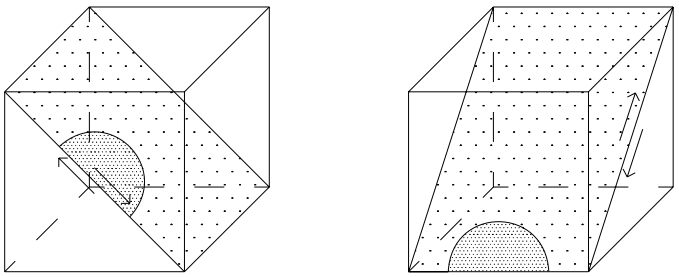

CASE A CASE B

Figure 2.3 The two different cases of shear cracks.

To get this criterion McDiarmid carried out a series of fatigue tests on a thin-wall tubular specimens subjected to constant amplitude alternating longitudinal load and alternating pressure across the wall thickness. He exposed the specimens for 15 different cases of principal stress amplitude ratio, out-of-phase angle and frequency ratio, shown in the Table 2.1. He even tested his criterion with previous preformed test result from the literature and the criterion gave a good correlation by the previous obtained result. Some difference between the McDiarmid's criterion and the different test series was obtained dependence on type of loading, specimens and if it was in or out-of-phase. The difference was following:

1. Combined bending and torsion: In-phase is the correlation +/- 5 % and out-of-phase +/- 10 %.
2. Thin cylinders, including effects of mean stress and in and out-of-phase: The correlation is within +/- 10 %.
3. Thick cylinders: 90 % of the tests have a correlation within +/- 10 %.

Case	$\lambda=\sigma_2/\sigma_1$	Phase angel	Frequency ratio σ_2/σ_1
1	0	Longitudinal stress only	1
2	0,3	0	1
3	0,5	0	1
4	0,8	0	1
5	1	0	1
6	2	0	1
7	∞	Transverse stress only	
8	1	180	1
9	2	180	1
10	3	180	1
11	1	180	1
12	1	0	2
13	1	90	2
14	1	0	3
15	1	180	3

Table 2.1 Test conditions on thin wall tubes, σ_1 is longitudinal and σ_2 is transverse [20].

The criterion in formula 2.6 can be applied to following multiaxial loading conditions by using test data from previous experiments in the literature:

1. Combined bending and twisting.
2. Combined bending and twisting with mean stress.
3. Combined bending and twisting, out-of-phase.
4. Thin wall cylinders.
5. Thin wall cylinders with mean stress.
6. Thin wall cylinders with mean stress and out-of-phase stresses at different frequencies.
7. Thin wall cylinders with out-of-phase loading including different waveforms and frequencies.
8. Thick wall cylinders.

McDiarmid's model is similar to Findley's model but McDiarmid has some modifications [10]:

- The model considers the both cracking types A and B.
- Findley's material parameter k is replaced with $\frac{t_{A,B}}{2\sigma_{uts}}$
- The critical plane is defined as the plane with the maximum shear stress amplitude and not the plane on which the damage is maximized. In some cases can this be completely different from the plane defined by Findley.

McDiarmid never tested his criterion for welded specimens and therefore it can only be applied for fatigue calculations for parent metals.

2.7.3 Dang Van

Dang Van proposed a limit criterion for fatigue life based on the concept of micro stress within a critical volume of the material. This model arises from that fatigue crack nucleation is a local process that begins in the small grains that have experience a plastic deformation and formed slip bands in the atomic structure. Cracks usually starts in the slip bands and therefore is the microscopic shear stress on the grain an important parameter. In the same way is the microscopic hydrostatic stress also an important parameter because it will influence the opening of the cracks caused by the shear stress. Dang Van came up to a simple failure criteria concerning this two parameter in a linear combination, see expression 2.7 [10]. A great advantage with Dang Van approach is that it can be suited for uniaxial and complex multiaxial stress state [3].

$$\tau(t) + a\sigma_h(t) = b \qquad (2.7)$$

$\tau(t)$ = the microscopic shear stress

$\sigma(t)$ = the microscopic hydrostatic stress

a and b = are constants

2.7.4 Susmel & Lazzarin

Susmel & Lassarin proposed a multiaxial fatigue criterion based on use of non-conventional bi parametric Wöhler curves. This method takes as its starting point the idea that fatigue damage is mainly shear dominated. The use of the critical plane approach has been justified by using hypotheses directly derived from the theory of cyclic deformation in single crystal. Susmels and Lazzarin approach follows the idea that fatigue damage in the presence of both smooth components and blunt notches depends on both shear stress amplitude and the maximum normal stress relative to the plane of shear stress amplitude. This assumption is based on the fact that these macroscopic stress components are proportional to the microscopic ones damaging the most unfavourable oriented crystals positioned inside the fatigue process zone. Therefore the plane of maximum shear stress amplitude is the plane on which the probability of initiating a fatigue crack reaches its maximum value. The criterion has been successful showing a high level of accuracy in predicting the fatigue life both in low, medium and high cycle fatigue field, independently of the complexity of the applied fatigue stress [17].

2.8 Strain-based models

For the strain approach there is no single theory that can be applied to a wide variety of materials and loading condition and give reliable result [3].

This approach is most used for low-cycle fatigue but it can be applied for high-cycle.

Yongming Liu, [3] divide the strain approach into three different groups:

- Critical plane approach
- Shear failure
- Tensile failure
- Characteristic approach

There critical plane approach can be divided into shear and tensile failure. In shear failure mode some approaches are Brown and Miller 1982, Lohr & Ellison 1980, Socie 1989, Fatemi and Socie 1988, Farahani 2000 and Pan 1999. Models based on tensile failure mode are Smith 1970 and Socie 1987 [3]. Some of these are low cycle fatigue models and are not accurate for civil engineering. Even strain-based models are typically associated with low-cycle fatigue and are for the same reason not applicable in civil engineering [10] and this is confirmed by Morel [11] that strain based models normally are devoted to low cycle fatigue but can be extended to high cycle fatigue. There seems to be approaches in strain based models that is valid also for high cycle fatigue or at least with some modification.

2.9 Critical plane approach based on strain

These criterions are similar to the stress based critical plane approaches but instead of calculate the critical stress plane a critical shear strain plane is calculated.

2.9.1 Brown & Miller

Brown and Miller came up to a multiaxial fatigue theory based on the critical plane approach. They based their theory on that crack initiation is a slip process governed by plastic deformation, the maximum shear strain is the controlling parameter and that the normal strain across the maximum shear strain amplitude plane assists in propagation. Their original theory was defined as expression 2.8, but after further work they came up to another promising criterion, see expression 2.9.

$$\frac{1}{2}\cdot(\in_1 - \in_3) = f(\frac{\in_1 + \in_3}{2}) \tag{2.8}$$

$\in_1, \in_3$ = principal strains

$$\frac{1}{2}\cdot(\in_1 - \in_3) + \frac{S}{2}\cdot(\in_1 + \in_3) = \text{constant} \tag{2.9}$$

S = a material constant

This model is developed to calculate the damage caused by low cycle fatigue, but some of the work that Brown and Miller performed came to be some sort of base for other more promising high cycle models like McDiarmid and Dang Van and therefore it is important to mention this method [10], [21].

2.10 Characteristic approach

This method is similar to the critical plane method in the calculation procedure. A plane is first determined and the strain (stress) components on the plane are combined together and used for fatigue life prediction. Unlike most of existing critical plane

models the characteristic plane in this model is not based on the physical observations of the crack but arises from the idea of dimension reduction. It assumes that the complex multiaxial fatigue problem can be approximated by using the strain components on a certain plane (characteristic plane). Then the objectives are to find the plane and the formula of combinations of the strain components on that plane. Through this type of definition of the characteristic plane, failure mode analysis is not required and the model can therefore be adopted for different materials. The materials can be different metals and still be analysed with this model. Correction factors for out-of-phase, plastic hardening and mean stress are also introduced into the model. Good correlations are found between predicted and experimental fatigue lives under propotional and non-propotional loading for both low and high cycle regime [18].

2.11 Energy-based models

Energy criteria of multiaxial fatigue can be divided into three groups, depending on the kind of strain energy density per cycle which is assumed as the damage parameter [22].

1 Criteria based on elastic energy (for high cycle fatigue)
2 Criteria based on plastic energy (for low cycle fatigue)
3 Criteria based on the sum of elastic and plastic energies (for low and high cycle fatigue)

From multiaxial fatigue tests it appears that criteria that do not include all the strain energy, but only the component connected with the critical fracture plane, seems to be the most promising. The known energy criteria of multiaxial fatigue failure are usually formulated for regular cyclic loading. There are some successful attempts in their application to non regular loading. The material nature must be considered (ductile, semi-ductile, and brittle) because different failure mechanisms have been observed for different types of material [22]. There are several methods treating energy based approach. Below are some methods that many reports are referring to.

- **Garud (plastic energy model)**
- **Ellyin (sum of elastic and plastic energies)**

The Ellyin method assumes proportional loading and includes also a formula which requires integration, see expression (2.10). Garud and Ellyin have created early models later modified and used by others.

$$W_f = \int_{cycle} s_{ij} de_{ij} \qquad (2.10)$$

W_f = total elastic plus plastic distortion energy density

s_{ij} = components of stress state deviator

e_{ij} = components of strain state deviator

2.12 Fracture-mechanics models

This method analyses growth of micro cracks often linked to each other forming single dominant crack that goes to failure. This type of analysis can be a proper way to consider elements of interest for this report. Unfortunately there are not possibilities to include everything in the report due to time.

The fracture mechanics approach is based on the Paris law, which the fatigue crack growth can be calculated with. The Paris law relates the number of cycles to the stress intensity parameter through the relationship in expression (2.11).

$$\frac{da}{dN} = C \cdot \Delta K^{m} \qquad (2.11)$$

$\frac{da}{dN}$ = the crack growth rate

C = material constant

ΔK = the stress intensity parameter which can be expressed instead:

$K = \sigma\sqrt{\pi \cdot a}$

a = the crack length

m =material constant, 3.0 for carbon steel

The differential equation can be solved and the new expression is for define the crack length for a given number of cycles. The problem with this approach is the calculation of the stress intensity parameter and that the local stress concentration factor also has to be known [33].

2.13 Combined and remaining methods

Some models are a combination of different methods and these models will be shown in this Section.

2.13.1 Combined critical plane and energy models

- Liu
- Chu, Conle and Bonnen
- Glinka, Wang and Plumtree

2.14 Welded components

Producing components by welding causes stress raising geometries which causes fatigue cracks during life. Niemi writes in [4] –In a welded component there will be several geometric features which act as stress raisers. Such stress raising discontinuities can produce essentially global or local effects and they frequently interact such that very high local stresses occur [4]. High local stresses causes crack initiation where notches or other imperfections due to the welding procedure work as starting points.

The calculation problem can be greatly simplified observing that in the medium/ high cycle fatigue regime and in the presence of sharp notches the plasticity contribution to stress field distributions is in general negligible and stress-strain fields can be studied just by using simple linear-elastic approaches [24].

It was stated [24] that a warning should be given for welds affected to multiaxial nominal loading. When calculation procedures are suggested they are often extremely simplified and resulting in approximate estimations. The most critical problem in assessing welded details subjected to complex stress is that principal stress directions may rotate during the load cycle when the applied loading is non-proportional.

There are five basic fatigue prediction models for welded components [4]. The method using hot-spot method is only accurate for failure at weld toe. This type of failure is normally consisted as a failure in parent metal.

- Nominal stress approach
- Local notch stress or strain approach
- Fracture mechanics approach
- Hot-spot approach (only for toe crack failure)
- Effective equivalent stress hypothesis

2.14.1 Nominal stress approach

To understand this method it is necessary to understand the meaning of nominal stress. The nominal stress can usually be determined by simple handbook formulas. Most engineers are familiar with Naviers formula. This formula calculates the nominal stress for an ordinary beam on a certain level affected by normal force and bending. In the nominal stress approach, fatigue strength is given in form of S-N curves determined from testing specimens. The specimens contain various attachments with different weld types causing discontinuity effects. In all cases the fatigue strengths are quoted as nominal stresses ignoring the stress field discontinuity caused by the attachments stress [4]. Maddox writes in his report [2] that S-N curves are derived from constant amplitude fatigue test data obtained from welded specimens by statistical analysis. Many are familiar with Eurocode 3 and have seen such S-N curves for welded details. Figure 2.4 shows given S-N curves for different details [2].

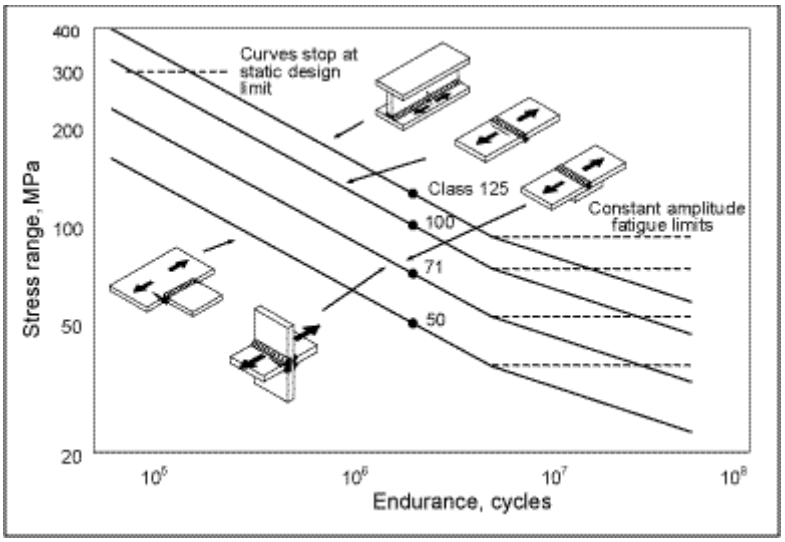

Figure 2.4 S-N curves for different details [2].

Using nominal stress approach like Eurocode 3 has limitations due to multiaxial loading. If the equivalent shear stress range is less than 15 % of the equivalent nominal normal stress range the effects of shear stress range may be neglected [23].

2.14.2 Local notch stress & strain approach

These approaches are based on the stress/strain state directly. The stress analysis will often be divided into a global finite element analysis at the structural stress level, coupled with a local finite or boundary element analysis of the notch area. This approach should be valid for a wide variety of joint types and loading conditions, including biaxial non-proportional loading [4]. The method seems to work for multiaxial fatigue problems even when load conditions are out-of-phase. This type of method needs finite element analysis which is not a part of this paper. Niemi suggest a novel linear-elastic approach based on Neuber's hypothesis. It is state that [25] multiaxial state of stress using Neuber's rule gives good results provided that one uses the second invariants of the stress and strain tensor deviators. But the use of the same method component by component does not give good results. This method is advanced to use and may result in complex calculations not suitable for hand calculation.

2.14.3 Hot-spot approach

In publication [16] the following description for hot-spot is given. -*Hot-spot is a term which is used to refer to the critical point in a structure where fatigue cracking can be expected to occur due to discontinuity or notch*. Usually the hot-spot is located at the weld toe. The hot-spot stresses account only the overall geometry of the joint and exclude local stress concentration effects due to weld geometry and discontinuities at the weld toe. Hot-spot stresses used in combination with modified Wöhler curves can be successful in predicting fatigue lifetime of welded details subjected to multiaxial fatigue loading [24]. However more work needs to be done in this area to check its validity. This paper will shortly describe the modified Wöhler method later on in Section 4.2.2. One must also remember that hot-spot stresses are defined from finite element analysis which requires computer assistance.

2.14.4 Effective equivalent stress hypothesis

Sonsino discovered that neither von Mises criterion nor maximum principal stress criterion was relevant for non-proportional loading. His method assumes that cracks initiate by shear and involves calculating the interaction of all shear stress components in a surface or volume element at the weld toe [16]. It has also been stated [16] that a correct use of von Mises hypothesis is valid for proportional loading with no change in direction of principle stress [16]. A feature of this approach is that it uses local notch stresses rather than nominal stresses for welded joints. The termination of notch stresses requires detailed finite element modelling of the weld toe as a notch. It is also relevant to note that although the local approach utilizing notch stresses is one possible method for designing welded joints. However it is not yet established in fatigue design rules for welded structures [5].

To calculate the fatigue life for steel specimens and welds, different variants of approaches have been developed based on the local stress concept. The basic idea with this concept is to treat the weld as a notch and calculating the local stress distribution in the weld toe. In combined multiaxial loading the nominal stress design curve can not be applied because they can give non-conservative results. Therefore the nominal design curve most be transformed into a local one, see Figure 2.5. This can be done by determination of the theoretical stress concentration factor K_{tb} for bending and K_{tt} for torsion. This concentration factors can be found with example finite or boundary element calculations or from analytical solutions. With help of von Mises stress hypothesis the equivalent stress can be determined, see expression (2.12).

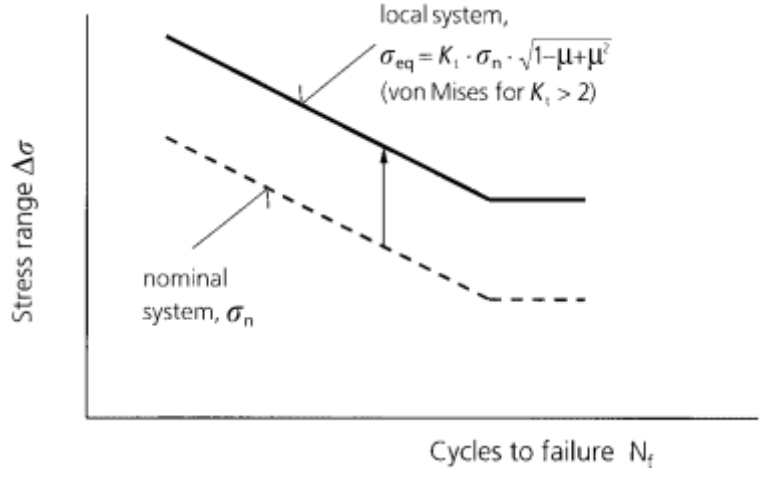

Figure 2.5 Transformation of an S-N curve from the nominal into the local system [26].

$$\begin{aligned} \sigma_x &= K_{tb} \cdot \sigma_n \\ \sigma_y &= \mu \cdot \sigma_x \\ \tau_{xy} &= K_{tt} \cdot \tau_n \\ \sigma_{eq} &= \sqrt{\left(\sigma_x^2 + \sigma_y^2 - \sigma_x \cdot \sigma_y + 3\tau_{xy}^2\right)} \end{aligned} \qquad (2.12)$$

σ_x, σ_y =Local stress components

σ_n =Nominal stress

τ_{xy} =Local shear stress

τ_n =shear stress

μ =Poisson's constant

K_{tb}, K_{tt}, = Stress concentration factors

This method can only be applied for multiaxial loading in-phase with fixed principal stress directions because of this the method can overestimate the fatigue life then the multiaxial loading is out-of-phase [26]. To overcome this problem a local stress-based modification of von Mises has to be done and therefore the so called effective equivalent stress hypothesis was developed.

The effective equivalent stress hypothesis, short named EESH, is a critical plane oriented integral hypothesis suggested by Sonsino [27]. EESH assumes that failure of ductile materials exposed for multiaxial stress state is initiated by shear stresses, $\tau_n(\varphi)$, (2.13). The shear stresses can be calculated from the stresses in the weld toe, influenced of the phase angle between bending and torsion, see expression (2.14). To calculate the equivalent stress it is necessary to determine the effective shear stress acting on the plane φ, which will de done with expression (2.15). When all this stresses are calculated the equivalent stress can be determined with expression (2.16) and with the σ_{eq} a new S-N curved can be calculated and adapted for the current load.

$$\begin{aligned}\sigma_n(\varphi) &= \sigma_x \cos^2(\varphi) + \sigma_y \sin^2(\varphi) + 2\tau_{xy}\cos(\varphi)\sin(\varphi) \\ \tau_n(\varphi) &= \tau_{xy}(\cos^2(\varphi) + \sin^2(\varphi)) - (\sigma_x - \sigma_y)\cos(\varphi)\sin(\varphi)\end{aligned} \tag{2.13}$$

$$\begin{aligned}\sigma_x(t) &= \sigma_{xm} + \sigma_{xa}\sin(\omega_x t) \\ \sigma_y(t) &= \sigma_{ym} + \sigma_{ya}\sin(\omega_y t - \delta_y) \\ \tau_{xy}(t) &= \tau_{xym} + \tau_{xya}\sin(\omega_{xy} t - \delta_{xy})\end{aligned} \tag{2.14}$$

$\sigma_{xm}, \sigma_{ym}, \tau_{xym}$ =Local mean stresses

$\sigma_{xa}, \sigma_{ya}, \tau_{xya}$ =Local stresses

t =Time

δ =Phase angle

$\omega_x, \omega_y, \omega_{xy}$ =Angular velocity

$$F(\delta) = \frac{1}{\pi}\int_0^{\pi} \tau_n(\varphi) d\varphi \tag{2.15}$$

This value is then used for obtain the effective equivalent stress in any phase angle.

$$\sigma_{eq}(\delta) = \sigma_{eq}(\delta = 0°) \times \frac{F(\delta)}{F(\delta = 0°)} \sqrt{G \exp\left[1 - \left(\frac{\delta - 90°}{90°}\right)^2\right]} \tag{2.16}$$

where

$$G = \frac{1 + K_{ta}}{1 + K_{tt}} or \frac{1 + K_{tb}}{1 + K_{tt}}$$

and

$$\sigma_{eq}(\delta = 0°) = \sqrt{\left(\sigma_x^2 + \sigma_y^2 - \sigma_x \cdot \sigma_y + fg^2 \cdot 3 \cdot \tau_{xy}^2\right)}$$

$$f_G = \frac{\sqrt{\sigma_x^2 + \sigma_y^2 - \sigma_x \cdot \sigma_y}}{\sqrt{3} \cdot \tau_{xy}}$$

Sonsino evaluated in [26] the equivalent stress hypothesis and some test was carried out for verify the theory and the result is shown in Figure 2.6. The tests was made on a welded flange-tube connection exposed for pure bending, pure torsion and with combined in-phase and out-of-phase loading. Most of the results where in the scatter 10 % from the S-N curve and the theory was also successfully applied for other welded joints.

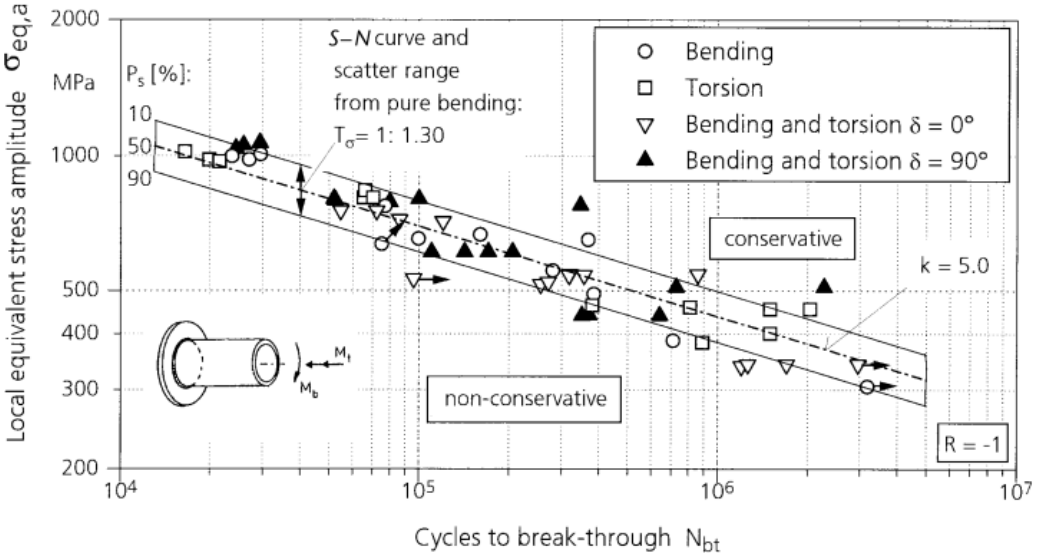

Figure 2.6. Application of the EESH for a welded flange tube connection [26].

3 Fatigue testing of multiaxial fatigue strength

3.1 Types of test specimen

Fatigue tests are performed in different ways depending on the type of multiaxial stress combination that are surveyed. The most common procedure is test with round shafts of pipes welded to steel plates affected to torsion in combination of normal loading. The pipes can also be rectangular. Other tests combine bending and torsion and even change direction of loading during the trial. Cruciform specimens with centre welds are used in surveys when investigations are made to determine if constant principal stress direction be treated differently from those with variable directions. Other questions are in what extent known hypotheses are applicable for welds affected to multiaxial stresses. Boxbeam specimens are used in surveys affected to bending-torsional loading. In the following some clarity are given due to test specimens.

3.1.1 Shafts and pipe specimen

Figure 3.1 (a) to (d) gives example on how these specimens may look like. Most of the surveys with pipes are related to bending only, torsion only or combined bending and torsion with proportional or non proportional loading. It can also be a combination of tension and torsion in combination in the same extent that was mentioned earlier. Some investigators prefer square hollow sections affected to combinations of bending and torsion proportional or non proportional loading. Then the loads can be varied in intensity so that different ratio appears between bending and torsion. This has different effects on the specimen. Square specimen shows crack initiation in the base material near corners when loaded with pure shear (torsion test). Pure shear caused by torsion test causes throat crack for pipe specimen. The shape of the specimen affected to same type of loading shows difference in failure. There are also tests made in pipes, Figure 3.1 (c), of same dimension welded to each other. The loading on such specimen follows the bending-torsion principle with non-proportional and proportional loading [28]. Shafts can be notched or un-notched, Figure 3.1 (b), from the beginning. The reason using notched specimen is that combined loading cases can be achieved. The specimen geometry and the loading configuration result not only in triaxial stresses and strains in the notch, but also three-dimensional stress-strain gradients [25]. The surveys with this type of specimen contribute to verify properties for base materials. The smooth specimen does not have the geometrical properties creating triaxial stresses and are therefore of interest.

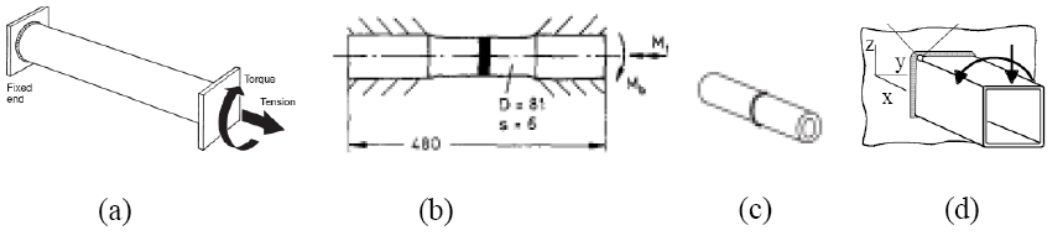

Figure 3.1 Examples on shaft and pipe specimen [25] and [28].

3.1.2 Cruciform specimen

This type of specimen is generally used for studying crack growth under biaxial stress conditions, see Figure 3.2. A three dimensional cruciform specimen with six arms was also designed. Severe stress raisers are present in this type of specimen making it possible to gain a homogenous strain or stress distribution [25]. Cruciform specimen with centre welds are used in surveys studying stress concentrations, change in ductility and geometry effects. The method is commonly used in mechanical industry investigating temperature effects and complex stresses on parent materials [32]. There are also variations in how these specimens are manufactured, see Figure 3.3 [21].

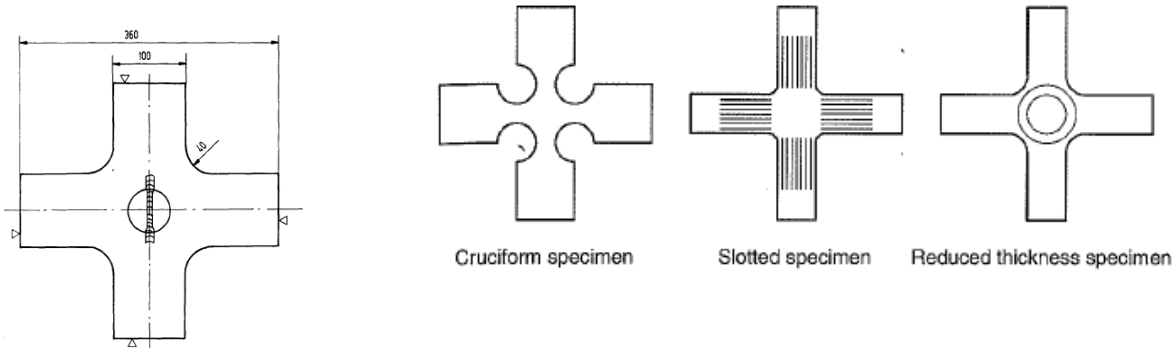

Figure 3.2-3.3 Cruciform specimen for testing of weld (left) [25], and for parent metal (right) [21].

3.1.3 Boxbeam specimen

These specimens, see Figure 3.5-3.6, are normally tested to bending, torsion and combined bending-torsion with proportional and non-proportional loading. Phase difference in non-proportional loading is generated by different frequencies for the bend and torsion load. Earlier studies with such specimens showed that no pronounced difference between proportional and non-proportional loading was found. The study included limited experimental data which must be considered [28].

Figure 3.5-3.6 Different types of box beams specimens [28].

3.2 Loading and test setup

As there been mentioned earlier under Section 3.1.1 the loading vary depending on test specimen. This is mainly due to what information or properties are analysed.

3.2.1 Welded pipe specimen

Welded pipes to steel plates are normally affected to bending only, torsion only or combination of bending-torsion loading. Some investigations are made on the basis of tension only, torsion only and the combination of these. The normal procedure is checking different ratios between the mentioned loads. These test causes failure in the welding, which normally appears in the weld toe. Before testing pipe specimens they may be stress relieved. Stress relieved means that the specimen has been reheated to reduce residual stresses caused by the welding procedure [28]. The change in ratio between the loads affects the specimen in different ways.

3.2.2 Notched/un-notched shaft specimen

To choose loading for shaft specimen varies from case to case. Smooth specimens are tested under bending as well as under torsion to provide baseline data. Observed fatigue life data are used to evaluate several multiaxial fatigue life prediction models, including a critical plane method, a von Mises approach, and an energy-based approach. Notched specimens (bar with circular notch) works as stress concentration, tested under combined bending and torsion in and out-of-phase loading. The aim with such a test is to observe crack initiation and small crack growth in the notch [32]. Four independent loads can be applied on a shaft, Tension, torsion, and two bending moments M_x and M_y. The maximum stresses on a shaft due to tension and torsion loading are located in an annual ring at the base of the stress concentration [10]. Bending and tension loads will produce a σ_z. A stress σ_o will also be produced due to notch constraint. Torsion moments result in a shear stress $\tau_{\theta z}$, see Figure 3.7 [10].

Fatigue life prediction is not of that importance in these testes. Both notched and un-notched specimens are used to give information regarding a base material and its ability to resist fatigue cracks. There are also some disadvantages with notched specimen. The change in notch geometry during a test modifies the original stress state [25].

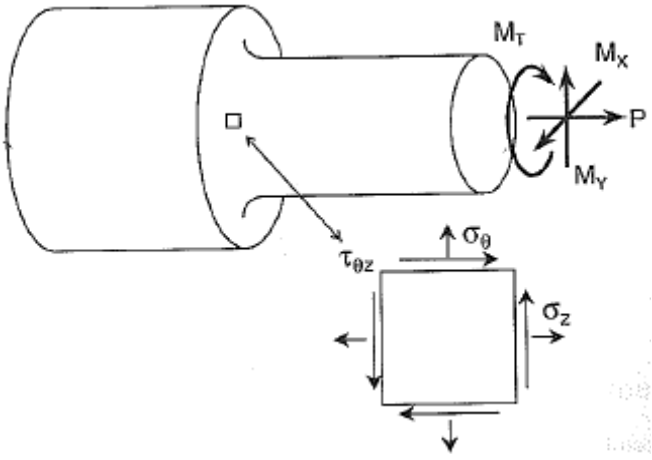

Figure 3.7 The loading of a notched shaft specimen [25].

M_τ, M_x, M_y = Moment

P = Normal force

σ_θ , σ_z = Normal stresses

$\tau_{\theta z}$ = Shear stress

3.2.3 Cruciform specimen

Cruciform specimen like Figure 3.2 with welding is normally affected by loading in two of the four legs. The applied loading is tension of some magnitude and can be varied in each direction. The loading can be alternated to cause non-proportional loading [27].

3.2.4 Box beam specimen

Loading modes for box beams are normally bending, torsion and combined bending-torsion proportional and no-proportional. Phase differences can be produced by using different frequencies bend and torsion loading. This leads to cumulative damage problem, because smaller stress variations will be added to the main cycle [28].

3.3 How test results are expressed

Test results from the different multiaxial fatigue test that have been done during the history are often expressed in a logarithmic diagram. On the x-axle the number of cycle to failure are expressed and on the y-axle the applied stress or force are expressed. In Figure 3.8 the test results on different welded specimens are shown. From this type of diagram the S-N curves are later developed.

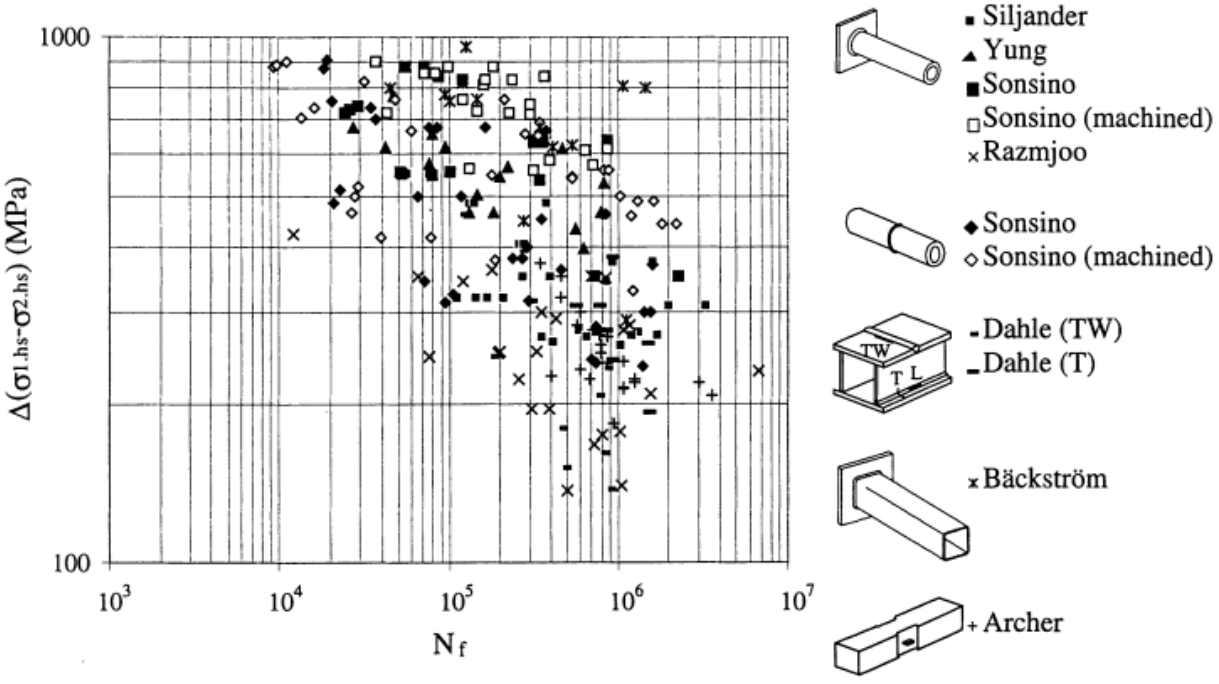

Figure 3.8 Example of how fatigue test results can be expressed [28].

Another more unusual way to display the test result in a diagram is to plot the cycles to failure as a function of the equivalent strain. In Figure 3.9 the test result from shaft

specimens subjected to axial torsion, compression and reheating is shown. This method to show the results is more common for multiaxial testing with different temperature ratios and is therefore more passable for the manufacturing industry and is not so useful in the civil engineering [32].

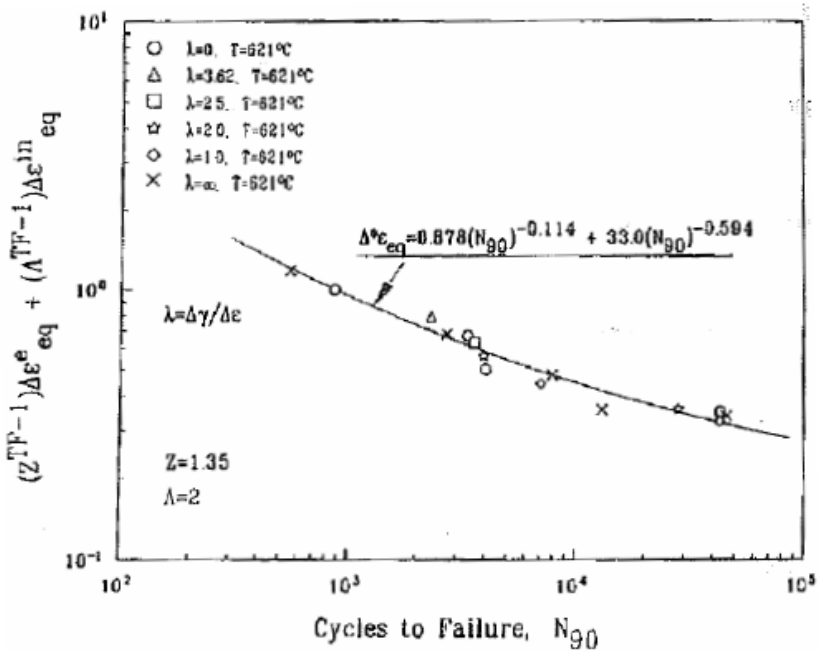

Figure 3.9 Fatigue test results, the cycle to failure plotted as a function of the equivalent strain [32].

In [20] McDiarmid use another method to display the test result, he plot the shear stress amplitude as a function of the maximum normal stress. In Figure 3.10 McDiarmid's test results are shown and the reason for this type of plotting is to show how the fatigue life between the two crack cases A and B.

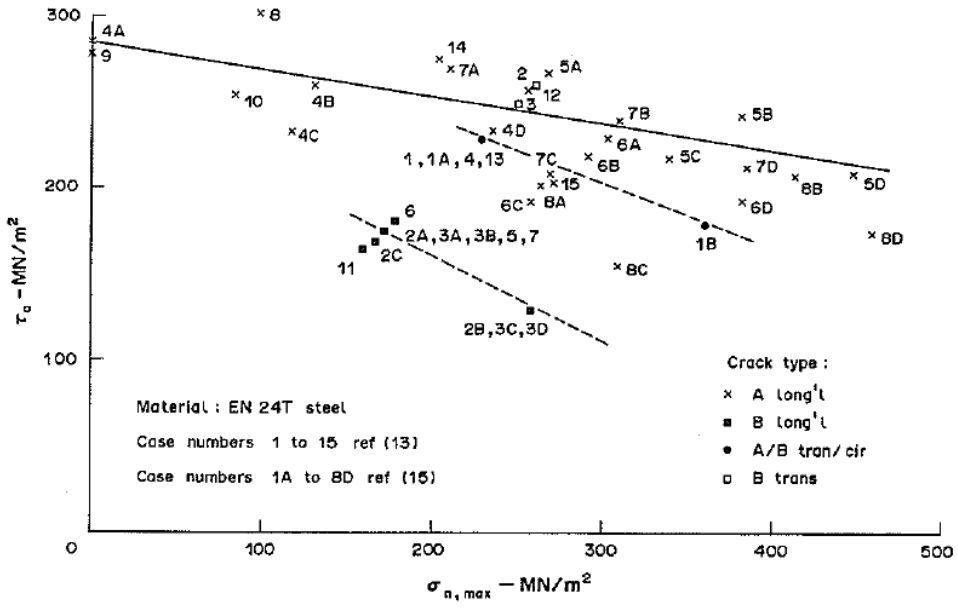

Figure 3.10 Shear stress amplitude as a function of the normal stress [20].

3.4 What kind of things have been studied

Some things that have been studied within multiaxil fatigue are phase difference between shear and normal stresses, proportional and non-proportional loading and the effect of mean stress.

McDiarmid have in [1] studied thin wall steel specimens subjected for loading under different phase angles under ratios and also the effect of mean stress was investigated. The total number of tested specimens was 60.

Sonsino have in [27] studied welded cruciform, flange-tube and tube-tube specimens subjected for loading in- and out-of-phase, in-phase difference 90°, proportional and non-proportional loading. In these tests Sonsino used 125 specimens.

In [28] Bäckström and Marquis have done an overview of test series carried out of different researchers in multiaxial fatigue there the stresses are proportional and non-proportional. In Table 3.1 a summary over these tests are shown. The tested specimens have all welded geometry.

Test results	Specimen (No.)	Bending or tension only (No.)	Torsion only (No.)	Bending/tension and torsion proportional (No.)	Bending/tension and torsion non-proportional (No.)
Archer	27	1	10	5	11
Yung and Lawrence	18	5	2	11	0
Siljander	40	10	10	10	10
Razmjoo	29	7	8	7	7
Bäckström	22	5	4	9	4
Dahle	53	6	22	21	4
Total	189	34	56	63	36

Table 3.1 An overview of different test series carried out of different researchers.

3.5 Load introduction

The type of loading on a specimen has a large effect regarding to fatigue. From literature like [1] the following advice are held. – In order to determine the resulting fatigue strength of the material under complex loading, one must consider not only the various mean and alternating stress components and the number of cycles, but also the time –dependence of the stress wave form, the frequency, and the phase-difference between stress components. One must remember that different professions chose loadings which give answers on fundamental questions of their interest. This can create a complication because adequate loads in machine industry not necessary have same interest for construction in civil engineering. There are also effects from welding to take in to account. From survey [2] interesting aspects about residual stresses was found. Maddox writes - Welding introduces residual stresses, which modify the mean stress experienced by a welded joint under fatigue loading. When residual stresses with loading interacts, the sum of stress can increase or decrease depending on circumstances. As one understands the subject has many aspects to overview. In the following, explanations are done to bring clarity in how different loading affects steel details.

3.5.1 Complex loading

Complex loading is normally caused by combined or multi-axial loading. To give an example on such a situation torsion combined with normal force can be mentioned. Several combinations are possible where the idea is that the loads shall act on more than one geometrical axis. In some reports the word biaxial load is used which means that the load is acting on two geometrical axes. This will be the case in most situations regarding to structural design for buildings.

3.5.2 Variable amplitude loading

In [1] describes this as loading applied to a component with variable amplitude. Many surveys show diagrams over stress changes over time. The amplitude can be of different shape and magnitude but also located with phase difference comparing to other stresses acting on the specimen at the same time. Tests with variable amplitude loading have shown shorter fatigue life than constant amplitude loading.

3.5.3 Proportional loading

Most design data have been obtained under unidirectional axial or bending loads. It is common for details in real structures to experience more complex loading. There for it is natural to use equivalent stress or interaction formula in conjunction with design data.

For some products the loading is proportional and the degree of multiaxility is low. In such cases quite simple solutions for equivalent stress has been chosen. Problems appear when the principal stress acts with an inclination relatively to the weld [4].

3.5.4 Non-proportional loading

In some constructions involving moving loads like cranes and bridges the various stress components fluctuate in different ways. The stress components may be out-of – phase and the number of cycles of each stress components may be different. Therefore it is questionable if a universal equivalent stress criterion could be found. Fatigue calculation methods using principal stress range based on non-proportional loading can lead to non-conservative life predictions [4]. The two most widely used equivalent stresses are von Mises stress σ_e, expression (3.1) and the maximum principal stress σ_1, see expression (3.2) [5]. This means that it is of great importance to guarantee what load effects are acting on the construction.

It is also of great interest to know if stresses in or out-of-phase cause the largest fatigue damage. When applied normal and shear stress acts in-phase the resulting maximum principal stress range has a higher value than when they act out-of-phase, see Figure 3.13. It will be obvious that in-phase loading should be more damaging than out-of-phase due to the principal stress range. However the opposite proves to be the case [5].

$$\sigma_e = \left(\sigma_x^2 - \sigma_x \cdot \sigma_y + \sigma_y^2 + 3\tau_{xy}^2\right)^{1/2} \tag{3.1}$$

$$\sigma_l = \frac{\sigma_x + \sigma_y}{2} + 0.5\left\{\left(\sigma_x - \sigma_y\right)^2 + 4\tau^2{}_{xy}\right\}^{0.5} \qquad (3.2)$$

σ_e = Equivalent nominal stress

σ_x = Nominal normal stress in x-direction

σ_y = Nominal normal stress in y-direction

σ_l = Maximum nominal principal stress

τ = Nominal shear stress

τ_{xy} = Nominal shear stress in x, y plane

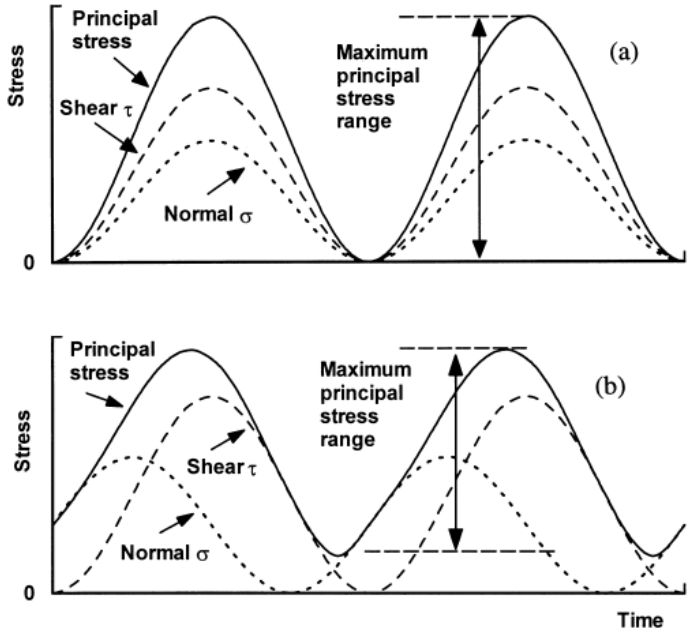

Figure 3.13 Showing in and out-of-phase loading [5].

Under multiaxial fatigue loading the fatigue assessment of welded attachments becomes more complex because when welded ductile steels are subjected to non-proportional loading the fatigue damage increases compared to proportional loading [7]. This situation is a consequence of the interaction between material ductility and the change during the load cycle of the maximum principal stress direction [7].

The combination of bending and torsion with a phase difference of 90˚ causes a reduction of the fatigue life compared to in-phase loading. This seems to be the case for booth variable and constant amplitude loading, see Figure 3.14 and 3.15 [6]. All Figures and loadings are related to welded constructions and confirm what has been said earlier.

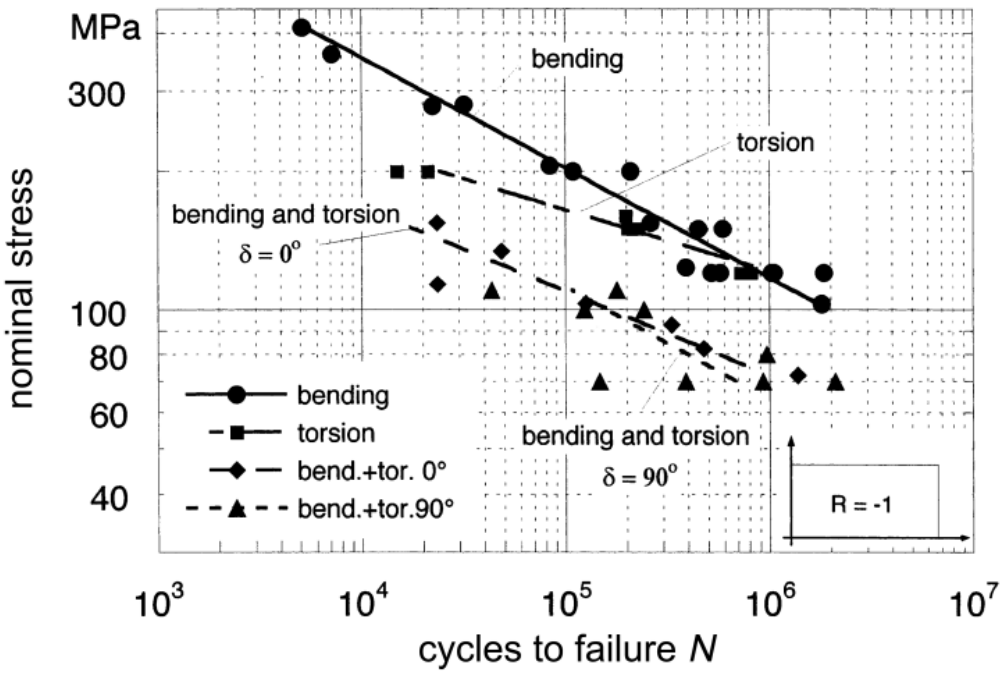

Figure 3.14 Constant amplitude [6].

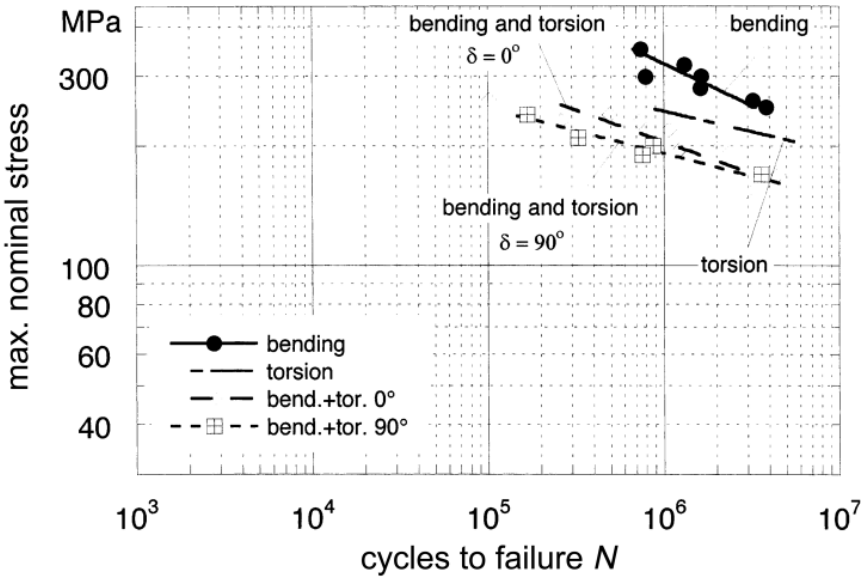

Figure 3.15 Variable amplitude [6].

4 Examination of some design methods

There are some methods that are more applicable than others in the field of civil engineering. In the following an inventory of suitable methods from what have been found and presented earlier is done. Methods that are presented earlier but are not included in this Section are consequently not representative or may be so complicated that they are deemed not to be suitable for hand calculations or civil engineering applications.

4.1 Hot-spot method

The hot-spot method has several advantages compared to other methods. For example the method is applicable when there is no clearly defined nominal stress or when the connection differs from the detail categories provided by the design codes for fatigue calculations based on nominal stress. Even cases when misalignment exceeds the limits specified by the code (which makes nominal stress calculations incorrect), the hot-spot method can be applied [35]. As mentioned earlier under Section 1.10.2 and 2.14.3, the fatigue stress is generally measured in the specimen near the point of crack initiation [4]. The crack initiation point is normally located at the weld toe or in the vicinity of a weld end. The Hot-spot method is included in some design codes for the purpose of fatigue life calculation. The difficulties encountered when using the hot-spot method may be the way of determining the stresses at weld toe from finite element models. Eurocode 3 prescribe that maximum principal stress in the parent material adjacent to the weld toe is the hot-spot stress. Local stress concentration affects needs not to be considered. These are included in the detail categories in annex B in Eurocode 3. The stress shall be calculated as expression (4.1):

$$\gamma_{Ff} * \Delta\sigma_{E.2} = K_f * (\gamma_{Ff} * \Delta\sigma_{E.2}) \qquad (4.1)$$

where: K_f is the stress concentration factor.

The variables in parenthesis are the design value of the stress range. There are no conditions denying the use of the method on multiaxial loaded specimens. The way of calculating the hot-spot stress also differs between various codes and recommendations. The normal way to solve such problem is to determine the stresses by using finite element calculation. It is recommended that the hot-spot stresses are determined as the stresses perpendicular to the weld toe [4]. Normally there is no information in codes on how the finite element model should be constructed. Fortunately there are recommendations given by, for example Niemi [4] among others on how this can be properly done. One recommendation is that the hot-spot stress should be determined from the tangent drawn between the points 0.4t and t, see Figure 4.1 [24]. Observe that this recommendation is not present in Eurocode 3. In Eurocode 3 the hot-spot method can be used also in combination with principal stress. This differentiates the calculation procedure due to principal stress method in general which is based on nominal stresses, where the affect of stress concentration is not taken into account. Shear and tensile stress are solved by finite element method and used in calculation to define principal stress. The principal stress can also be obtained from the finite element calculation directly. The use of hot-spot stresses may differ for codes. For example in the Swedish national code BSK-99 hot-spot stresses are not

mentioned at all. Codes allowing hot-spot approach are, for example, EC 3 and IIW [39].

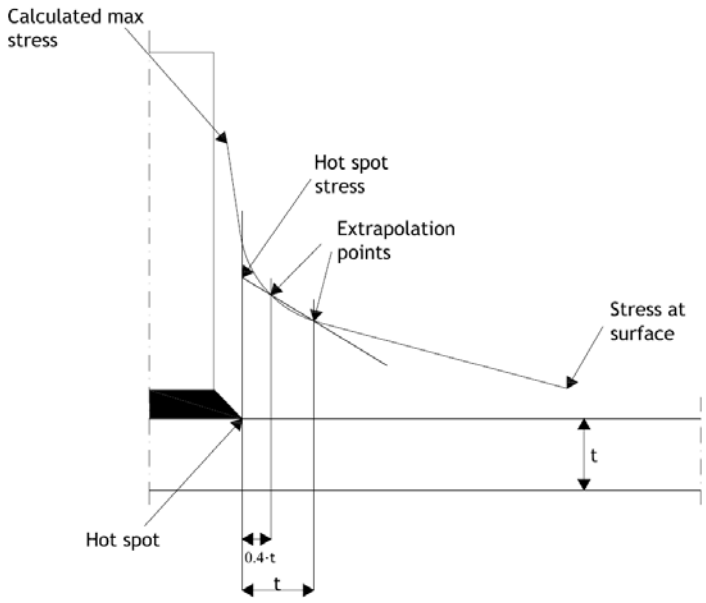

Figure 4.1 Derive hot-spot stress.

Designing with hot-spot method may involve some problems because of the poor guidance in codes. For example in EC 3 there are given S-N curves which should be used when the hot-spot stresses are used. All these S-N curves assume stress perpendicular to weld. As long as the details are affected by loading corresponding to the S-N curves in annex B there is generally no problems. The difficulty begins when principal stress from hot-spot calculation is used as design value. One important issue is that stresses creating principal stress may be in-phase or out-of-phase. This would probably affect the fatigue life in a considerable way. Also the S-N curves will be affected, at least the slope that corresponds to the fatigue class. EC 3 gives a note that local stress concentration effect is included in the detail categories in annex B. In EC 3 there is a restriction on the use of principal stress for fatigue calculation based on nominal stress approach, that the direction of this stress in relation to the weld does not change significantly (what is considered significant in this respect is, however, not specified). The cause to inconvenience in hotspot method based on principal stress lies in the procedure when principal stress is derived. In context this means that each predicting method based on principal stress will get the same problem. The hot-spot method may be used on the parent metal only. Hot-spot stress is calculated at the weld toe of fillet and butt welds, and corresponds to fatigue failure in parent metal. Root cracking on the other hand is related to failure of the weld itself and must be considered by different methods [35]. There are also limitations regarding the stress direction. Stresses should act mainly perpendicular to the weld length. Stresses parallel with the weld should be solved by a nominal stress approach [35]. Mutliaxial stresses act in- and out-of-phase with arbitrary direction depending on the loading situation. Such loading may lead to complications depending on if the hot-spot principal stress is used or if the stress components perpendicular and parallel to the weld are resolved. The damage is then calculated with Palmgren-Miners rule with appropriate choice of detail class. Here it should be mentioned that hot-spot stress is

combined with hot-spot detail class. In the same way nominal stress is combined with a detail class for nominal stress. This should not be any problem because there is no mixing in detail classes for hot-spot or nominal stress and should result in a relevant prediction. If principal stress is used, derived from hot-spot method, there will appear problems with detail class. In such case parallel and perpendicular stress are combined to one stress, the principal stress, and compared with one detail category. As was mentioned earlier S-N curves assume stress perpendicular or parallel to weld. If the principal stress has an angular towards the weld this criterion will not be fulfilled. The maximum principal stress does not necessarily agree with the maximum stress range in a detail [41]. In such a case, the stress considered as structural hot-spot stress is the larger of the absolute values of the following [41] see Figure 1.15 under Section 1.10.2.

- The principal stress with largest stress range if this is within +/- 60˚ of the normal to the weld toe
- If the principal stress with largest range is outside the above range, the stress component normal to weld toe, $\sigma_{perpendicular}$, or the smaller principal stress σ_2 which ever shows the larger range.

In context this means that the designer should choose the largest value of principal stress in range or if a larger stress is discovered outside this range, then this one should be chosen. When the hot-spot stress has been calculated, a suitable detail category should be chosen according to EC 3. The number of cycles should then be calculated by expression (4.2) or (4.3) by EC 3. If the calculated numbers of cycles are less than 5 million cycles, expression 4.1 should be used. Otherwise, expression (4.3) is valid.

$$N_i = 5 \times 10^6 \left[\frac{\Delta\sigma_D / \gamma_{Mf}}{\gamma_{Ff} \Delta\sigma_i} \right]^3 \tag{4.2}$$

$$N_i = 5 \times 10^6 \left[\frac{\Delta\sigma_D / \gamma_{Mf}}{\gamma_{Ff} \Delta\sigma_i} \right]^5 \tag{4.3}$$

Eurocode 3 do not present curves for principal stress for a given stress direction. Without S-N curves it becomes impossible to fulfil fatigue life prediction. For cases of a considerably biaxial stress state the strain ratio $\varepsilon_2/\varepsilon_1$ should be taken into account using expression (4.4) [41]. From expression (4.4) the hot-spot stress may then be calculated. It should be mentioned that Eurocode 3 does not give such recommendations given by [41].

$$\sigma_{hs} = E\varepsilon_1 \cdot \frac{1 + \nu \frac{\varepsilon_2}{\varepsilon_1}}{1 - \nu^2} \tag{4.4}$$

ε_2 = strain parallel to weld toe

ε_1 = strain perpendicular to weld toe

E = Young's modulus

V represents Poisson ratio.

4.1.1 Modified hot-spot method

This method has been presented by Susmel and Tovo [24]. It is not included neither in EC 3 or IIW. To correctly use hot-spot stresses when predicting multiaxial fatigue strength of welded details, they have to be always resolved into two stress components [24]. One component is perpendicular and one is parallel to weld toe. The component perpendicular to weld causes mode I crack propagation. The other component, parallel to weld, causes mode II propagation [24]. The different fracture modes are shown in Figure 4.2 (a) to (c). Mode II in Figure 4.2 (b) can be neglected if the stress is not singular [24]. The stresses are solved by finite element analysis in each direction, where σ indicates stresses perpendicular and τ indicates stresses parallel to weld, see Figure 4.2 (c). To finally get the hot-spot stress there is a certain routine to be used. The hot-spot stress is defined as the tangent drawn between the points 0.4t and t as shown in Figure 4.1 [24]. The way to achieve shear stress is done in similar way. There have been studies made with modified Wöhler curves when these have been correctly weighted by stresses in mode I and mode II. It is possible to predict both crack initiation and fatigue lifetime due to this method [24].

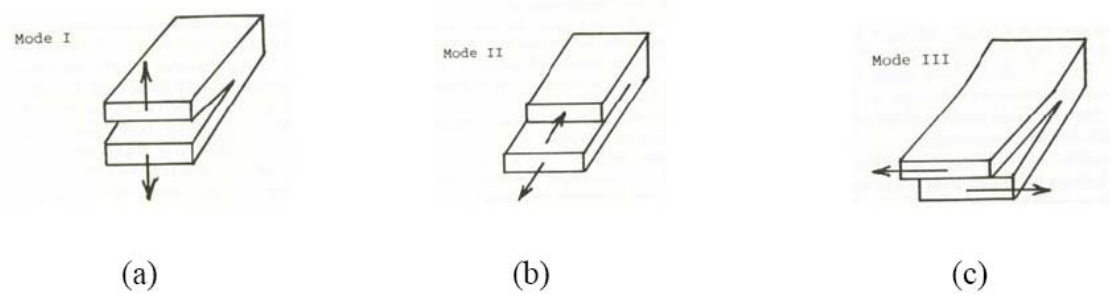

Figure 4.2 (a) to (c) showing different cracking modes.

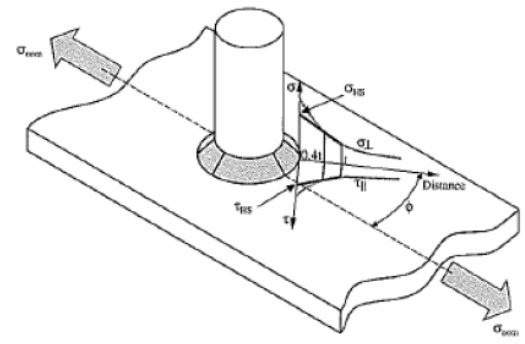

Figure 4.3 Derive hot-spot stress [24].

4.1.2 Interaction Formulas

Many codes have interaction formulas for calculation the fatigue lifetime under multiaxial loading conditions. The advantage with interaction formulas is that they are easily performed with hand calculation. The method can be applied to both cracking in welds and in the parent metal. Codes like Eurocode 3, Finnish standard SFS 2378 and the Swedish standard BSK-99 are examples where multiaxial fatigue situations are treated with interaction formulas. Weld toe failure is a parent metal failure while root cracking is related to weld failure. Even complete non-welded details are presented in the interaction method which makes it general in use.

Eurocode 3 declares that in the case of combined stress range $\Delta\sigma_{E.2}$ and $\Delta\tau_{E.2}$ the expression (4.5) should be fulfilled.

$$\left(\frac{\gamma_{Ff}\Delta\sigma_{E.2}}{\Delta\sigma_c/\gamma_{MF}}\right)^3+\left(\frac{\gamma_{Ff}\Delta\tau_{E.2}}{\Delta\tau_c/\gamma_{MF}}\right)^5\le 1.0 \qquad (4.5)$$

Expression (4.5) is based on Palmgren-Miners rule, which is presented in expression (4.6).

$$\left(\frac{\Delta\sigma}{\Delta\sigma_c}\right)^3+\left(\frac{\Delta\tau}{\Delta\tau_c}\right)^5\le 1.0 \qquad (4.6)$$

There are several design codes using the same principles for calculating the fatigue damage under multiaxial fatigue loading. There are, however, some differences between the codes. The parameter 1.0 that regulates the maximum value of the sum of the damage in Eurocode 3 has value of 1.23 in the Finnish standard SFS 2378. The International Institute of Welding proposes that the value 0.5 should be used instead of 1.0 for out-of-phase loading and 1.0 for in-phase loading. Most designers are familiar with the fact that Eurocode 3 uses slope m=5 for details affected by shear stress. The Finnish code uses slope m=3 in the case of shear, as well as for normal stress. Such differences can be one reason why the sum of damage parameter is higher in the Finnish code comparing to Eurocode 3, for example. Also the fact that different codes use different partial safety factors also makes a direct comparison between the different codes more difficult. Bäckström [36] declares that the value is purely empirical. The International Institute of Welding recommends 0.5 because studies have shown that Eurocode 3 can give results that are non-conservative. This recommendation is valid if the loading spectrum is not close to constant amplitude. It is a good point to take the load effect into consideration. However many studies has clearly declared that out-of-phase loading is more severe than in-phase loading with respect to the fatigue life. In earlier drafts of Eurocode 3 there are some instructions regarding fatigue calculations under multiaxial loading conditions. If the shear stress is less than 15 % of the equivalent nominal normal stress, the effect of the shear stress on the fatigue damage can be neglected. In the Swedish code BSK 99 the interaction formula is as shown in the expression (4.7). For some details, the multiaxility is already included in the C-value, given by the BSK 99 (i.e. inherent in the test results used to derive the specific C-value or S-N curve). In this case, the requirement of fulfilling expression (4.7) can be overseen.

$$\sqrt{\frac{\sigma_{rdII}^2}{f_{rdII}^2}+\frac{\sigma_{rd\perp}^2}{f_{rd\perp}^2}+\frac{\tau_{rdII}^2}{f_{rvd}^2}+\frac{\tau_{rd\perp}^2}{f_{rvd}^2}} \le 1.10 \qquad (4.7)$$

When checking detail categories for Eurocode 3, SFS 2378, BSK and recommendations given by International Institute of Welding differences are obtained in the calculated fatigue strength. One reason for the difference is that the different codes use somewhat different C-values for the same detail sometimes. Some examples on the difference between the design codes are shown in Figure 4.4.

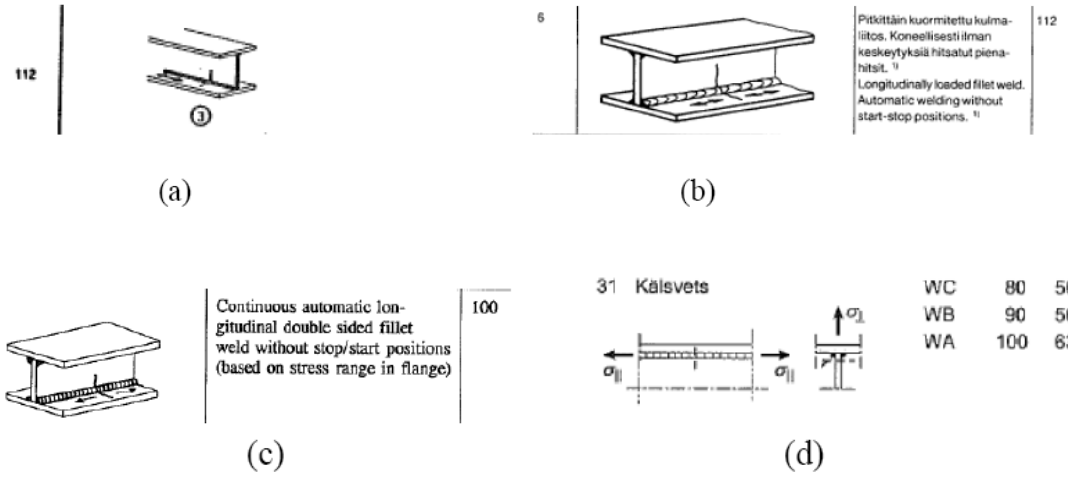

Figure 4.4 (a) to (d) different detail categories from EC 3 (a), SFS 2378 (b), IIW (c) and BSK 99 (d).

Figure 4.4 shows how the category can vary for a detail comparing different design code recommendations. The Swedish national design code has class WA -WC. These factors consider welding class, which regulates transition between weld and adjacent material. Bäckström and Marquis [36] give one explanation on design life calculations contain a degree of conservatism. This is usually 5 % failure probability based on a two-sided confidence interval of 75 %. Larger deflection between detail classes can be found. It has been stated [36] that classes may differ up to 50% or more. One shall also remember that all details are made to predict fatigue life on details affected to non multiaxial stresses. However they are used for multiaxial details with different result. In the following Section earlier made tests are analysed to bring clarity in agreement with real fatigue life.

4.1.3 Modified Wöhler curve method

The Modified Wöhler Curve method, also known as the modified S-N curve, is a method proposed by Susmel and Lazzarin to estimate the multiaxial fatigue life for steel components. The method is described in [40] and can be applied to both smooth and notched components subjected for either in-phase or out-of-phase multiaxial cyclic loading. The basic idea with the method is that the crack initiation occurs on the plane on which the shear stress amplitude reaches its maximum value, this plane is called: the critical plane. Susmel and Lazzarin validated the method with data

obtained from the literature and they found out that the accuracy in the method was significantly better than other prediction criteria like McDiarmid and Gough. Later Susmel and Tovo, in [7] extended the modified Wöhler curve method to fit welded joints subjected to both in-phase and out-of-phase multiaxial cyclic loading. One of the modifications and assumptions required was that the method should be based on that the crack initiation is mode II and it occurs on the plane where the shear stress amplitude, $\Delta\tau_n/2$, has its maximum value. The crack initiation is also influenced by the stress component normal to this plane, σ_n. From this the stress ratio, ρ_w, can be calculated as shown in expression (4.8). This stress ratio affects the position of the S-N curve, and thus also the predicted fatigue life.

$$\rho_w = \frac{\Delta\sigma_n/2}{\Delta\tau_n/2} = \frac{\Delta\sigma_n}{\Delta\tau_n} \tag{4.8}$$

$$\Delta\sigma_n = \frac{\Delta\sigma_x}{2}$$

$$\Delta\tau_n = \sqrt{\left(\frac{\Delta\sigma_x}{2}\right)^2 + \Delta\tau_{xy}^2} \qquad \text{for in-phase loading}$$

$$\Delta\tau_n = \Delta\tau_{xy} \qquad \text{for out-of-phase loading}$$

$\Delta\sigma_x, \Delta\tau_{xy}$ = the nominal stresses

Figure 4.5 Shows a schematic log-log diagram of how the stress ratio influences the S-N curves. On the y-axis is the shear stress range and on the x-axis is the number of the cycles.

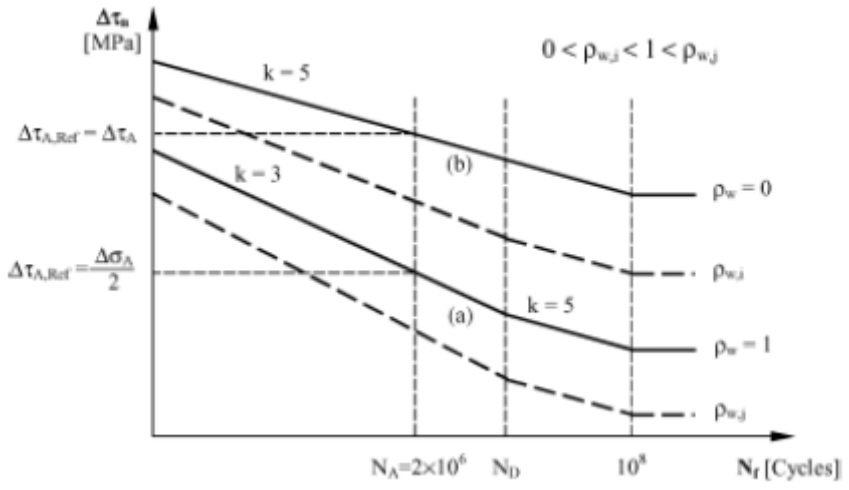

Figure 4.5 Modified Wöhler diagram for welded connections [7].

The position of the fatigue curve in the diagram can be determined from the reference stress values for different structural details given in design codes, for example EC 3. In Figure 4.5 curve (a), with the ratio equal to 1, is the uniaxial standard fatigue curve

and the curve (b) in the same Figure with the ratio equal to 0, is the standard curve for torsion fatigue. From Figure 4.5 can it be noticed that with increasing ρ_w, the modified Wöhler curves moves downwards. An assumption can be made that the relationships between the ρ_w versus the slope k and ρ_w versus the reference shear stress for different cycles, $\Delta\tau_{A,Ref}(\rho w)$, can be expressed as simple linear functions. The reference shear stress and the slope k can be calculated for multiaxial situations with expression (4.9) and (4.10) in the cycle region $N_f < N_D$, see Figure 4.5.

$$\Delta\tau_{A,\mathrm{Re}f}(\rho_w) = 2\left[\left(\frac{\sigma_A}{2} - \tau_A\right)\rho_w + \tau_A\right] \tag{4.9}$$

σ_A, τ_A = The reference stress at 2 million cycles, provide in design codes.

$$k(\rho_w) = 2\left[k(\rho_w = 1) - k(\rho_w = 0)\right] \times \rho_w + k(\rho_w = 0) \tag{4.10}$$

$k(\rho_w = 1)$ = Is the inverse slope (k) of the bending fatigue curve.

$k(\rho_w = 0)$ = Is the inverse slope (k) of the torsional fatigue curve.

And if the cycle region instead is $N_D < N_f < 10^8$ the expression (4.9) has to be rewritten as expression (4.11).

$$\Delta\tau_{A,\mathrm{Re}f}(\rho_w) = 2\left[\left(\frac{\sigma_D}{2} - \tau_D\right)\rho_w + \tau_D\right] \tag{4.11}$$

σ_D, τ_D are the nominal stresses at N_D cycles, in EC 3 N_D is equal to 5 million cycles.

By using these formulas the fatigue life can be estimate for constant amplitude multiaxial loading, by using following equations:

if $N_f < N_D$ use expression (4.12)

$$N_f = \left[\frac{\Delta\tau_{A,\mathrm{Re}f}(\rho_w)}{\Delta\tau_n}\right]^{k(\rho_w)} \times N_A \tag{4.12}$$

if $N_D < N_f < 10^8$ use expression (4.13)

$$N_f = \left[\frac{\Delta\tau_{A,\mathrm{Re}f}(\rho_w)}{\Delta\tau_n}\right]^{5} \times N_D \tag{4.13}$$

4.1.4 Principal stress method

This method has been discussed shortly under Section 1.10.1. In the design principle proposed by Eurocode 3 is based on the nominal stress. Nominal stresses do not consider local stress raising effects on a specimen. As there have been mentioned earlier such stresses can be determined by using ordinary handbook formulas. In the simplest form nominal stress can be determined by dividing a known force by the

area. There are many ways of using nominal stresses in fatigue calculations. As was mentioned in Section 4.2.2 interaction formula calculation is one possible way. All calculation methods using nominal stresses can be called nominal stress methods. In this Section more focus has been given the use of von Mises formula when determine principal stress caused by two stress components. The principle stress can be explained as some kind of resultant stress acting in a specific direction acting on a plane where shear stress is zero. Expression (4.14) and (4.15) give the equivalent stress and maximum principal stress by von Mises [38] (σe is equivalent stress).

$$\sigma_e = \left(\sigma_x^2 - \sigma_x\sigma_y + \sigma_y^2 + 3\tau_{xy}^2\right)^{1/2} \tag{4.14}$$

$$\sigma_1 = \frac{\sigma_x + \sigma_y}{2} \pm 0.5\left\{\left(\sigma_x - \sigma_y\right)^2 + 4\tau_{xy}^2\right\}^{1/2} \tag{4.15}$$

The former formula has been used in fatigue design codes for pressure vessel for the principle stress in (4.15) is more common in structural engineering applications [5]. Eurocode 3 allows the use of principal stress for fatigue prediction calculation. There is however no recommendations as to which fatigue class (S-N curve) should be used with the principle stress for example, the following text can be found in EC 3:

At locations other than weld throats, if the normal and shear stresses induced by the same loading event vary simultaneously, or if the plane of the maximum principal stress does not change significantly in the course of a loading event, the maximum principal stress range may be used.

Also in EC 3, the following can be found:

If the plane of the maximum principal stress does not change significantly in the course of loading event, the maximum principal stress range may be used.

The first problem is what is considered to be *significant* concerning the change in direction of the principle stress. The second problem is what formula should be used for calculating number of cycles to failure. It should be mentioned that the text refers to load combinations of normal and shear stress ranges. Here comes a complication in the method. As there have been mentioned in Section 4.2.2 "interaction methods" detail categories are used predicting fatigue life. It should be obvious that calculating a principle stress where the both acting stress components have some magnitude creates a larger principal stress than one of the components alone, see Figure 4.6. The fatigue damage is based on stress range and should therefore be derived from the principal stress. The stress range which is defined as $\Delta\sigma$ =stress range = (σ_{max} - σ_{min}) may be a contributed factor to error. This is because the principal stress is calculated due to von Mises formula (for details in civil engineering), sees expressions (4.15), which contain a square root and generates two possible solutions. It is of great importance that booth roots are tested in analysis to derive maximum stress range before the number of cycles to failure can be calculated, see Figure 5.5 and 5.4 in Section 5.3). The most rational way to calculate number of cycles to failure using principal stress should be by expression (4.16) to (4.18) taken from EC 3. Expression (4.16) is used to calculate cycles to failure regarding to shear stress. Expression (4.17) and (4.18) treats damage due to normal stress. One important factor not to be forgotten is that codes generally use stress range as damaging factor in fatigue

calculations. Figure 4.6 (b) shows how the principal stress range decreases in out-of-phase loading. The consequence of such behaviour results in a longer fatigue life. This means in reality that the detail should last longer before failure. The calculation of the fatigue under out-of-phase loading situation may thus be overestimated when principal stress is used. Maddox [5] writes: "*One aspect which is known to be potentially unsafe is the method of assessing complex loading situations, particularly those in which the principal stress change during the fatigue load cycle*". Further on, in the same report the following can be found: "*It will be observed that for same applied normal and shear stress ranges, the maximum principal stress is smaller for non-proportional loading, suggesting that it should be less damaging than for proportional loading, the opposite proves to be the case*". Using S-N curves obtained under uniaxial loading with principal stress seems to potentially generate incorrect results. The fatigue behaviour of details affected by multiaxial loading may not compatible with S-N curves obtained under uniaxial loading, which leads to incorrect predictions.

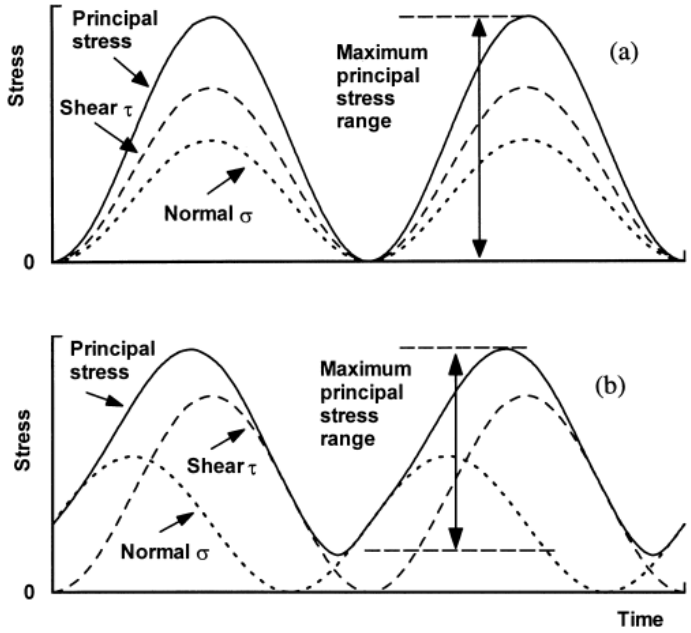

Figure 4.6 Showing principal stress from shear and normal stress in (a) and out-of-phase loading (b) [5].

$$N_i = 2\times10^6\left[\frac{\Delta\tau_c / \gamma_{Mf}}{\gamma_{Ff}\Delta\tau_i}\right]^5 \tag{4.16}$$

$$N_i = 5\times10^6\left[\frac{\Delta\sigma_D / \gamma_{Mf}}{\gamma_{Ff}\Delta\sigma_i}\right]^3 \tag{4.17}$$

$$N_i = 5\times10^6\left[\frac{\Delta\sigma_D / \gamma_{Mf}}{\gamma_{Ff}\Delta\sigma_i}\right]^5 \tag{4.18}$$

As was mentioned earlier there are no specifications given in EC 3 as to what S-N curve should be used with the principle stress in fatigue calculations of details under multiaxial fatigue conditions. In order to bring some clarity to the subject, let's consider a welded girder loaded in four-point bending. The web plate near the flange to web connection in the constant moment region is affected by normal (bending) stress only. EC 3 gives detail categories from 125 to 100 depending on the type and quality of welds and welding. The same specimen affected by shear is assigned fatigue class 100. When calculating principal stress there is no consideration taken as to which of the stresses (shear or normal) is dominant. If there were recommendations given in EC 3 on C-class and slope when principal stress method is used, it would be easier to calculate number of cycles to failure and choose the right expression (4.16) to (4.17). The formulas include factor 5×10^6 which corresponds to $\Delta\sigma_D$ stress range at constant amplitude fatigue limit by EC at this given cycles. Fortunately there is also further guidance given by [5] which can be used for the subject. For example there seems to be differences from tests when beams and flange tube specimens are tested.

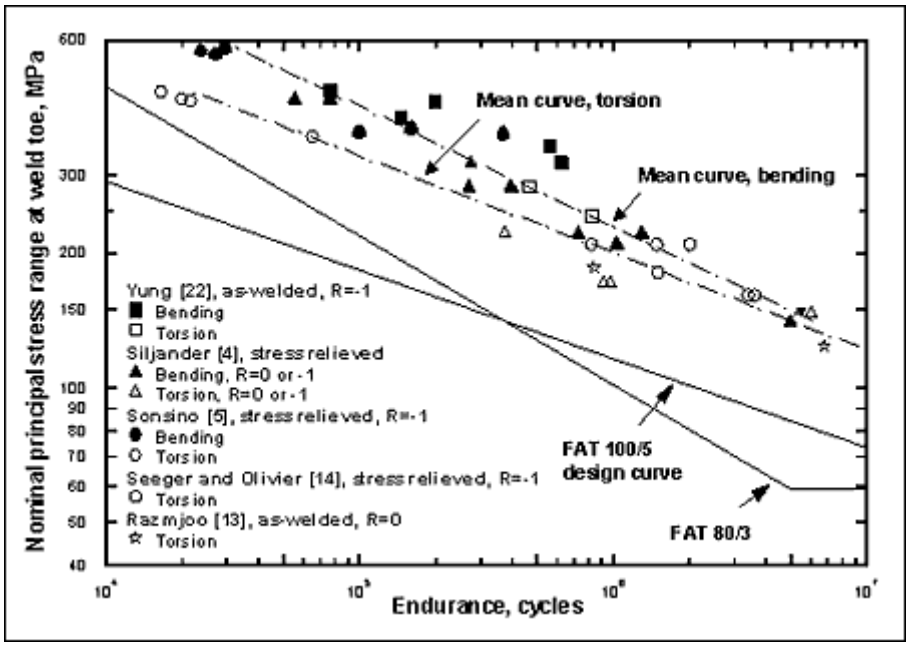

Figure 4.7 Showing test results for flange-tube welded joints failing from the weld toe, tested under bending or torsion [5].

From Figure 4.7 test results carried out on flange-tube welded joints shows that the mean curves of the fatigue life with respect to shear stress and bending stress have different slopes. This result shall be compared with the different fatigue classes in EC. Specimens affected by shear have an S-N curve with a slope m=5 while specimens affected by normal stresses have a curve with slope m=3. The test result seems to agree well with this. Therefore it may be accurate to separate specimens affected to shear and normal stress at least for flange-tube specimen failing from the weld toe. Maddox [5] has also presented results showing flange-tube and welded beam specimens subjected to in and out-of phase loading. In Figure 4.8 and 4.9 the results are shown for flange-tube and welded beam specimens. The result differs from each other in a quite prominent way. Slope m=5 seems to correspond best to results from flange-tube experiments while slope m=3 is more representative in the case of beam specimens. This kind of comparison is of great value for designers in civil

engineering. Bridge girders are better related to the beam tests and can therefore be treated in a similar way. Such girders can be exposed to non-proportional loading which also can be treated with the same slope of the S-N curve. As was mentioned earlier there are indistinct recommendations in EC 3 on what class to use in fatigue calculation using principle stress. From the experimental results presented in [5] it can be seen that class 80 with slope 3 can be used to describe the fatigue strength of beams under shear and normal stress conditions. In report [5] the following explanation has been given "*In contrast, the fatigue cracks in regions of combined bending and shear in beams loaded in bending were of the usual mode I type, propagating normal to the direction of the principal stress. Such a fatigue fracture mode would be expected to result in an S-N curve closer in slope to the FAT80/3 curve than the FAT 100/5 curve"*. On the other hand further results are needed to confirm these indications including more attention to the modes of fatigue failure obtained under complex loading [5].

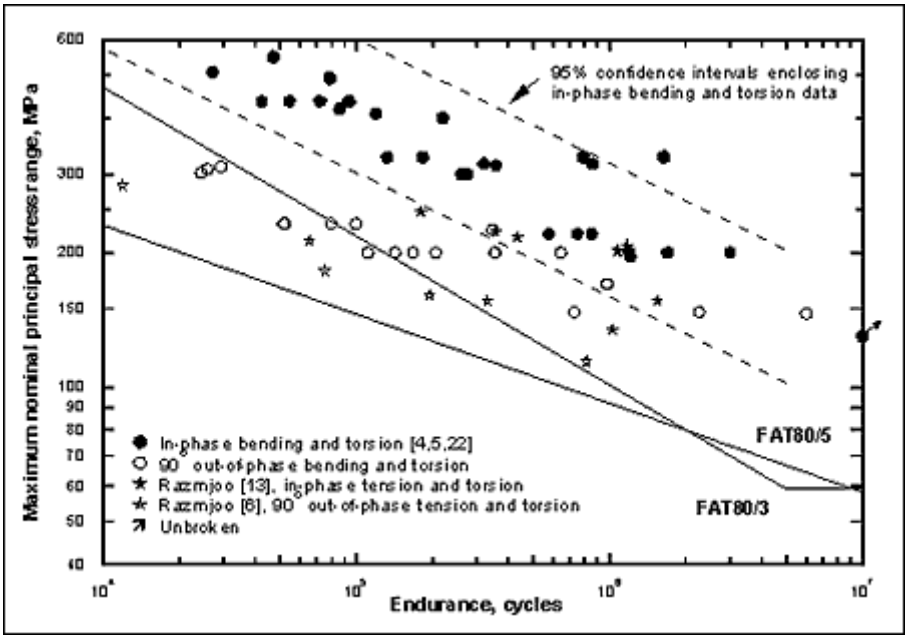

Figure 4.8 Fatigue test results for flange-tube welded joints failing from weld toe, tested under combined bending or tension and torsion loading [5].

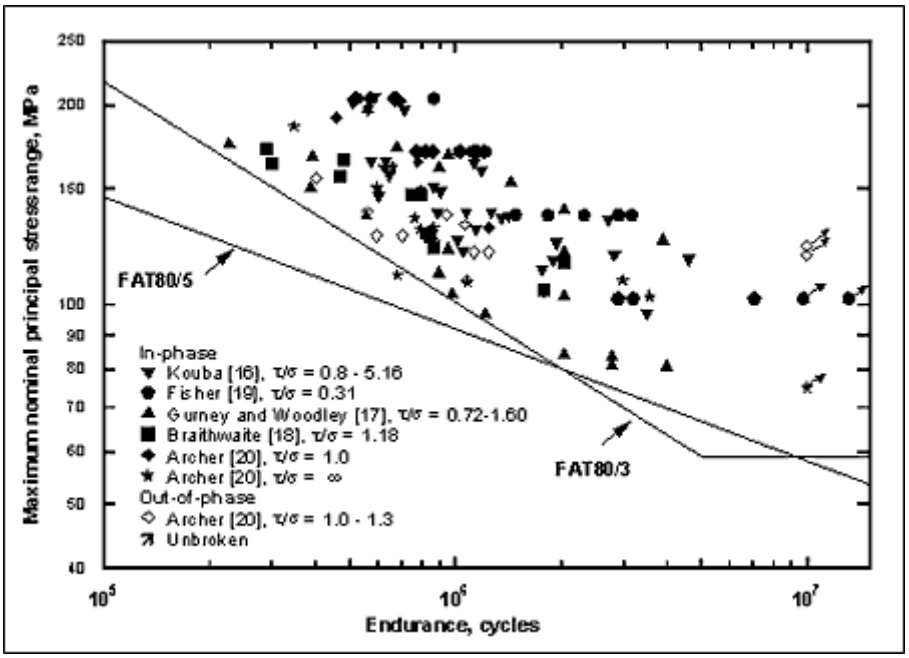

Figure 4.9 Fatigue test results for welded beams with fillet welded web attachments under combined bending and shear [5].

There are no clear and definitive solution given but results from this survey indicates that there is a good correspondence in behaviour. This solves even the problem what formula should be used because expression 4.16 contains the exponent 3 which corresponds to m=3 which was the best slope for beam specimens. There is one important issue not to be forgotten. Observe that the ratio in complex loading is in range 1.0 – 1.3. Different ratios must be considered because they could generate results that diverge from the experimental results. From [5] some explanations are given –*it seems reasonable that change in failure mode from mode I to mode III will result in a different S-N curve. What is not clear is if the mode III shear mode of fatigue cracking can be produced by loadings other than torsion. It is possible that for all other practical cases of fatigue loading on welded joints, when the weld toe is the most likely location for fatigue cracking, shear stresses are always accompanied by normal stresses and that they encourage the mode I failure. This warrants further study, as does the influence of applied shear stress in cases when fatigue cracks may occur at other locations, notably the weld root in load carrying fillet welds.* From this recommendations there seems to be need for further analyses to bring absolute clarity in the subject.

4.1.5 Modified critical plane

Bäckström and Marquis have in [28] made an analysis of 233 experimental results from eight different studies with help of a modified critical plane model for welds. The tested specimens consist of welded specimens in loading modes such as bending, torsion, proportional and non-proportional and combined bending-torsion. All the applied loads were under constant amplitude. All these 233 results showed a failure at the weld toe, weld root/throat failure are not considered. The modified critical plane used by Bäckström and Marquis is a modified criterion from the criterion suggested by Findley 1959, see Section 2.7.1. Findley's method was developed to suit non-welded material and therefore it was necessary to modify the criteria to fit welded

specimens. One of the most important changes is that to calculate the acting stresses, the hot-spot method should be used and therefore is this method mentioned as the *hot-spot critical plane approach*. It has been stated [37] that Marquis suggested five modifications of the original criteria, to make it more suitable for welded structures.

1. The critical plane is assumed to be orientated as a shear plane parallel to the line of the weld toe. All the other planes are ignored. The reason for this is that most of the cracks are initiated along the weld toes where high stress concentrations and local geometric irregularities exist. In Figure 4.10 is a tube-to-plate weld shown and the orientations of the possible critical planes are also illustrated.

2. The maximum normal stresses on the critical plane are calculated by assuming yield stresses normal to the weld toe. If the joint is stress-relieved the maximum stress will be the applied hot-spot stress during the load history.

3. To estimate the local normal stress along the weld toe, a hot-spot technique suggested by Niemi in [4] should be used. The methods to estimate the stresses are either based on FEM analysis or strain gauge, describe by Niemi in [4].

4. Stress gradients created by shear can not be effectively measured by using the strain gauge method, instead the hot-spot stress stress based on FEM analysis should be used for determining the shear stress along the weld toe.

5. The damage function, *f* in Findley's criterion, is assumed to be linear in the $\log(N_f)$ versus $\log(\Delta\tau')$ diagram. The new criterion for welded material will be like expression (4.19).

$$\Delta\tau'_{hs} = \Delta\tau_{hs} + 2 \cdot k \cdot \sigma^{\max}_{n,hs} = \tau^{*}_{f}(N_f)^{b} \qquad (4.19)$$

τ_{hs} =hot-spot shear stress

$\sigma^{\max}_{n,hs}$ =is the maximum of either the yield strength of the material, or for stress relieved joints, the largest applied hot-spot stress during one load cycle.

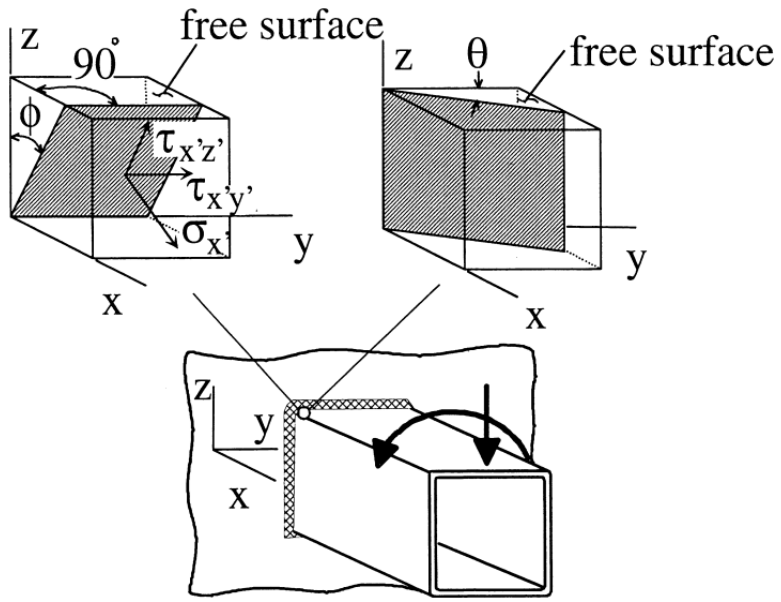

Figure 4.10 The orientation of the damage plane at the weld toe [28].

In the analysis of the modified critical plane in [28] Bäckström and Marquis used 233 test result to check the accuracy of the method. In all the calculations, Findley's material constant k had the value 0.3 which is a common value for structural steel. In Figure 4.11, test results obtained by using the hot-spot critical plane approach are showed. In the Figure the relationship between maximum hot-spot shear and the fatigue life of different welded joints, are plotted. To get the data points in Figure 4.11, the given failure cycles from the test results are used and with help of expression (4.19) the hot-spot shear stress can be estimated.

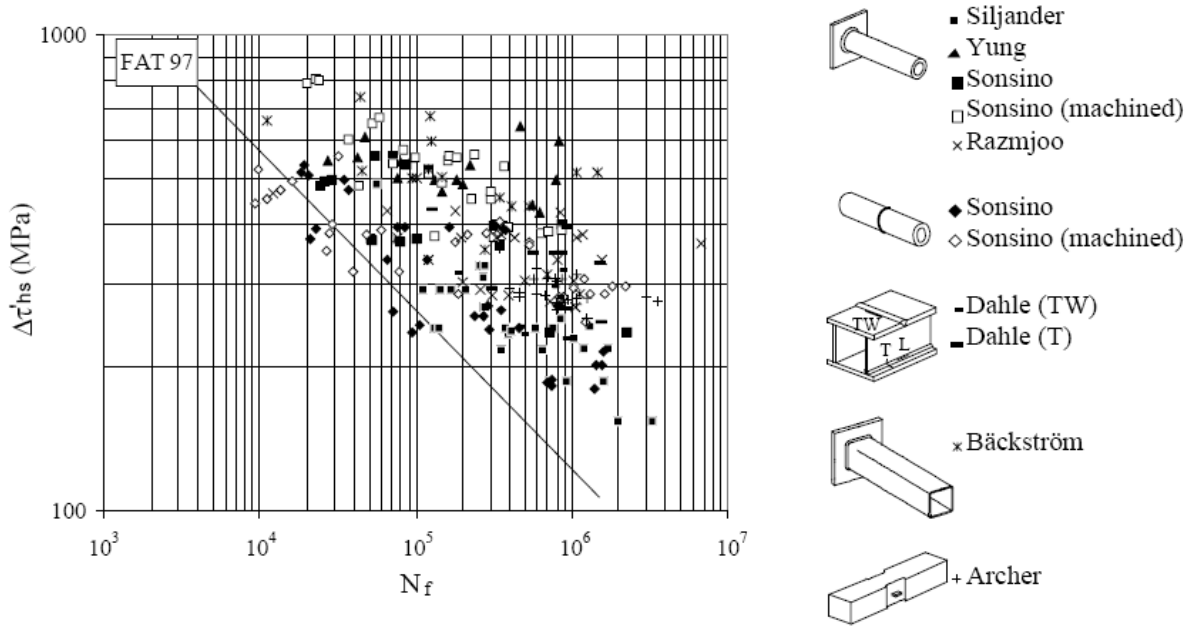

Figure 4.11 Test results for welded joints under multiaxial loading using the hot-spot critical plane approach [28].

From the results shown in Figure 4.11, Bäckström and Marquis found that the best design fatigue curve for all 233 data points was FAT 97. The standard deviation for the scatter is 0.47 for a curve based on the slope 3. For slope 5 the deviation will increase to the value of 0.58. This standard deviation values are log-values because of the log-scale in the diagram. Concerning Figure 4.11 Bäckström and Marquis discussed some of the results and one of their first conclusions was that the non-proportional loading seems to have an influence on the fatigue life. This phenomenon has also been reported from other researchers in the literature, but it has also been reported that proportional and non-proportional loading have been equally damaging [28].

In Figure 4.12 Bäckström and Marquis summarize the available data for proportional and non-proportional loading and calculated the expected fatigue life with the modified critical plane method. From the Figure 4.12 it can be seen that non-proportional loading is more harmful than the proportional loading.

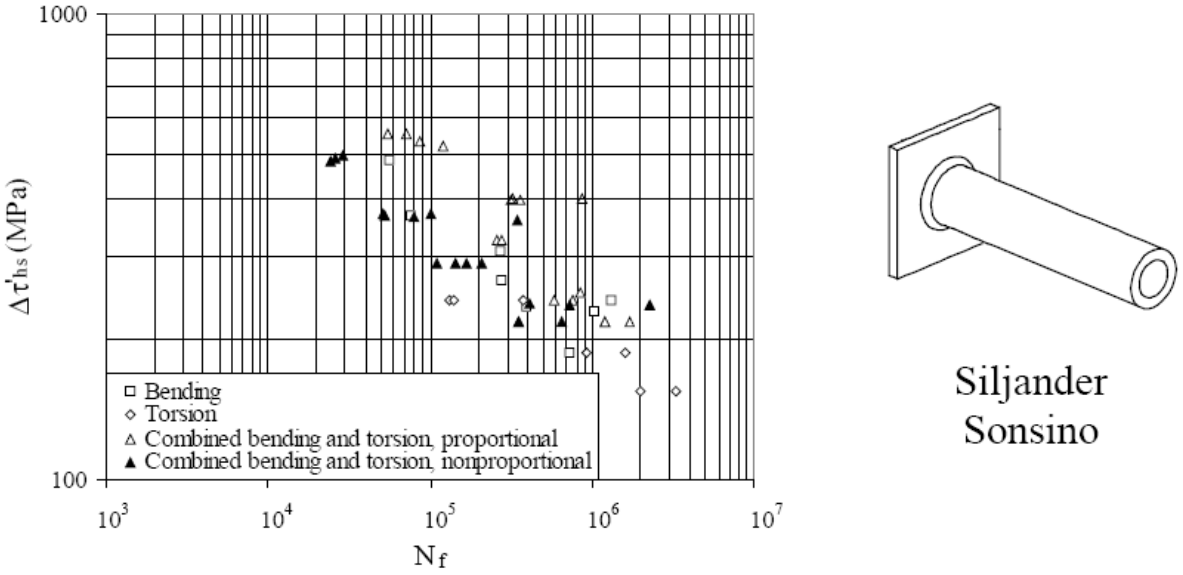

Figure 4.12 Test results for proportional and non-proportional loading by using the modified critical plane method [28].

Lehtonen compared different European standards [39] and the critical plane approach suggested by Bäckström and Marquis. Lehtonen used three different fatigue tests series, all of them are welded structural steel specimens. Two of these test series are performed under biaxial/multiaxial loading and are therefore of interest in this report. The first test results are from Bäckström [28] and the tests are carried out on a rectangular hollow section welded to a plate, see Figure 4.13. In the Figure 4.13 the loading paths are showed, these different paths show the type and direction of loading Applied on the tested specimens. For example is load path A causes only bending (normal stress) and the load path C causes only for torsion (shearing stress). Loading path F is out-of-phase loading. In Figure 4.14 the predicted fatigue life by using the finish standard SFS 2378, EC 3 and the modified critical plane are showed.

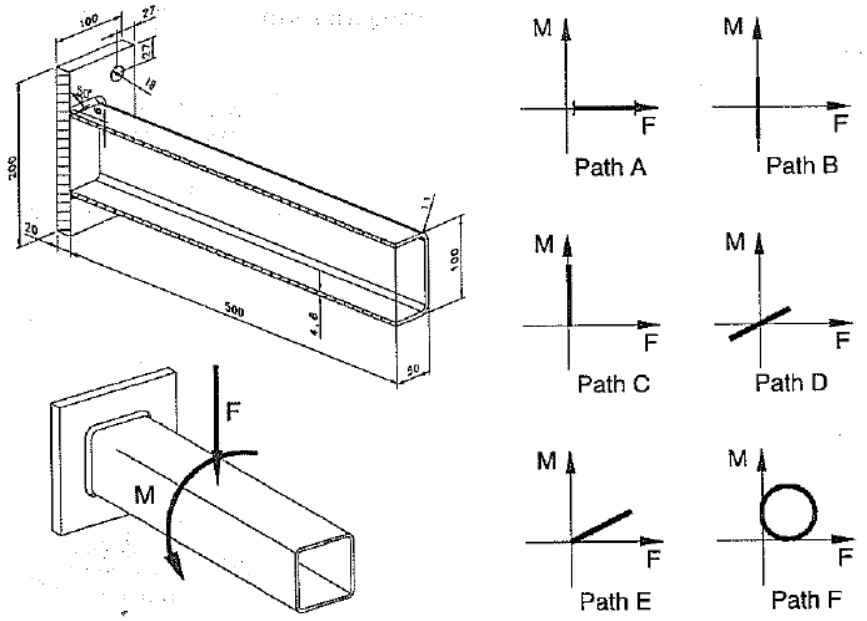

Figure 4.13 Geometry of the tested specimen and the loading paths [39].

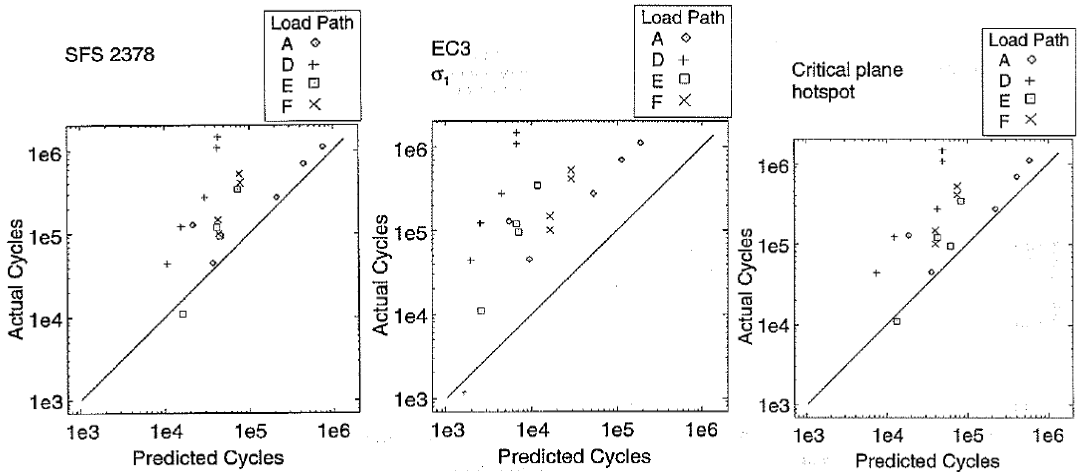

Figure 4.14 Fatigue life prediction using SFS 2378, EC 3 and the modified critical plane approach [39].

From Figure 4.14 it can be seen that the scatter from the modified critical plane results are smaller than for EC 3 and SFS 2378. This can be taken as evidence that the method can be reliable in predicting the fatigue life.

The other test series was carried out by Siljander, the specimens had a circular hollow section welded to a plate, see Figure 4.15. The load paths are also showed in the same Figure. The tests were carried out under constant amplitude loading. The predicted numbers of cycles for the two design standards and for the modified critical plane method are showed in Figure 4.16.

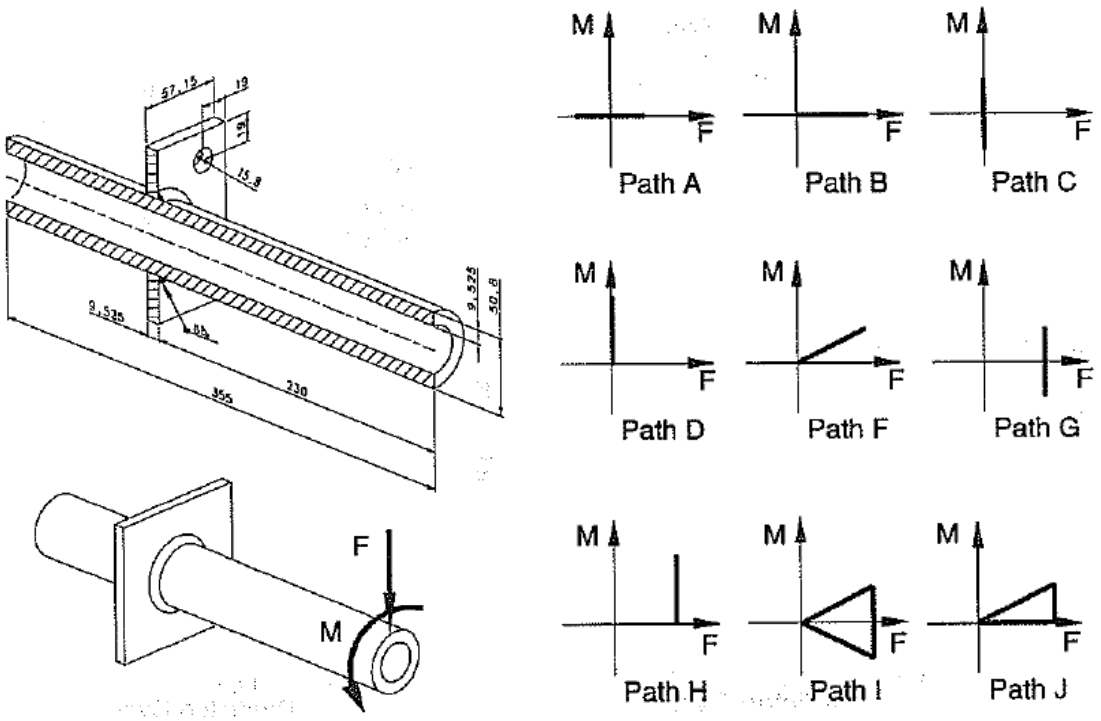

Figure 4.15 To the left, the geometry of the specimens, to right the load paths [39].

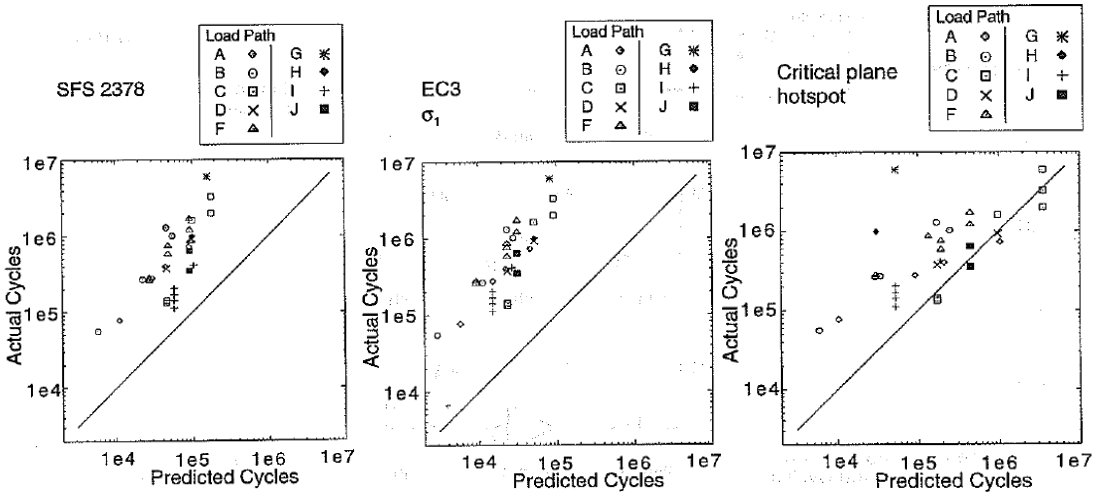

Figure 4.16 Fatigue life prediction using SFS 2378, EC 3 and the modified critical plane approach [39].

4.2 Method agreement compared to test results

The performance on how the methods presented in Section 4.1, in predicting the fatigue life have been tested by many different researchers. In this chapter their results will be summarised.

4.2.1 Test results from interaction methods

There is a large amount of fatigue tests reported in the literature which were made on specimens having different shapes and subjected to various types of loading conditions generating multiaxial fatigue situations. The variation of test specimen is dependent on what stresses due to fatigue has been investigated. Observe that the test specimens may be prepared before testing in different ways. The most common way is stress relieving or machining before testing. One must also remember that design codes consider the tested details in different way. For example in Eurocode 3 there are some restrictions regarding calculating effective stress range on stress relived details. Eurocode 3 considers also machining were restrictions are given in the detail requirements. Figure 4.17 shows that slope m=3 for an S-N curve describe the trend of test data for stress relived specimens accurately. Figure 4.18 shows test result on stress relieved, machined specimens. Slope m=3 for on S-N curve matches not the test results accurate for such specimens. Figure 4.19 shows test results for as-welded specimens. A slope of m=3 on S-N curve matches test results with good accuracy.

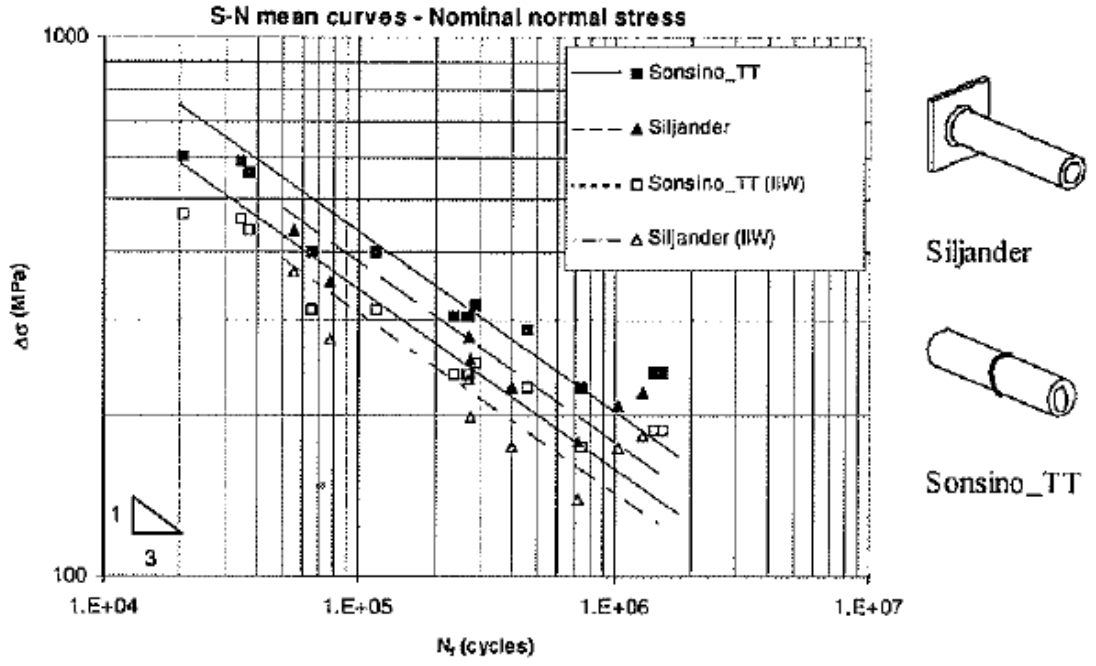

Figure 4.17 Showing test results on stress relieved specimens [36].

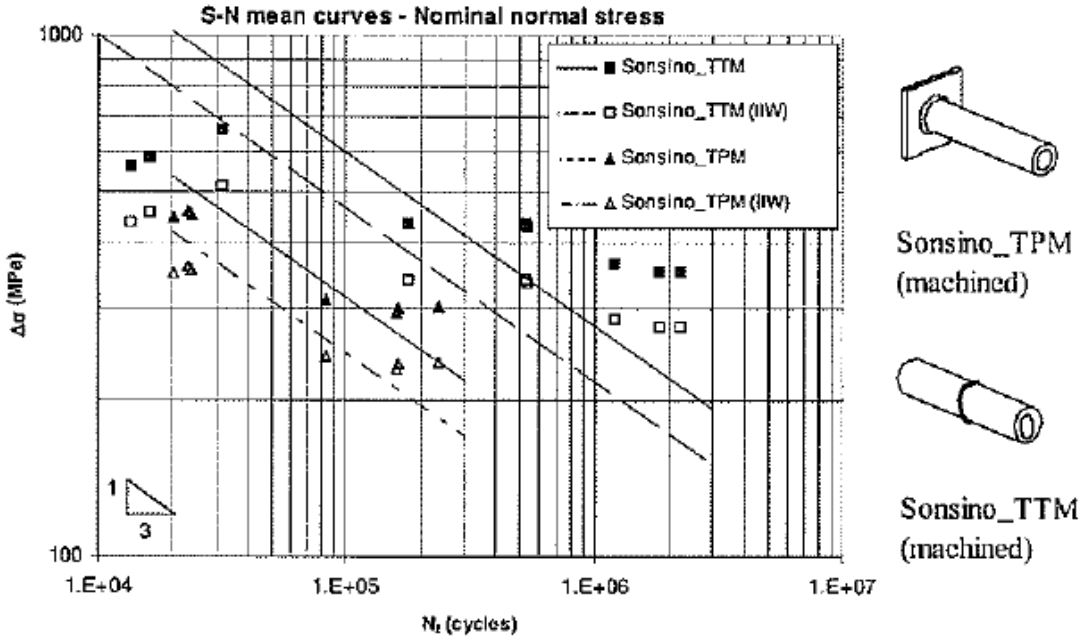

Figure 4.18 Showing test results on stress relieved and machined specimens [36].

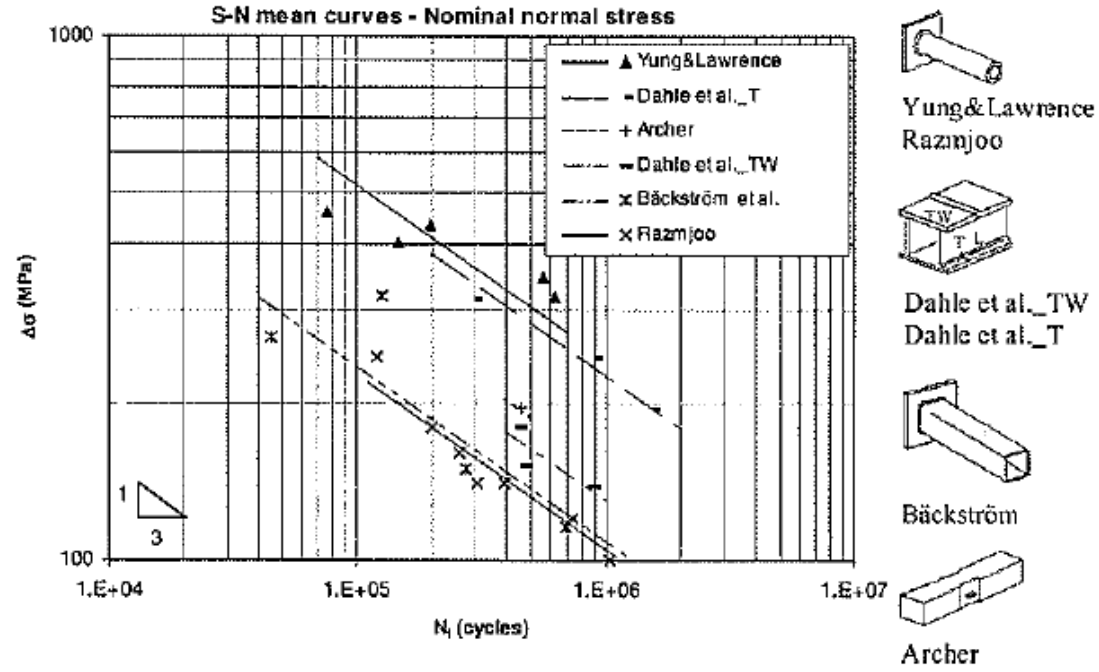

Figure 4.19 Showing test results on as-welded specimens [36].

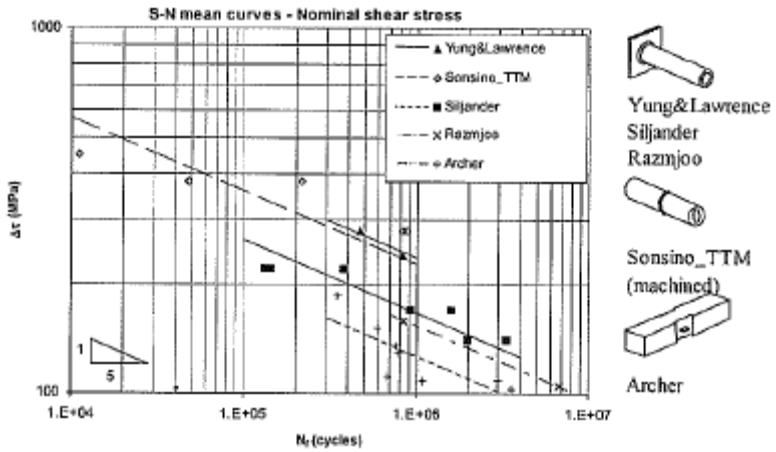

Figure 4.20 Showing nominal shear stress obtained from test data [36]

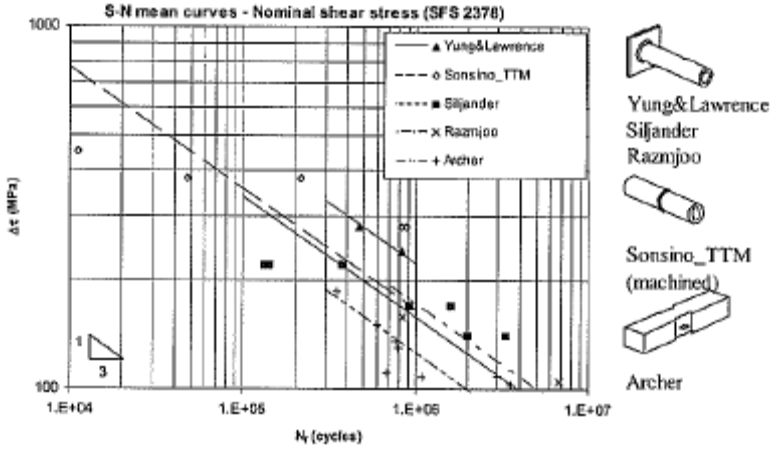

Figure 4.21 Showing nominal shear stress obtained from test data [36]

Figure 4.17 to 4.21 show the test results obtained on specimens loaded in bending only or torsion only [36]. From these results the fatigue strength of the tested specimens can be derived. Interaction equations works poorly in cases where cracks propagates from different locations. The best correspondence was found for cases were cracks propagate from one common location [36]. Calculation of the theoretical fatigue life to failure is normally made by using detail categories which corresponds to the actual loading case. Eurocode 3 regulates the fatigue strength at 2 million cycles for each detail category. In these values standard deviation is included along with probability calculations defining the final fatigue strength. Comparing the fatigue life from experiments with that from calculations causes problem because there is no probability or standard deviation included in the real result from experiments. One way to solve the problem is by making line regressions with slope 3 or 5 for the experimental results and generating the fatigue strength at 2 million cycles without any correlation [36]. Slope 3 was used for normal stress experiments while slope 5 was used for specimens affected by shear. By using the uncorrelated fatigue strength from line regression resulted in better comparison between experimental fatigue lives and predicted.

When comparing calculated fatigue life time with the experimental results some interesting results was discovered. In [36] it is shown that SFS 2378, IIW and EC 3

give results, which are conservative but with a significant scatter. Some test specimens give experimental results which exceed the calculated fatigue life. The opposite is shown to be true for other specimens. It has been stated [36] that more investigations are needed before optimisation can be done due to the generally conservative estimates. Figure 4.20 and 4.21 shows the scatter from the tests.

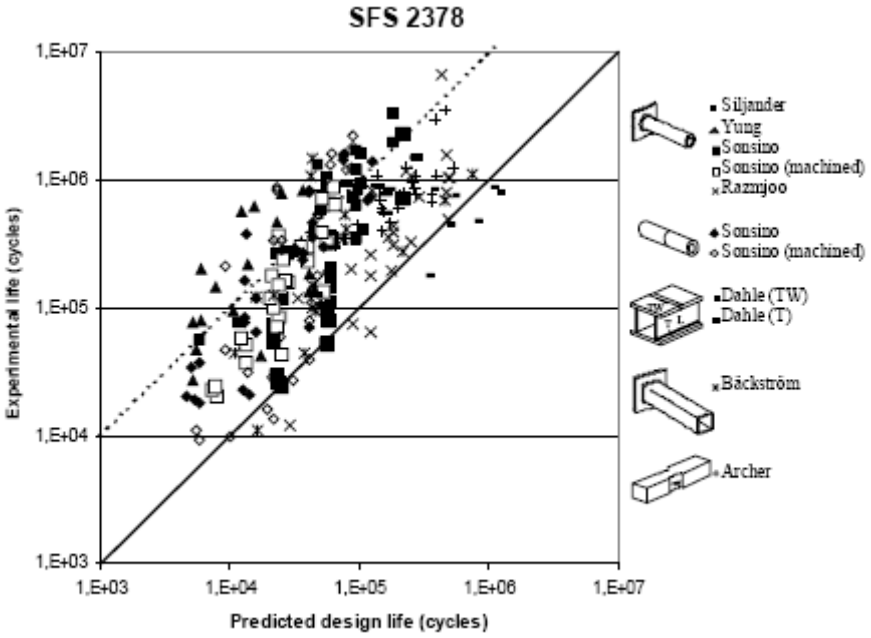

Figure 4.22 The fatigue test results for welded joints under multiaxial loading using nominal stresses and interaction equation from SFS 2378 [16].

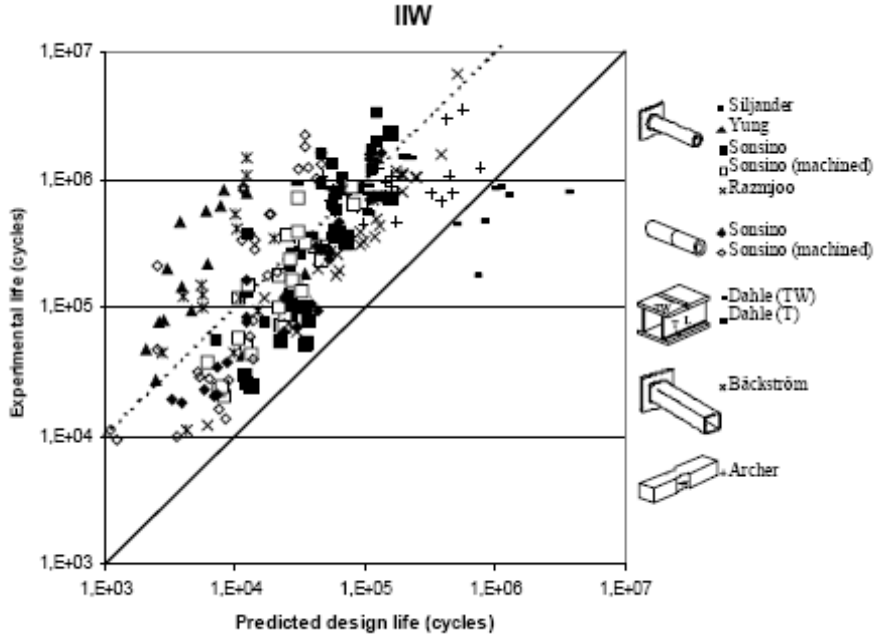

Figure 4.23 The fatigue test results for welded joints under multiaxial loading using nominal stresses and interaction equation from IIW recommendations [16].

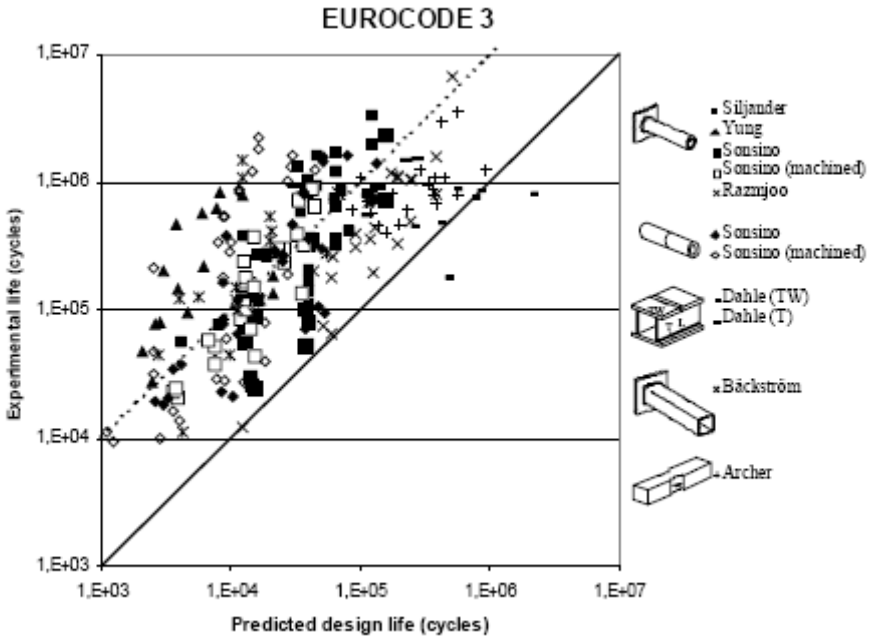

Figure 4.24 The fatigue test results for welded joints under multiaxial loading using nominal stresses and interaction equation from Eurocode 3 [16].

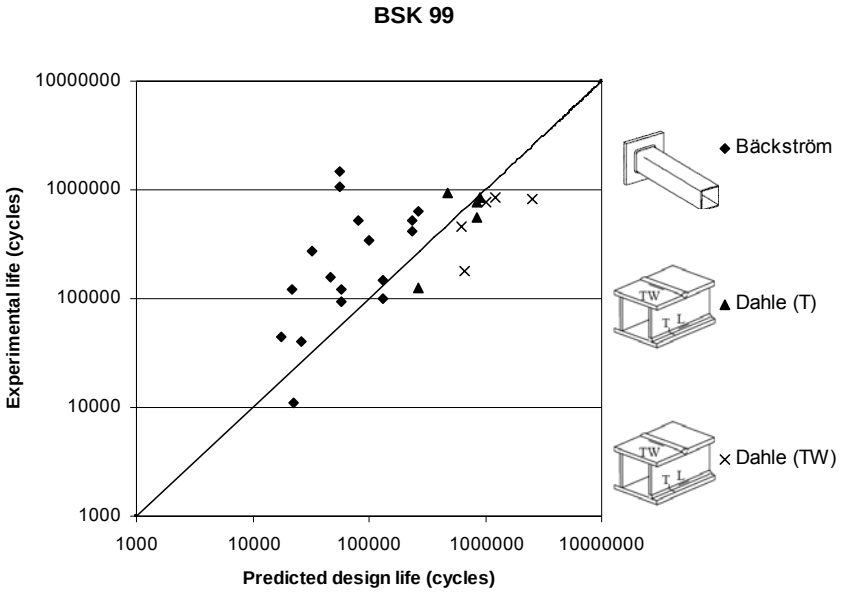

Figure 4.25 The fatigue test results for welded joints under multiaxial loading using nominal stresses and interaction equation from BSK 99.

Figure 4.22 - 4.25 shows a clear trend that experimental life is higher compared to predicted values. One significant property that should be taken into consideration is the fatigue classes used in the calculations. Bäckström and Marquis use the fatigue classes shown in Figure 4.26 and Table 4.1 in theirs calculation [36]. Figure 4.25 has been obtained by using test data from the literature and the calculations together with the test data are showed in appendix A.

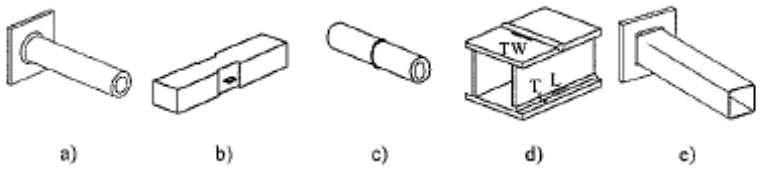

Figure 4.26 The test specimen geometry [36]

Test series	Figure 1	SFS 2378		Eurocode 3		IIW	
		$\Delta\sigma_C$	$\Delta\tau_C$	$\Delta\sigma_C$	$\Delta\tau_C$	$\Delta\sigma_C$	$\Delta\tau_C$
Archer[11]	Fig. b	71	63	80	80	71	80
Yung and Lawrence[12]	Fig. a	63	63	50	80	50	80
Siljander *et al.*[9]	Fig. a	63	63	56	80	56	80
Sonsino[7,8]							
Tube-to-tube (TT)	Fig. c	80[3]	63	71	100	71	
Tube-to-plate (TP)	Fig. a	71	63	56	100	56	100
Razmjoo[13]	Fig. a	63	63	50	80	50	80
Bäckström *et al.*[14]	Fig. e	71	63	45	100	45	100
Dahle *et al.*[15]							
TW	Fig. d	112	63	90	100	112	100
T	Fig. d	100	63	100	80	90	80

Table 4.1 Showing fatigue classes for different specimens [36].

It should be mentioned here that the tests described earlier in this chapter are performed under proportional loading. Non proportional loading was also investigated by Bäckström and Marquis [36]. Figure 4.27 shows that non proportional is more harmful than proportional loading.

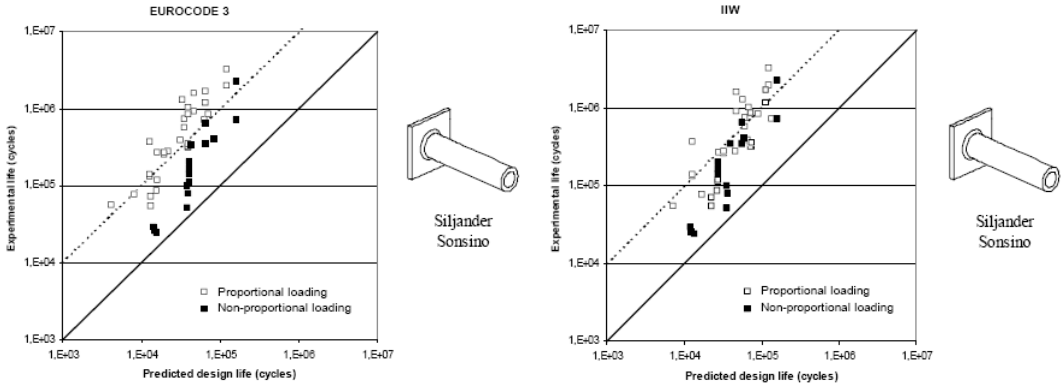

Figure 4.27 and 4.28 showing proportional and non proportional loading using fatigue classes from Table 4.1 and interaction equation from EC 3 and IIW [16].

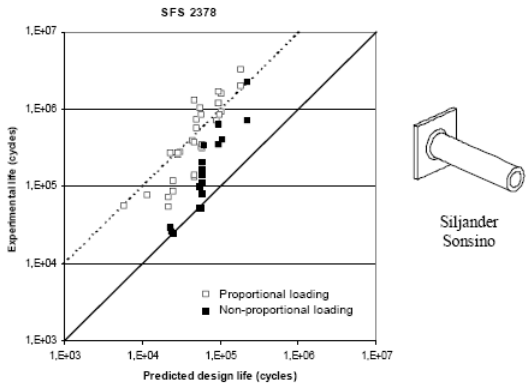

Figure 4.29 showing proportional and non proportional loading using fatigue classes from Table 4.1 and interaction equation from SFS 2378 [16].

After introducing test and test results some interesting aspects should be mentioned. By using fatigue classes from Table 4.1 the result shows some conservatism. As was mentioned earlier, fatigue classes include safety due to reducing the mean fatigue strength with 2 standard deviations. Interaction methods seem to give a good correspondence to reality at first view. Therefore it is of interest to compare test results with predictions without any safety factors or reductions. Such study was made in [16] and shows some other aspect of the same issue.

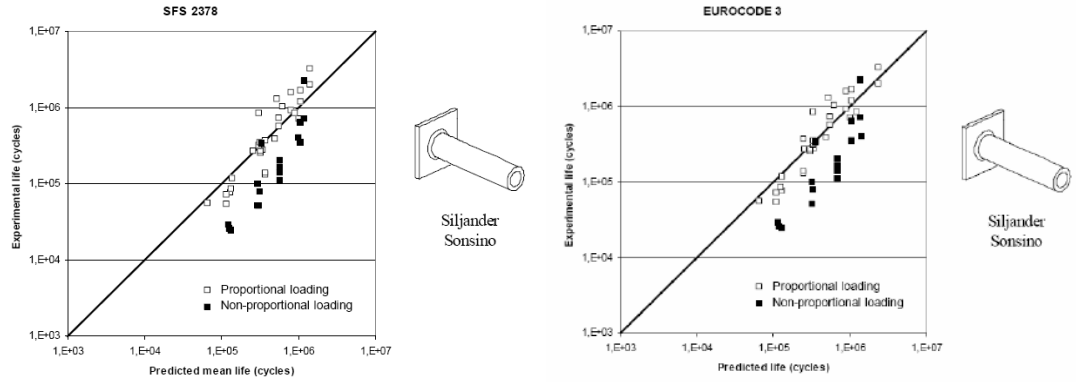

Figure 4.30-4.31 The fatigue test results of tube to plate welded joints under proportional and non-proportional loading using mean S-N curves (SFS 2378 or EC 3) [16].

After studying Figures 4.30 to 4.31 a trendline for non-proportional loading appears. Most of the experimental results are located below the line where predicted and experimental cycles correspond. This means that experimental fatigue lives are less than predicted ones. One interesting observation is that most of the values are highly represented on the unsafe side. On the other hand this may be included in the safety parameters included in the fatigue classes, because normally designers shall use the given fatigue classes given in each design code. The fatigue class which should represent this kind of multiaxial case should have lower defined fatigue strength. This phenomenon has also been discussed in [16]. Different cracking modes were reported by different researchers and specimens. It was mentioned earlier that interaction formulas works in fatigue prediction when cracks caused by shear and normal stress

start from a common point. If different cracking modes appear under multiaxial loading this may explain the divergence in accuracy. The issue regarding prediction of fatigue life under multiaxility has been in focus by several leading researchers. The following can be found in [38]: "*it is not likely that the multiaxial fatigue behaviour under non-propotional loading can be solved by simple calculation procedure, as suggested in ASME code for out-of-phase loading modification of von Mises , or in the Eurocode by considering individually nominal or structural normal and shear stresses and then adding their damaging increments together*".

4.2.2 Modified Wöhler curve in view of test data from the literature

The researchers behind the modified Wöhler curve, Susmel and Tovo in [7], tested the accuracy of the method by using a number of test data taken from the literature. The selected data were obtained on welded joints subjected to bending, tension, torsion, in-phase and out-of-phase biaxial cyclic loading. In Figure 4.32 an example of the test series is shown with a drawing (a) of the tested joint, diagram (b) and (c) are the two standards Wöhler curves for axial and torsional loading showed together with the experimental data. Diagram (d) have the experimental failure plotted versus the predicted fatigue life from the uniaxial and torsional standard curves. In diagram (e) the predicted failure versus the experimental failure is plotted. The predicted failure is calculated by using experimental fatigue curves. These experimental fatigue curves are obtained from every single test series, the reference stress and slope value k is adjusted to fit the test data. In Table 4.2, the difference between the experimental and standard values is showed. It can be observed that under bending/tension loading the experimental k-value has a range between 2.2 to 5.4 when the Eurocode 3 suggested a slope of 3. Under torsional loading the experimental k has a value between 2.9 to 7.4, the Eurocode 3 give a value of 5. If the experimental value, k is lower than the k value from EC 3 there is a large risk that the predicted fatigue life would be overestimated. All the test data used by Susmel and Tovo [7] to verify the accuracy in the modified Wöhler curve method is summarised in appendix B together with the different load paths.

Bending/ Tension						Torsion					
	$\Delta\sigma_{A,Ps}$ =50%		k				$\Delta\tau_{A,Ps}$=50%		k		
R	Experim.	FAT	Experim.	FAT	Fig.	R	Experim.	FAT	Experim.	FAT	Fig.
-1	218.8	102.2	4.4	3	B1b	-1	176.3	144	4.8	5	B1c
-1, 0	180.9	102.2	3.9	3	B2b	-1	219	144	7.4	5	B2c
-1, 0	168.4	102.2	5.4	3	B3b	-1, 0	151	144	6.2	5	B3c
-1	130.6	102.2	5.4	3	B4b	-1	94	115.2	3.7	5	B4c
-1, 0	178.3	115.2	3.8	3	B5b	-1, 0	149.6	144	5.5	5	B5c
0	80.8	102.2	3	3	B6b	0	119.4	115.2	4.5	5	B6c
-1	67.2	64.8	2.2	3	B7b	-1, 0	90.5	144	6.6	5	B7c
0	-	115.2	-	3	B8b	-1	100.6	115.2	2.9	5	B8c

Table 4.2 Comparison between experimental and standard fatigue curves [7].

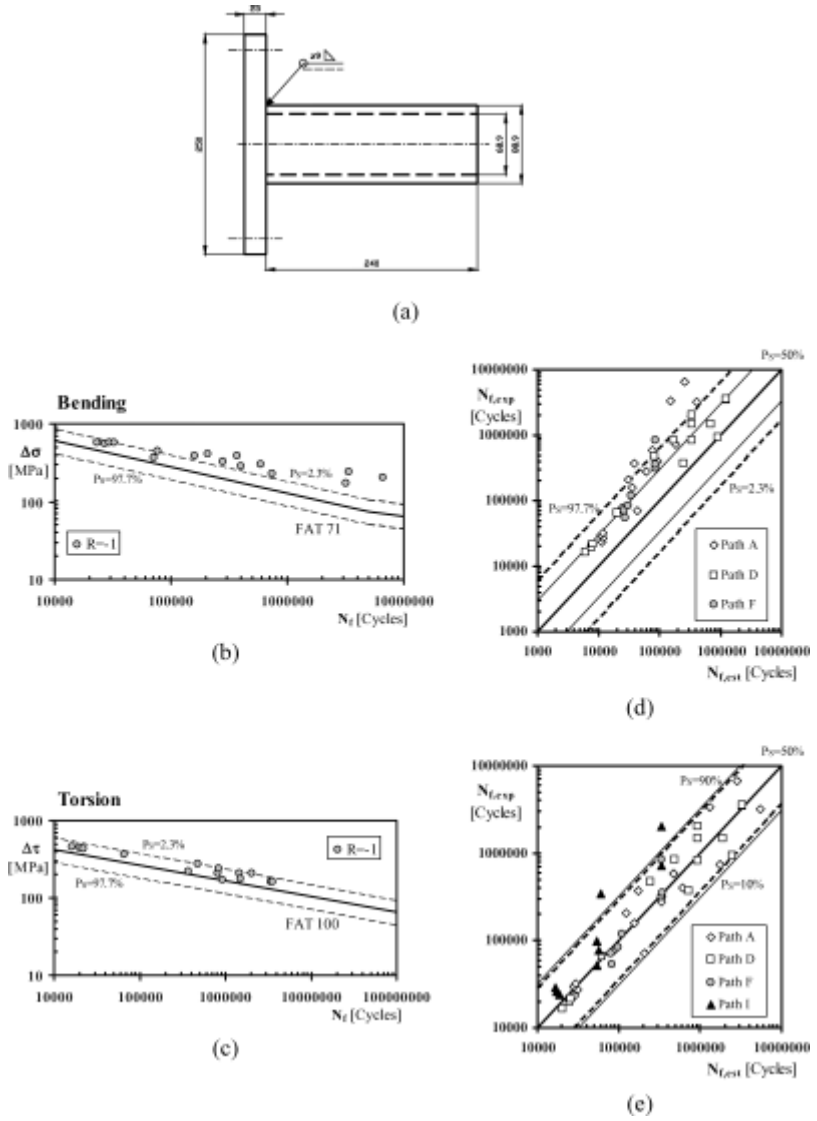

Figure 4.32 Geometry of specimen (a), Standard curves and experimental data (b, c), Experimental fatigue life versus predicted fatigue life by using the standard curves (d) and experimental curves (e) [7].

Susmel and Tovo have carried out own fatigue tests [24] on welded steel details and also used the Modified Wöhler curve to estimate the fatigue strength. The specimens were of two types, the first one was made by two round bars welded to a steel plate, see Figure 4.33 (a). The second one was made by a tube passing through a hole in a steel plate, the tube was welded to the plate, see Figure 4.33 (b). The total numbers of the tested specimens were 22, eleven for each type. The loading condition was uniaxial loading with a load ratio 0.1. Because of the geometry of this specimen, biaxial stresses will arise in the along the welds, see Section 1.12.1 and Figure 1.24 for the stresses in the weld. The stresses will be in-phase and the magnitude of the shear and normal components of stress depends on the angle Φ. In Figure 4.33 c and d the fatigue test results are plotted versus the nominal axial stress range. In these diagrams Susmel and Tovo also found the best fitting standard fatigue curve in EC 3 for the both geometries, FAT 80 was the best curve to describe the situation. They also write in [24] that the fatigue cracks were initiated at the weld toe for all the tested specimens, but the position of cracks vary. For the A-type specimens most of the

cracks were initiated at the angle, Φ = 0°, see Figure 4.34 for the crack position. In the B-type the cracks were initiated at the angle Φ = 40-50°, see Figure 4.34 for the positions.

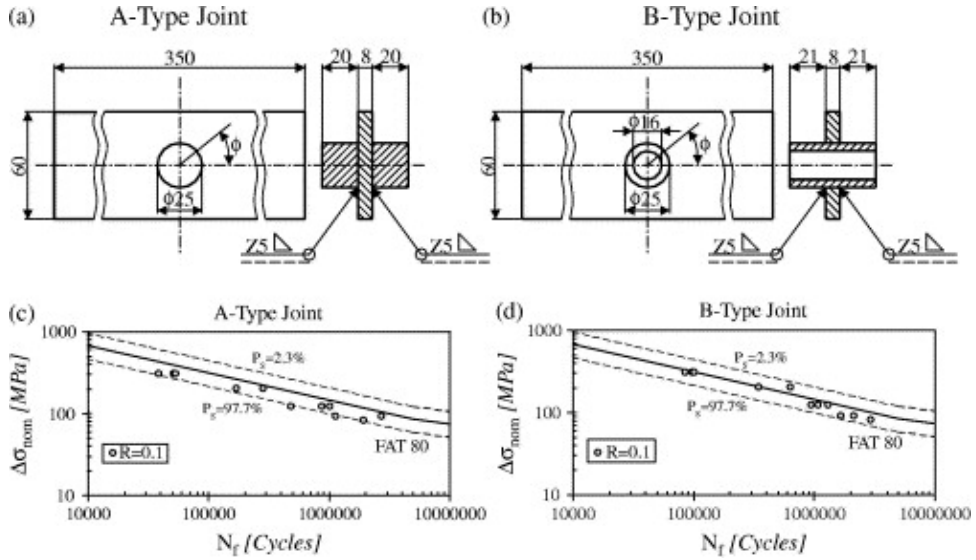

Figure 4.33 Specimens geometries and the fatigue test results [24].

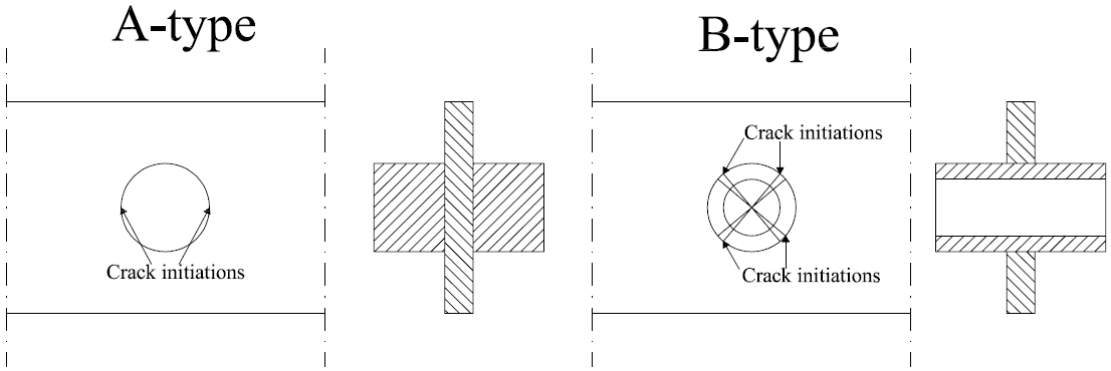

Figure 4.34 The position of the crack initiations in the specimens.

In their paper [24] Susmel and Tovo conducted some interesting calculations using the modified Wöhler curve method. They have used the method to predict both the fatigue life and the place where the cracks should be anticipated. To find a method to predict the site of crack initiation is very interesting because this gives a possibility to find the weakest points in the welds. Hot-spots stresses obtained from FE models were used in the modified Wöhler curve method. As mentioned earlier, the size of the biaxial stresses depends on the Φ angle and in Figure 4.35 this phenomenon is showed. The ratio between the hot-spot shear stress and the nominal stress reaches its largest value at the angle of 45°. The ratio between the normal hot-spot stresses and the nominal stress has a different behaviour for the both details. For the A-type the normal hot-spot stress is about 20 % larger than the nominal stress at the angle 0°, this is an effect of the stress concentrations at the weld toe. At the angle 90° there is no normal stresses. In the B-type the hot-spot stress is about 20 % smaller than the nominal stress, which has a higher value because of the hole in the plate gives a smaller area and therefore gives a larger nominal stress. From Figure 4.35 it is easy to see that the stress amplitude and the stress ratio changes when the angle Φ change.

Because of this and to make some simplifications in the calculations, Susmel and Tovo in [24] calculated the fatigue life for four points along the weld at the angles 0°, 22.5°, 45° and 67.5°. It can also be mentioned that the A-type loading was mainly mode I, the B-type loading was mode III.

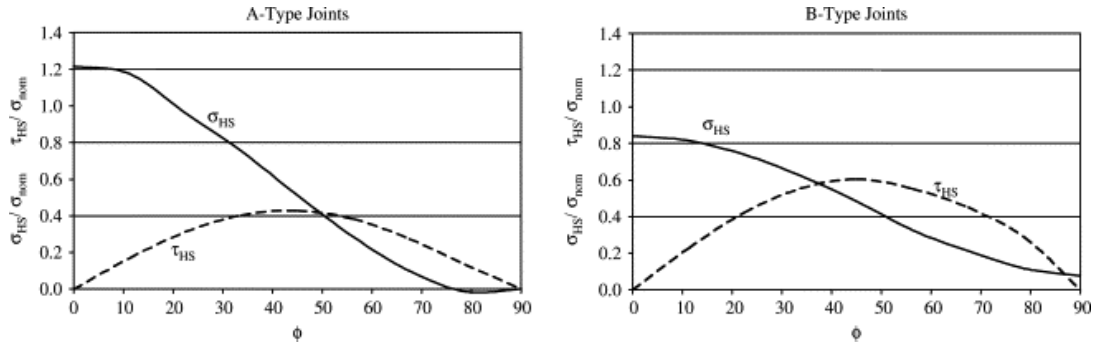

Figure 4.35 The hot-spots stresses along the weld toe for the different angles [24].

It was also necessary to find the best fitting standard fatigue curve, which should be used to calibrate the Modified Wöhler curve method. The best fitting curve, according to EC 3, was for torsion the FAT 80 and for the normal stress the FAT 71. By using these two curves the modified Wöhler curves can be estimated for the different hot-spots stress ratios and this is showed in Figure 4.36, but the Wöhler curves are here plotted as a function of the nominal stress. From the Figure it can be noticed that for the A-type joint it is the angle 0° which gives the lowest Wöhler curve, the same angle at which all of the cracks were initiated. For the B-type joint the lowest Wöhler curve in the medium and low cycle fatigue was the curve for the angle 45°, for high cycle fatigue the curve for angle 0° was the lowest one. Also this was in a quite good agreement with the observed crack initiation sites.

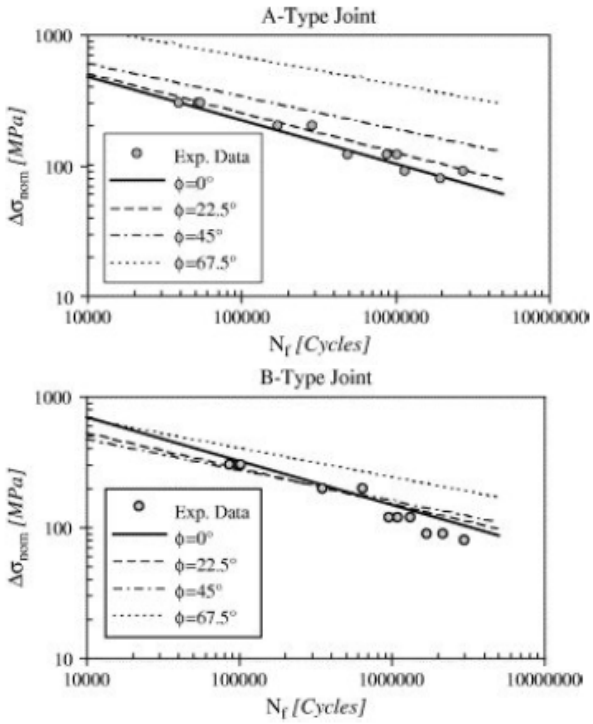

Figure 4.36 The modified Wöhler curves and the experimental data [24].

The accuracy of the modified Wöhler curve when hot-spot stresses were used seemed to have a good agreement with the tests. In Figure 4.37 the predicted cycles to failure are plotted versus the experimental cycles to failure.

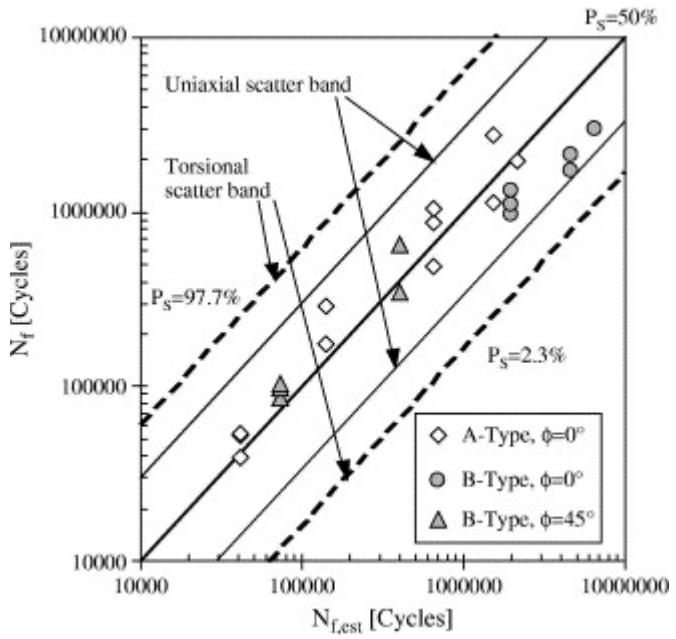

Figure 4.37 The predicted life cycles versus the experimental failure cycles [24].

4.2.3 Comparison between Modified Wöhler curve and Eurocode 3

To evaluate the reliability of the modified Wöhler curve method in predicting the multiaxial fatigue life of welded connections, Susmel and Tovo compare its accuracy with results from the methods proposed in EC 3. In Figure 4.38, all the calculations performed by Susmel and Tovo in [7] are summarized. Two different curves are used as calibration information, the axial and torsional standard curves and the experimental curve. Figures 4.38 (a) and (b) show the results from the method proposed in the EC 3. Under in-phase loading the prediction of the fatigue life is conservative, under out-of-phase loading the precision of the life predictions gets better. When the approach suggested by EC 3 is applied by using the uniaxial and torsional experimental curve as calibration information, Figure 4.38 (b), the results become more critical and under out-of-phase loading the results are non-conservative. Figure 4.38 (c) and (d) shows a summary of the results obtained from the modified Wöhler-curve. When the standard curves are used as calibration information, see Figure 4.38 (c), the error interval for out-of-phase loading is in about ± 300 %. For in-phase the error interval for the life prediction is a little conservative. When the experimental curve is used the error interval is within ± 300 % for both in and out-of-phase. In Figure 4.38 (e) and (f) the error frequency distribution is shown and from this distribution diagram it is quite obvious that the modified Wöhler curve gives a more accuracy than the EC 3.

When the standard curve is used for calibration, the modified Wöhler curve has 60.3 % of the experimental data within the error interval of ± 150 % and for EC 3 is only 45.5 % of the experimental data in the same error interval. If the experimental curve is used, the error interval for the modified Wöhler curve is 73 % within the error interval ± 150 %. For EC 3 the accuracy gets lesser, 44.4 % of the experimental points are

within the error interval of ± 150 %. Susmel and Tovo mention that an important and interesting point with the error frequency for the modified Wöhler curve is that the peaks of the error distribution are always positioned in the conservative zone, for EC 3 is the error distribution scattered in both the non-conservative zone and in the conservative zone.

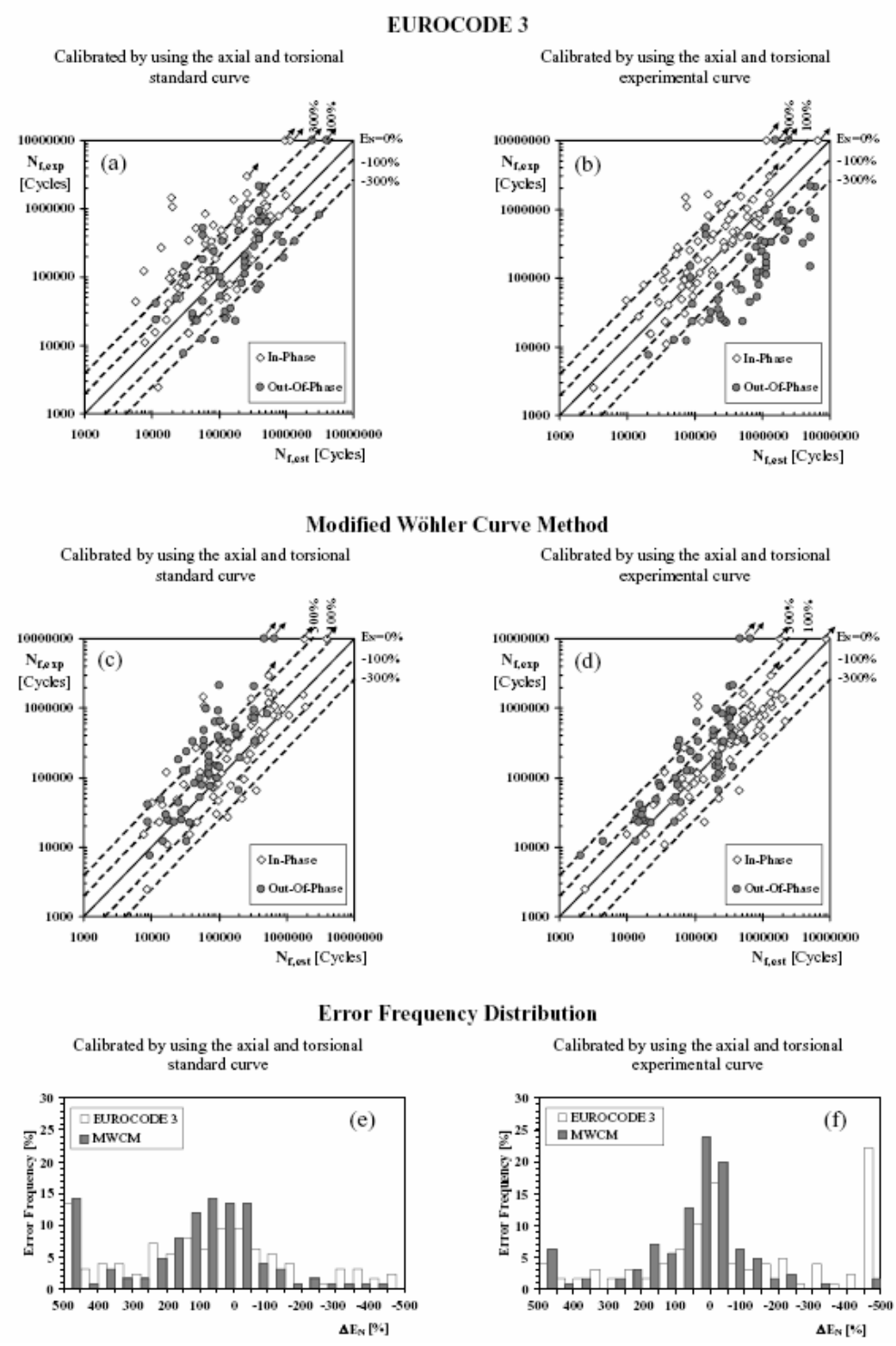

Figure 4.38 Comparison between modified Wöhler curve and EC 3 [7].

4.2.4 Fatigue life using principle stress – comparison with test data

As was shown earlier under Section 4.1.4, good correspondence between test results and fatigue classes given by EC 3. Details affected to shear corresponds well to slope 5 while details affected to normal stresses has slope 3. In Figure 4.39 welded flange-tube specimens affected to in-phase loading by bending and torsion corresponds to slope 3 while out-of phase loading corresponds to slope 5. Figure 4.39 shows that something happens when loading is out-of-phase compared to in-phase loading.

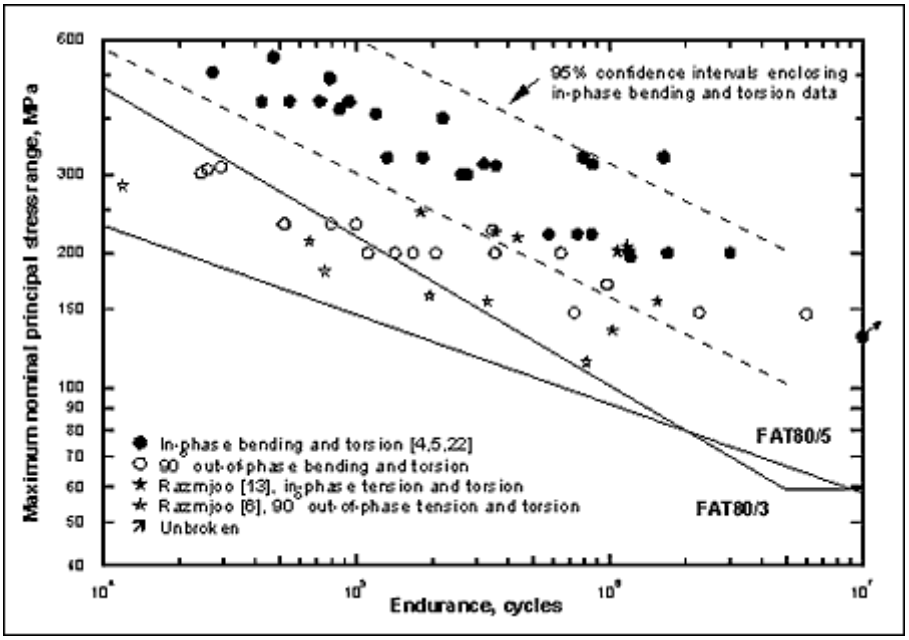

Figure 4.39 Fatigue test results for flange-tube welded joints failing from the weld toe, tested under combined bending or torsion and torsion loading [5].

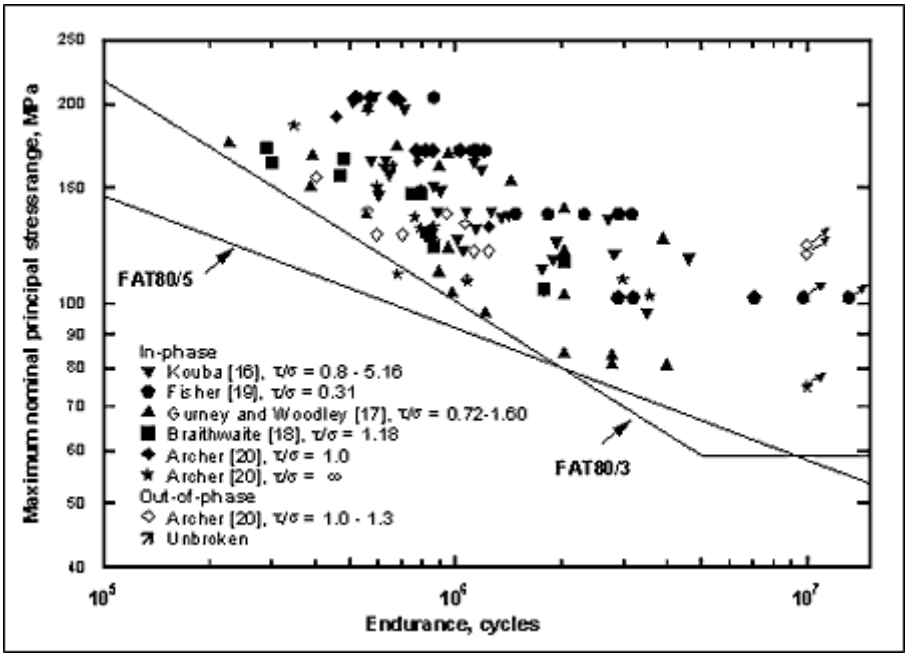

Figure 4.40 Fatigue test results for welded beams with fillet welded web attachments under combined bending and shear [5].

The interesting issue here is that for flange–tube welded joint (loaded in torsion) which creates shear in the welding slope m=3 corresponds best with the test results instead for the slope m=5 which is normally the value for shear. Recommendations from EC for details subjected to shear is fatigue class 100 or 80 with slope m=5. The interesting part is that normal stress due to bending has slight effect on the test result for in-phase loading. The effect is more prominent when loading is out-of-phase. In-phase loading may be represented by 80/3 curve but the influence of out-of-phase loading creates a larger scatter and requires 80/5 curve. In out-of-phase loading the shear stress component has more influence [5]. It seems likely that 80/5 is a suitable curve for flange-tube welded specimens affected to combined bending or tension and torsion. However more data are needed to clearly verify the curve for wider range of shear to normal stress ratios and variation in tube size and thickness, see Figure 4.39 [5]. Welded beam specimen differs from flange-tube specimens due to shear stress arise. The shear stress was caused by torsion for flange-tube specimens while it comes from ordinary loading for beams. In Figure 4.39 the scatter of in and out-of phase loading can be presented by the same curve. Fatigue class 80 with slope m=3 corresponds well to the test results. As Figure 4.40 shows that some test result are outside 80/3 line. There should be remembered that in reality other coefficients like γ_{mf} and γ_{Ff} from EC 3 creates further safety. Clearly more data are needed for non proportional loading to draw firm conclusions [5]. Here there was a limited amount of specimens used in out-of-phase loading, see Figure 4.40. The change in loading ratio may contribute to divergence in result. Booth tests show important trends and may contribute to easier design when using codes like EC 3 or IIW.

4.3 Conclusions

In this Section will conclusions about the different methods be presented. The conclusions are from well-known researchers in fatigue, but also conclusions from the authors to this master thesis.

4.3.1 Conclusions from the hot-spot method

The hot-spot method seems to be a potential method to predict multiaxial fatigue life. On the other hand this master thesis does not present any experimental data where the method is compared to experiments. Hot-spot method is an interaction method where the stresses are determined by FEM analysis. Hot-spot stresses may be determined as the principal stress at the weld toe. It is therefore likely that inconveniences may appear in prediction fatigue life despite the set of detail categories valid only for hot-spot method. As there have been discussed under principal stress method, principal stress range is decreasing when loading is out-of phase. This lack in calculation process causes miss-predictions and may be the case when principal stress range is determined by FEM analysis. One advantage when using hot-spot method is that the number of detail categories is reduced due to the difference compared to the hand calculation method deriving damaging stresses. Hot-spot method concludes toe failure which reduces the failure modes and detail categories. The poor guidance from codes does not improve the situation. To summarize the method, it seems promising but without good experimental results. Therefore it should be used with caution in the fatigue design of details subjected to multiaxial loading. If the method is used, designers should be careful with out-phase loading. However there is still needs for

further investigations and surveys to improve the hot-spot method for multiaxial fatigue conditions.

4.3.2 Conclusions from the modified Wöhler-curve method

The modified Wöhler curve method for welded details has shown to be a method which can predict the fatigue life very accurately. The method is not so old, Susmel and Tovo worked with this method for the first time in 2001 [40], and in 2004 they published the first paper where the modified Wöhler curve's accuracy was tested for welded details. Because of this, the method has not been evaluated by other researchers and therefore it is early to draw any firm conclusions regarding its general applicability. However, the tests performed by Susmel and Tovo in [7] confirm the good performance of the method. However the test-series that they used were of very similarly type, most of them were tubes welded to a steel plate, only one series consisted of box beams with welded attachments. The method needs therefore to be tested with other types of specimens to see if the accuracy and applicability will be the same. The same applies regarding the possibilities of predicting crack initiation sites by using this method. It will be of interest to test if it is possible to predict crack initiation sites in more complicated specimens by using the modified Wöhler curve method. If this shows to be successful, the designer would have a great tool to find the weakest parts in a welded steel structure. The greatest advantages with the modified Wöhler curve method is the simplicity in the calculations, it is possible to use with simple hand calculations. This makes it possible to implement the method in future design codes and even get designers to use the method in structural engineering.

Susmel and Tovo make some conclusions concerning modified Wöhler curve in their paper [7]. They list following conclusions:

1. The modified Wöhler curves method applied in terms of nominal stresses is successful in estimating the fatigue lifetime of welded connections subjected to multiaxial constant amplitude cyclic loading. Its formulation agrees with the standard code recommendations: it accounts for inverse slope changes and it does not take into account the mean stress effect.

2. When the criterion is calibrated by using the experimental bending (or axial) and torsional fatigue curves, it is capable of collapsing all the data into the widest scatter band related either to the uniaxial or torsional data. This holds true independently of the loading path type and the load ratio values.

3. When the criterion is calibrated using standard fatigue curves, it provides conservative predictions.

4. The modified Wöhler curves method is much more accurate than the procedure proposed by Eurocode 3 and it holds true independently of out-of-phase angle and load ratio values.

5. Further work needs to be done in this area to extend the use of this approach to welded attachments under variable amplitude multiaxial loading.

Susmel and Tovo make some further conclusions about theirs proposed modified Wöhler curve [24]. In Section 4.2.2 it have been described that the modified Wöhler

curve can predict the fatigue life and the site for the crack initiation and that hot-pot stresses can be used in the method. About this Susmel and Tovo writes [24] that the Modified Wöhler curve method are capable of predicting both the position of crack initiation sites and the fatigue lifetime on the tested specimens by using Hot-spots stresses. But they also mention that they don't have validate the method under non-proportional loading by using Hot-spot stresses, this needs to be done in further work.

4.3.3 Conclusions from interaction method

Using interaction formulas may be a good procedure in cases when the multiaxial loading effects are proportional. At least tests indicates some conservative results but with different variation in scatter when different design codes are applied. Some margin comes from the statistical analysis defining the fatigue class, which normally is defined as the stress range at $2 \cdot 10^6$ cycles to failure at 97 % survival probability. For non-proportional loading the interaction formulas tend to work poorly. There seems to be some error in the method when calculating damage from each stress component and summing them together. When creating S-N curves the regression line for test results is placed with slope 3 or 5 generating the fatigue class. Test results may scatter to the regression line and cause some divergence in calculations [36]. Even stress ratio that has been mentioned in Section 1.9 causes impact on estimation. Experiments carried out at a stress ratio R = -1 had higher fatigue life than specimens loaded at R = 0 even when the normal-to-shear stress ratio was constant. Some portion of compressive load cycle was non-damaging [36]. On the other hand other authors declare that it is not likely that multiaxial fatigue under non-proportional loading can not be solved by adding their damaging increments together. But by modifying the interaction formula better correspondence was found and made the method suitable for non-proportional loading. There fore designers should be suspicious using interaction methods for details affected by non-proportional loading or at least make predictions at the moment with some margin to prevent early failure.

4.3.4 Conclusions from principle stress method

In EC 3 among other codes the guidelines on how the principle stress should be used in assessing the fatigue strength of welded details subjected to multiaxial loading are rather poor and may cause difficulties for designers in evaluating fatigue life. There are, for example, differences in the slope for the S-N curves describing the fatigue life of different details. Flange-tube welded specimens had best correspondence to slope m=5 and fatigue class 80 while beam specimens corresponds best to m=3 and class 80. One explanation is that the flange-tube specimens are affected by torsion which gives rise to Mode III crack extension. For beam specimens, the shear stresses cause a Mode I crack propagation. It is possible that slope m=5 and class 80 is only required if the shear stress caused by torsion or to loading which induces mode III type shear fatigue fracture [5]. Many details in civil engineering correspond to beam type specimens and could there fore be treated as such. This simplifies the design process when cycles to failure are searched. Expression (4.17) with exponent 3 fulfils the requirement where m=3 should be used because the slope is presented as the exponent. Still some warning is required because the presented experiment in small scale does not include all possible variation between normal and shear stress. The ratio σ/τ in the experiments shows good correspondence to predictions for moderate values. There are also differences for loading in and out-of-phase. For proportional

loading ratio σ/τ seems not to be so significant. Experimental results show a larger scatter from ratio 0.31 to infinity which all corresponds well to slope m=3 and fatigue class 80. For non-proportional loading experiment for ratio σ/τ 1.0 – 1.3 showed good correspondence to fatigue class 80 and slope m=3. Fat 80/3 curve proves to be suitable for booth proportional and non-proportional combined loading when the shear stress component is not due to torsion [5]. Flange tube specimens were tested for ratio σ/τ 0.14-1.0 there slope m=5 and fatigue class 80 gave the best correspondence. If designing details similar to experimental specimens the actual loading ratio should be considered. Ratio value should not exceed tested values. As was mentioned earlier further investigations are required before absolute unambiguous is achieved. It should be mentioned that in some design codes there are restrictions regarding maximum change in direction of principal stress. For example in British Standard BS 7608 the greatest algebraic difference between the principal stresses occurring on principal planes should not be more than 45˚ apart in any loading cycle [5]. EC 3 contains the text - principal stress should not change significantly. A change in principal stress usually between ±20˚ was introduced in test. It will be seen that there is reasonable correlation between the results, suggesting that this difference was not significant [5]. By following the result it may be reliable to have differences up to 20˚ and fulfil the requirements regarding EC 3 at least according to [5]. As was mentioned earlier all experiments were based on weld toe failure. The influence of applied shear stress in case when fatigue cracks occur at other locations than the weld toe, may result in other failure modes other than mode I. This requires further study [5].

4.3.5 Conclusions from modified critical plane method

The modified critical plane method can be used to put fatigue data to a single S-N-curve and the accuracy is quite good. Figures 4.11 and 4.12 are a good proof of this. The problem with this method is how the critical plane in the weld should be assumed. Finding the most critical stress may also be difficult and often it is necessary to use FEM analysis. The method need also further work so it can applied for weld root/throat failure. These short comes make it complicated to use the critical plane in codes for structural design, but if the method is further developed and simplified it might be appropriate for incorporation in future design codes. This has already been pointed out of many of the researchers. There is no doubt that the method has potential. It can be seen in Figures 4.14 and 4.15 that the modified critical plane gives a more accurate prediction of the fatigue life compared to EC 3 and the finish standard SFS 2378. Even if the method gives reliable answers and if it will be further developed to fit design codes, it will be hard to get structural designers to accept this method in the reality, because it will probably always be more complicated and expensive to use the modified critical plane than, for example the methods based on interactions formulas.

In the literature some researchers have drawn conclusions about the modified critical plane method to estimate the fatigue life for welded joints. Some of researchers were positive to the approach but some were also critical, they indicate that the method can lead to an over-estimation of the fatigue life. In the following text the conclusions, found in the literature from different researchers will be presented.

Bäckström and Marquis draw some conclusions of the modified critical plane in [28] and the main conclusions were that the method need further work. The first point that

needs to be improved is how accounting for the presence of residual stresses should be done. It needs also further work with the definitions of the damage planes in the welded joints. They also write that it is important to understand and find the reason for increased damage during non-proportional loading compared to proportional loading. They also mention that the scatter of the test results was 70-100 % larger for multiaxial loading than for the uniaxial loading. The reason for this may depend on the geometry of the specimens tested, test methods, plate thicknesses and the definition of fatigue failure, but it can also depend on the accuracy of the method.

Sonsino [38] writes the following: Critical plane approaches of Findley-type fail for non-proportional loading with changing stress directions, because in case of changing principal directions, lower equivalent stresses are calculated , which lead to an over-estimation like the classical hypotheses.

Maddox [2] writes that the most promising methods to predict fatigue life under non-proportional seems to be the modified critical plane approach. But he also writes that the method needs further work to develop the approach to make it more easy and reliable to use in design codes.

5 Application of design methods

In this chapter the promising calculations methods that were studied will be applied and compared to test results found in literature.

In the literature there are several multiaxial fatigue tests on steel specimens, for tests carried out on welded specimens the range is significantly smaller. This, together with the trouble to find and receive available test data makes the data pool available within the frame of this study very small. The test series also need to include different loading conditions, for example in or out-of-phase loading, and it was necessary to find a tested specimen with a geometry that can be found in the design codes. The best test series which can be found and fulfil all the requirements was the one performed by Archer in [42]. These test series were carried out on a box beam with welded attachments under different phase and frequency loading. All the test data are showed are in appendix C Table C1. Most of the test specimens are pipes or other types of specimens with complex loading to give as much information as possible for loading and stress situations. This makes it difficult to compare an ordinary detail from a structure with a test specimen. A survey is reported in [5] shows that shear caused by torsion has different cracking mode than beams with shear stresses due to concentrated loading. This makes the choice even more difficult. .

5.1 Geometry of the specimens

The test specimens used by Archer in his tests were made from structural hollow section of steel BS4848 according to the standard British. On the box beam two attachments were welded with fillet welds. The thickness of the walls of the box beams was reduced in the welded section. The reason for this is to allow high shear stresses in the box beam without any risk for yielding caused by bending forces. A drawing over the test specimen is shown in Figure 5.1 [42].

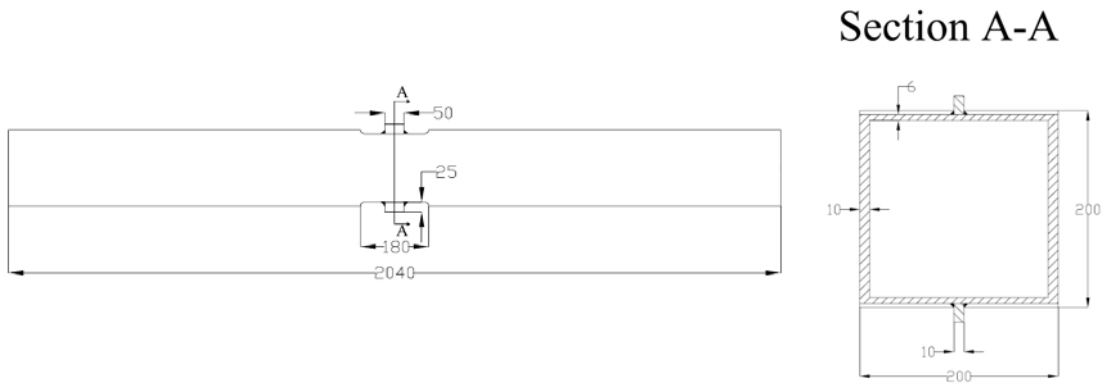

Figure 5.1 Test specimen geometry, dimensions in millimetres.

5.2 Loading and stresses in the specimen

To create stresses in the specimen four concentrated loads were added, see Figure 5.2 for the position of the concentrated loads. The box beam was simply supported on two supports with a distance of 1315 mm. To create shear stress, two vertical concentrated loads were applied. The two loads were acting in 180° out-of-phase, which gave a

pure shear stress in the attachment. This phase angle make the two loads to be in opposite of each other, if one of them is in compression then the other one will be in tension [42].

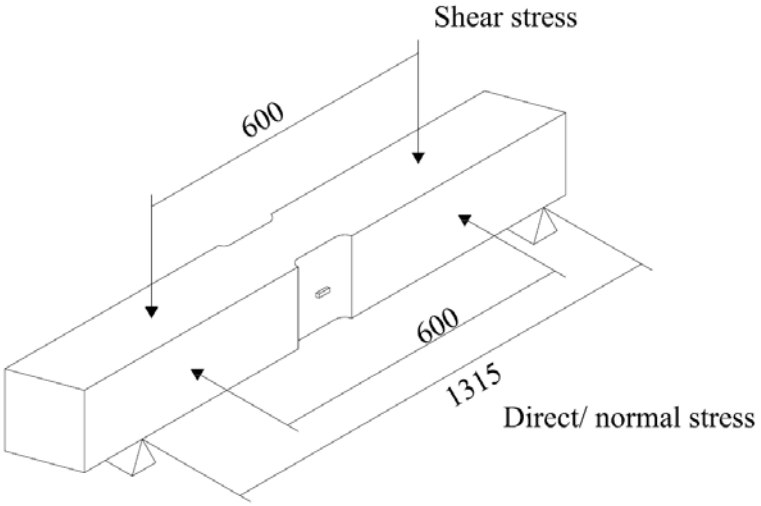

Figure 5.2 The loading of the specimen, dimensions in millimetres.

The tests were carried out with different phase angles, frequency and stress ratios. In appendix C, Table C1 the different tests are shown. Test specimens 1 to 11 were loaded either in pure shear or pure direct stress. Theses tests were not included in the calculations because the loading is only uniaxial. Specimens 12 to 15 were tested with in-phase biaxial loading with shear and normal stress. Specimens 16 to 19 were loaded with an out-of-phase angle, 90° between the shear and normal stress. The remaining specimens were loaded with four different relationships, see Figure 5.3, and the normal stress frequency was twice that of the shear stress. The reason of the last loading types is that this will create a lot of different principal stress variations. By using the principal stress formula 3.2 in Section 3.5.4 the principal stress can be obtained. In Figure 5.4 and Figure 5.5 two tests are shown with two different loading types and as it can be seen in the Figures the principal stress have a different behaviour for the both loading types [42].

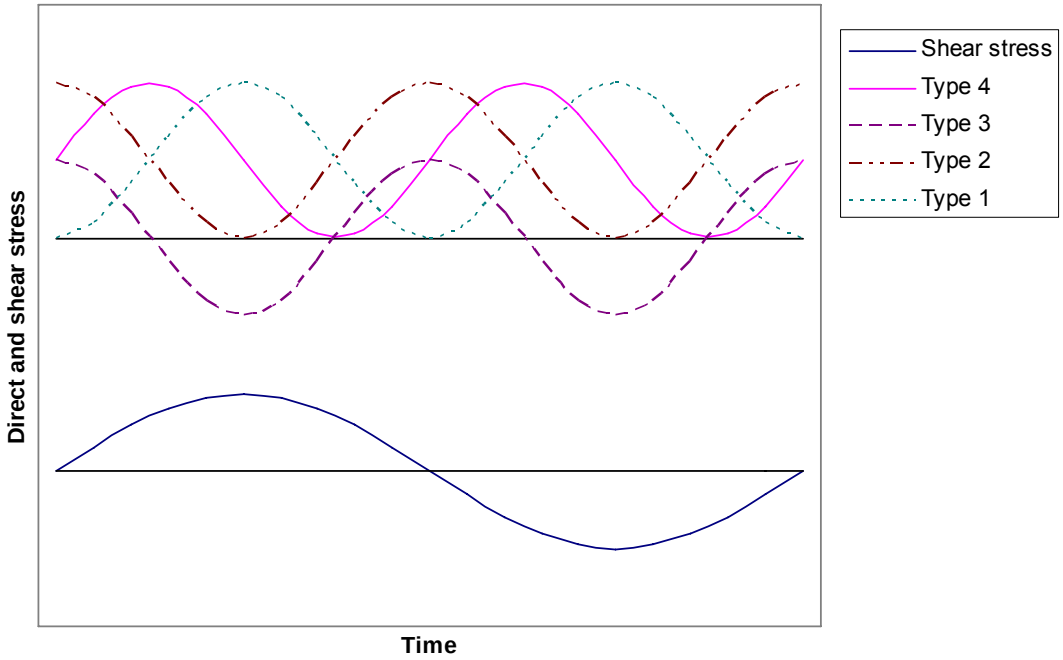

Figure 5.3 The variation of the stress for the different frequency.

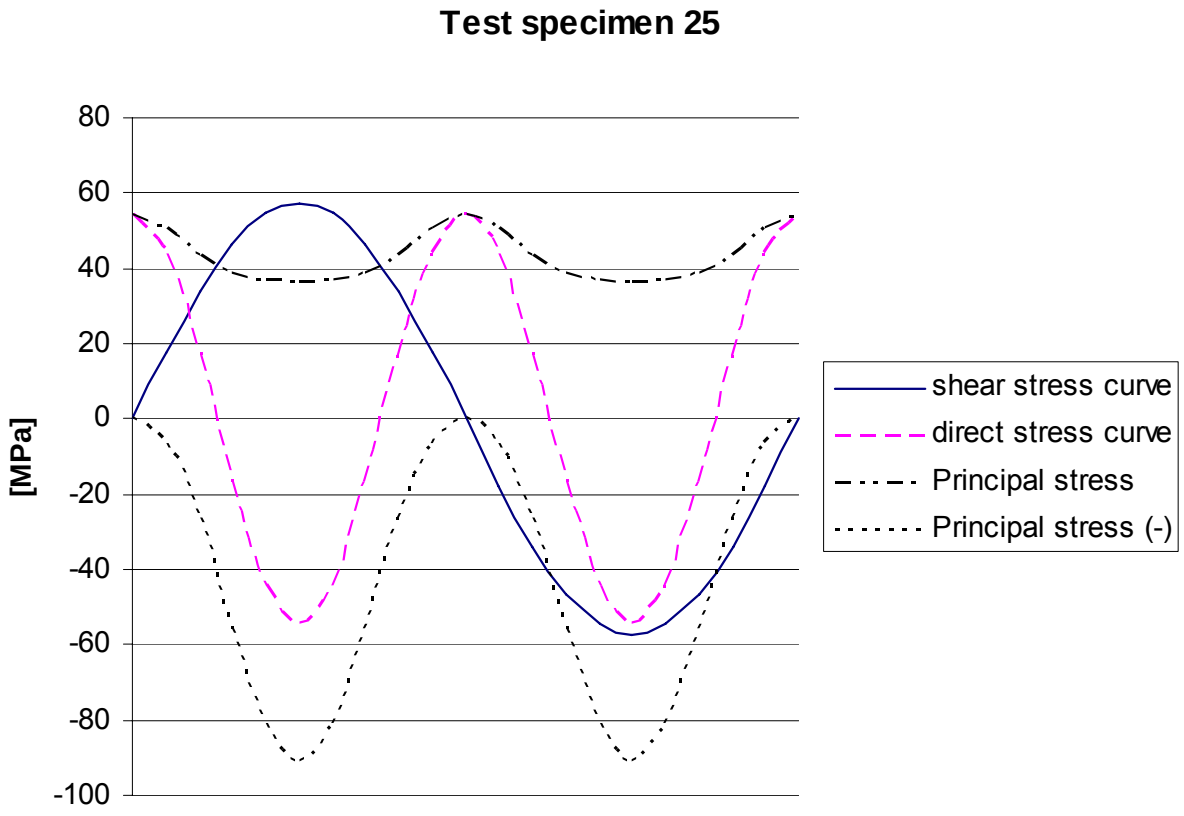

Figure 5.4 The principal stress for test specimen 20 and in loading type 1.

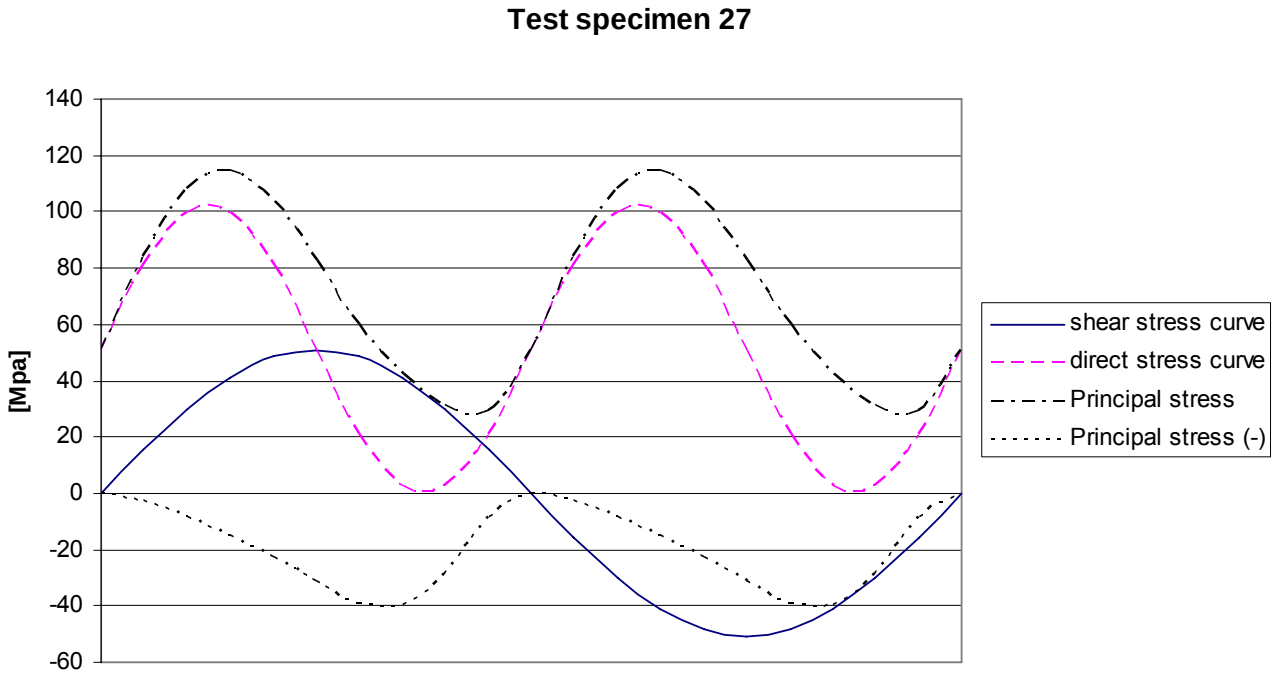

Figure 5.5 The principal stress for test specimen 27 and in loading type 4.

5.3 The calculations

All the calculations are made in Microsoft Excel. In the coming sections a short description of the calculation procedure is given of each design code. All the calculations are based on the search for predicted number of cycles to failure for the given specimen by Archer [42]. This means that the given fatigue prediction formula from the codes needs to be rewrite, so that the variable (n_i) may be calculated. The test results have been received from Archer [42] who contains a wide spectrum of experiments (see also appendix C). It should also be mentioned that Archer has made experiments on uniaxially loaded specimen subjected to pure normal or pure shear stress only. Such test result has no interest for this paper but are presented in appendix C. More interesting are the test results from combined shear and normal stress in and out-of-phase loading and with frequency differences. Archer used double frequencies on normal stress compared to shear stress in some cases, see appendix C. The combined results correspond to multiaxial loading cases and will be evaluated further on to predict the fatigue life. There are also experiments where the number of cycles is out of range which means that they have not showed any failure at $10 \cdot 10^6$ cycles. These experiments did not go to failure and are therefore neglected from further analysis. Normal stress is denoted direct stress in appendix C and may be confusing for the reader at first. Some design codes allow the use of principal stress there also complications may arise. Archer [42] has made the experiments with different period time on normal stress and shear stress, see Figure 5.3. From Section 4.1.4 it should be remembered that the principal stress is decreased in cases of phase-difference of stresses. This means that in the calculations booth normal and shear stress is plotted regarding test results presented in appendix C. After this plot the principal stress may be generated. When the principal stress has been plotted the stress range may be derived which is used to calculate the predicted number of cycles to failure. The

predicted number of cycles and experimental number of cycles are presented in diagrams for each design code. When principal stress approach is used this will be mentioned and annotated for each design code that allows this method.

5.3.1 BSK 99 (interaction method)

This design code does not allow principle stress method. The interaction formula in BSK 99 is given by the expression (5.1).

$$\sqrt{\frac{\sigma_{rdII}^2}{f_{rdII}^2}+\frac{\sigma_{rd\perp}^2}{f_{rd\perp}^2}+\frac{\tau_{rdII}^2}{f_{rvd}^2}+\frac{\tau_{rd\perp}^2}{f_{rvd}^2}} \le 1.10 \qquad (5.1)$$

$\sigma_{rd\parallel}$ = Normal stresses parallel to weld

$\sigma_{rd\perp}$ = Normal stresses perpendicular to weld

$\tau_{rd\parallel}$ = Shear stresses parallel to weld

$\tau_{rd\perp}$ = Shear stresses perpendicular to weld

$f_{rd\parallel} = f_{rk}/1.1\cdot\gamma_n$ (design value parallel to weld)

$f_{rd\perp} = f_{rk}/1.1\cdot\gamma_n$ (design value perpendicular to weld)

$f_{rv\parallel} = 0.6\cdot f_{rk}/1.1\cdot\gamma_n$ (design value parallel to weld)

$f_{rv\perp} = 0.6\cdot f_{rk}/1.1\cdot\gamma_n$ (design value perpendicular to weld)

$$f_{rk} = C\left(2\cdot 10^6 / n_t\right)^{1/3}$$

γ_n = Safety class

C = Depends on detail category and welding class (WA-WC) in BSK 99

In the present calculations the following C values has been used. Observe also that detail number 41 (from BSK 99) has been used there the designer is allowed to use one higher class if the welding length is shorter than 100mm. The Archer [42] test specimen has a welding length of 50mm which fulfils the criterion. It should also be mentioned that $\gamma_n\cdot 1.1 = 1.0$ has been used to avoid including the effects of various safety factors. C = 71 for class WA

C = 63 for class WB

C = 50 for class WC

When solving (n_t) from expression (5.1) and (5.2), the number of cycles n_t corresponds to n_i (number of cycles to failure) described in the beginning of Section 5.4.

$$n_t = 2\times 10^6 \left(\frac{1}{\frac{\sigma^2}{1.1^2 + C^2}} + \frac{1}{\frac{\tau^2}{0.6^2 \cdot C^2 \cdot 1.1^2}} \right)^{3/2} \qquad (5.2)$$

Expression (5.2) contains the variables σ and τ which is equivalent to $\sigma_{rd\parallel}$, $\sigma_{rd\perp}$ and $\tau_{rd\parallel}$, $\tau_{rd\perp}$. The tests have been done with combined shear and normal stress with values given in appendix C. These values from appendix C for shear and normal stress are used in Expression (5.2) for each combination given a prediction of number of cycles to failure. The predictions values has then be plotted in a diagram together with a inclined line of 45 degrees which represents the limit when prediction equals to experienced cycles to failure. The results are plotted in Figure 5.6 to 5.8.

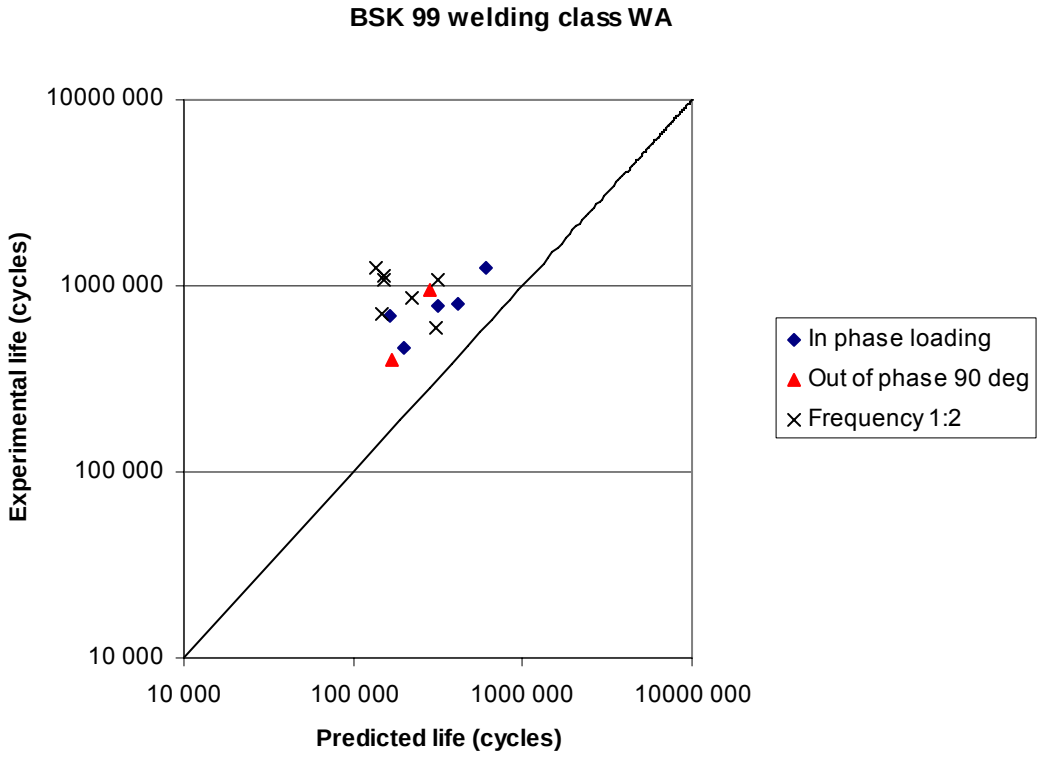

Figure 5.6 Results from calculation with BSK 99 interaction method for welding class WA.

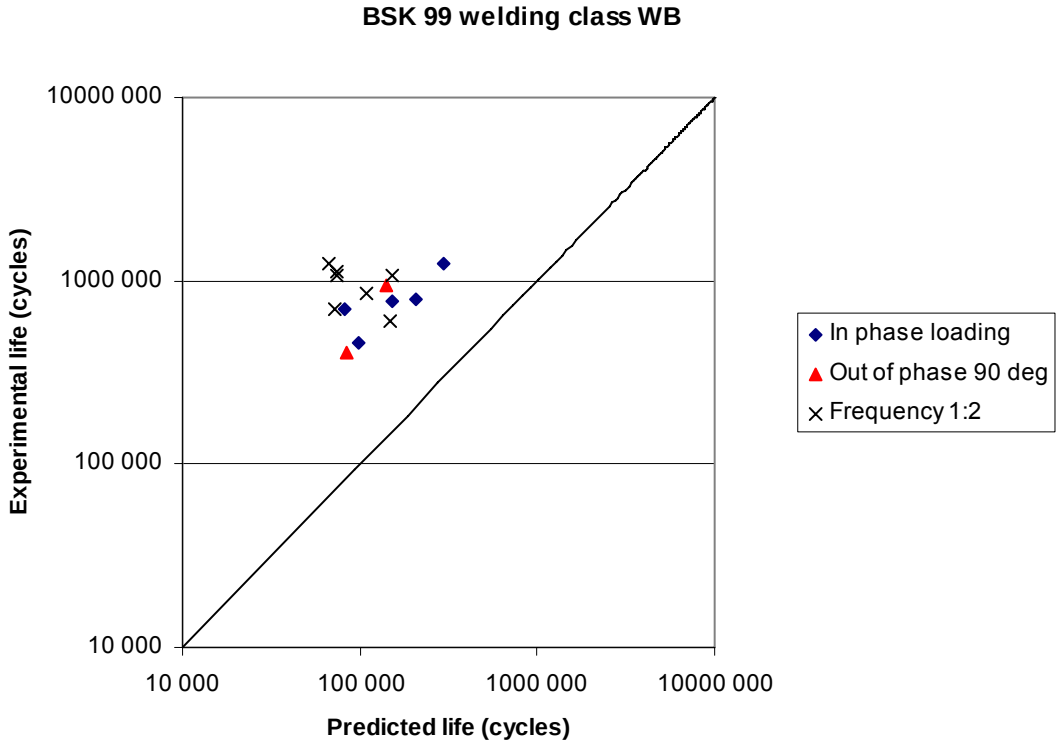

Figure 5.7 Results from calculation with BSK 99 interaction method for welding class WB.

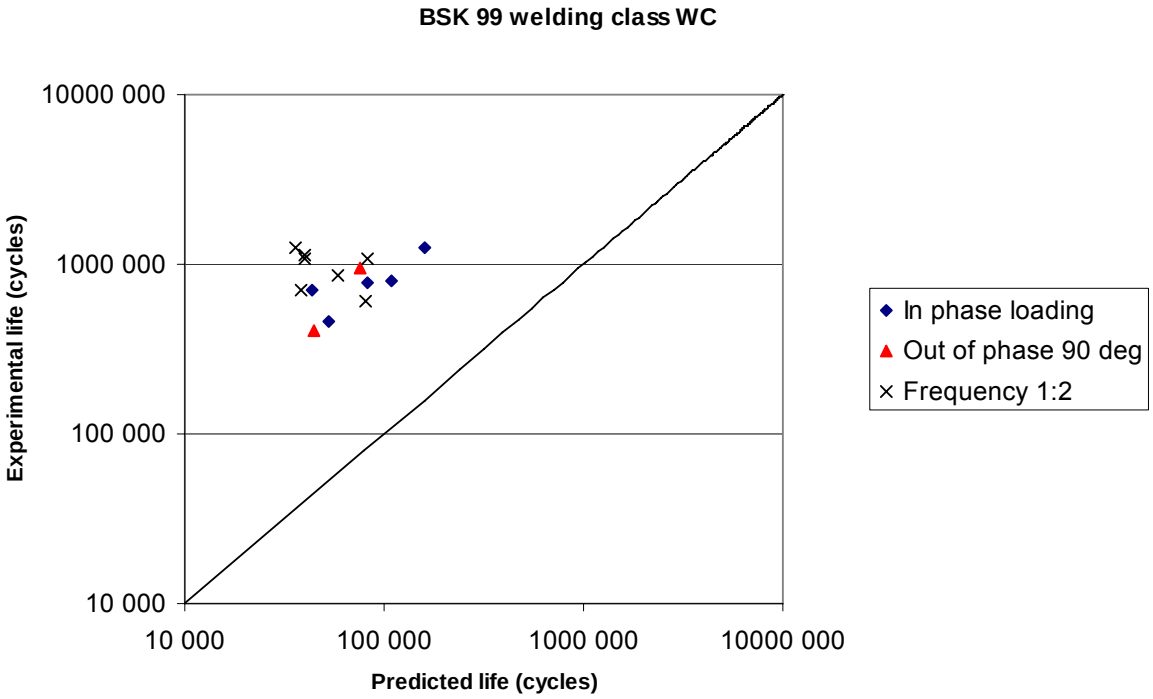

Figure 5.8 Results from calculation with BSK 99 interaction method for welding class WC.

Figure 5.6 to 5.8 shows clearly that predicted fatigue life cycles is less than the ones obtained from the tests. This means that this kind of detail can experience more cycles than calculated before failure. Result shows also that some conservatism is included in the calculation method. The conservatism should even increase a bit when safety factors are added in to the calculations. The method seems to work for in and out-of phase loading with predictions well on the safe side, at least for this type of test specimen. An analysis on utility ratio between predicted (characteristic strength) and experienced number of cycles resulted in further information. This is presented in appendix D and shows that the estimation of fatigue life time is approximately 60 % conservative for welding class WA, 80% for welding class WB and 90 % for welding class WC for in and out-of-phase loading. Even when the frequency difference was taken in to consideration the conservatism was approximately 75 %, 88 % and 93 % for welding classes WA, WB and WC. For this type of specimen the interaction expression (5.1) results in safe estimations of the fatigue life.

5.3.2 EC 3 (Interaction method)

The Palmgren-Miner rule should be fulfilled which means that the damage from each component normal and shear stress should be added together and the sum shall not exceed 1.0, see expression (5.3) to (5.5).

$$D_{d.\sigma} + D_{d.\tau} \leq 1 \tag{5.3}$$

$$D_{d.\sigma} = n_i / N_i \tag{5.4}$$

$$D_{d.\tau} = n_i / N_i \tag{5.5}$$

n_i = Number of cycles of stress range $\Delta\sigma_i$ that specimen experienced

$$\left(\frac{\gamma_{Ff} \Delta\sigma_E}{\Delta\sigma_R / \gamma_{Mf}} \right)^3 + \left(\frac{\gamma_{Ff} \Delta\tau_E}{\Delta\tau_R / \gamma_{Mf}} \right)^5 \leq 1.0 \tag{5.6}$$

γ_{Ff} = Partial safety factor for fatigue loads (in this calculation 1.0 is used)

γ_{Mf} = Partial safety factor for fatigue strength (in this calculation 1.0 is used)

$\Delta\sigma_E$ = Equivalent constant amplitude stress range (normal stress)

$\Delta\sigma_R$ = Fatigue strength (for normal stress value 80 according to detail category for this type of specimen by EC.)

$\Delta\tau_E$ = Equivalent constant amplitude stress range (shear stress)

$\Delta\tau_R$ = Fatigue strength (for shear stress value 80 MPa according to [5])

$$N_i = 5 \times 10^6 \left[\frac{\Delta\sigma_D / \gamma_{Mf}}{\gamma_{Ff} \Delta\sigma_i} \right]^3 \tag{5.7}$$

$$N_i = 2 \times 10^6 \left[\frac{\Delta\tau_c / \gamma_{Mf}}{\gamma_{Ff} \Delta\tau_i} \right]^5 \tag{5.8}$$

From EC 3 expression (5.7) and (5.8) can be received. These formulas permit the calculation of maximum possible life cycles to failure for a specimen. In the calculations the partial safety factors γ_{Ff} and γ_{Mf} have the value of 1.0. Expression (5.3) shows the two components contributing to the sum of 1.0. The formula has been taken directly from Eurocode 3 there the exponent varies for normal stress and shear stress. From scientific review it is of interest to compare results with slope 3 with recommendations from EC 3 were slope 3 should be used for normal stresses and slope 5 for shear stresses. When expression (5.3), (5.7) and (5.8) are combined together with fatigue strength $\Delta\tau_R = 80$ for shear and $\Delta\sigma_R = 80$ for normal stress the theoretical number of experienced cycles (n_i) can be calculated by expression (5.9).

$$n_i = \frac{1.0 \cdot 5 \cdot 10^6 \cdot \left(\frac{\Delta\sigma_c}{\Delta\sigma} \right)^3 \cdot 2 \cdot 10^6 \cdot \left(\frac{\Delta\tau_c}{\Delta\tau} \right)^3}{2 \cdot 10^6 \cdot \left(\frac{\Delta\tau_c}{\Delta\tau} \right)^3 + 5 \cdot 10^6 \cdot \left(\frac{\Delta\sigma_c}{\Delta\sigma} \right)^3} \tag{5.9}$$

This value will then be compared with the real number of cycles to failure from experiments. It should be mentioned that the fatigue strength values has been derived from tests where the fatigue class value has been correlated by two standard deviations together with 5 % failure probability and a two sided 75 % confidence interval. The result of this shall produce theoretical life cycles less than real experienced life cycles. Figure 5.9 shows the calculated values with slope 3 plotted into a diagram with the inclined line where predicted and experienced fatigue life cycles are equal. When studying appendix D the safety to failure between predicted and experienced fatigue life cycles are presented some interesting information can be received. For example specimens affected to in-phase loading have one result at 18.5 %. This means that the experienced cycles of life are more than predicted ones. However the results have a large scatter with all of the results on safe side. Out-of-phase loading shows positive safety values which gives a margin of 34.4 % at minimum to failure. Even experiments with frequency differences have positive safety values with minimum at 39.4 %. For these loading cases the method seems to work appropriately. There is no simple explanation why specimens affected to in-phase loading shows results which is less safe than other loading for slope 3. One explanation is that the shear effect creates a larger influence than by the recommendations from EC 3 with slope 5. But it should also be remembered that partial safety factors are set to 1.0 which bring safety margin to calculations when these are adjusted. It must also be remembered that a high percentage on safety factor to failure results in bad correspondence between reality and predicted calculation. The idea with calculations should be to give a precise prediction compared to reality and result in a better and more cost effective detailing. This means that the method may handle this kind of problem with more precise predictions when loading is in-phase. Some specimen may go to failure and are expected because the detail categories have 5 % failure probability. As there has been mentioned earlier the detail category is based on experiments with line regression, 5 % failure probability based on a two-

sided confidence interval of 75 %. Due to the 5 % failure probability, it may be possible for a specimen to exceed failure limit. This will cause a small overestimation compared to recommendations in EC 3 where slope five should be used for shear stresses.

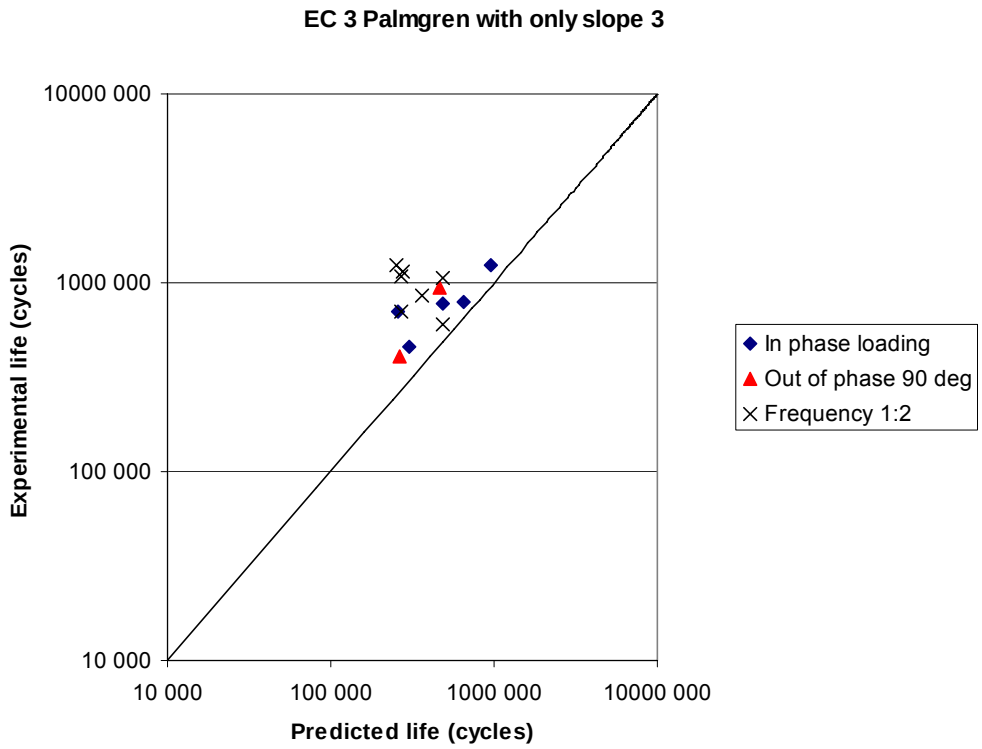

Figure 5.9 Showing results with interaction formula from EC 3 with slope 3.

The recommendations from EC 3 is that expression (5.6) with exponent 3 for normal stress and exponent 5 for shear stress should be used for predicting the cycles to failure. In Figure 5.10 are the results from the calculations with the exponent 3 and 5 given.

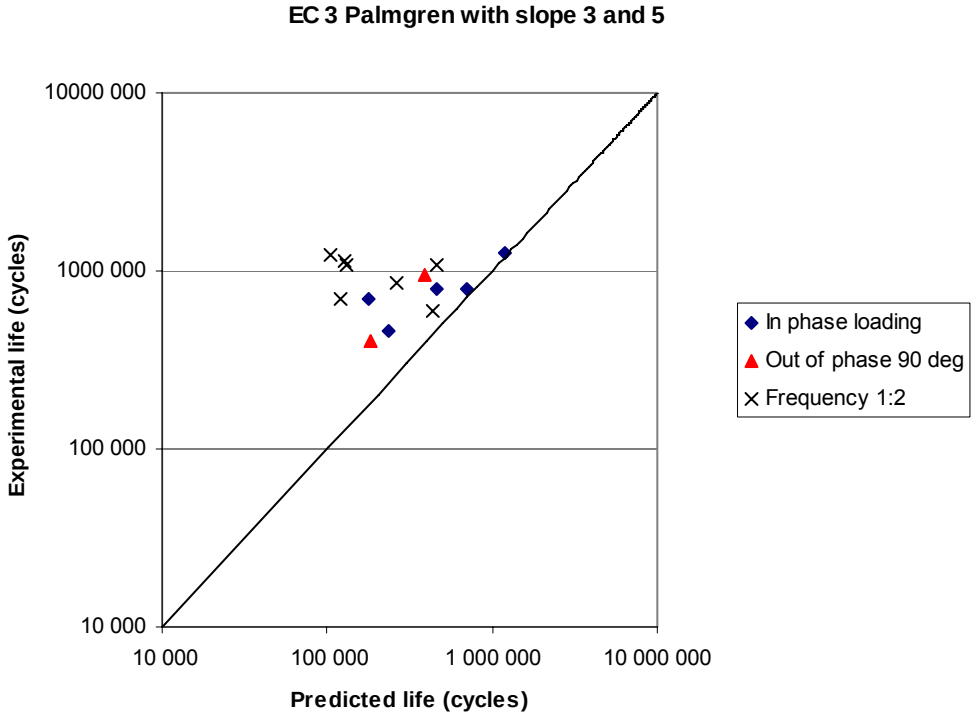

Figure 5.10 Plot over calculated results compared to EC 3 recommendations with slope 3 and 5.

All results are located more on the safe side regarding to the conservatism in the calculation. The scatter increases while two values still are close to the line where predicted life cycles are equal to experimental real life cycles. On the other hand appendix D shows that no values are on unsafe side and the margin to failure is 23.7 % in the worst case. Observe that also in this case safety factors γ_{Ff} and γ_{Mf} are set to 1.0 which results in more conservative predictions when changed. The common conclusion seems to be that the method is suitable for fatigue predictions for this type of specimen anyway.

5.3.3 EC 3 (Principle stress method)

When using the principle stress method by EC 3 the designer should know how the principal stress is derived. However expression (5.10) is the general formula for principal stress calculation for specimens like the tested one. In Section 4.1.4 it was mentioned that principle stress was not allowed to change significantly in course.

$$\sigma_l = \frac{\sigma_x + \sigma_y}{2} + 0.5\left\{\left(\sigma_x - \sigma_y\right)^2 + 4\tau^2{}_{xy}\right\}^{1/2} \tag{5.10}$$

The tested specimen has only normal stress in combination with shear stress, which makes expression (5.10) possible to simplify to expression (5.11).

$$\sigma_l = \frac{\sigma}{2} + 0.5\left\{\left(\sigma\right)^2 + 4\tau^2\right\}^{1/2} \tag{5.11}$$

To derive the variation in principal stress it is necessary to verify normal and shear stress variation. The easiest way to do this is to plot the normal and shear stress in one Figure (see Figure 5.4 and 5.5 in Section 5.3). From these curves it easy to derive the principal stress because shear and normal stress is defined in any arbitrary point. In Figure 5.4 and 5.5 under Section 5.3 the principle stress variation has been plotted. It should be remembered from Section 1.8 that the stress range is main parameter causing fatigue. The stress range is calculated by expression (5.12).

$$\Delta\sigma = \text{stress range} = (\sigma_{max} - \sigma_{min}) \qquad (5.12)$$

When the stress range is known the number of cycles to failure is of interest. Expression (5.13) can be used to calculate the number of cycles to failure.

$$N_i = 2\times 10^6 \left[\frac{\Delta\tau_c / \gamma_{Mf}}{\gamma_{Ff}\Delta\tau_i}\right]^5 \qquad (5.13)$$

$\Delta\sigma_i = \Delta\sigma =$ calculated stress range

$\Delta\tau_c =$ Fatigue strength

From surveys done by [5] results shows that FAT 80/3 could be used for beam specimens. This will be used in the calculations because no other recommendations are given by EC 3. In Figure 5.11 are the results from EC 3 principal stress method showed.

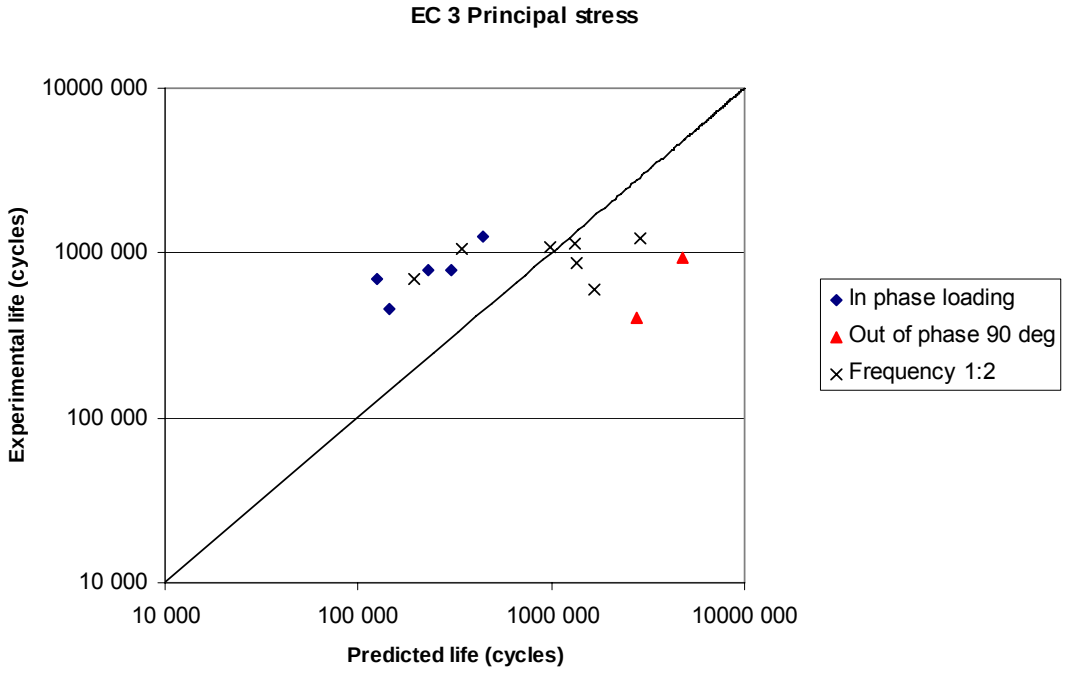

Figure 5.11 Showing results using FAT 80/3 recommended by [5].

One interesting conclusion given by [5] was that Fat 80/3 proves to be suitable for in and out-of-phase loading when the shear stress is not due to torsion. This test shows

that in-phase loading has a conservative prediction while out-of-phase loading together with different frequency loading on normal stress and shear stress got non-conservative prediction. It should be mentioned that [5] also had a small series of specimen and declares that more test are needed. Result from this thesis work shows that principle stress method is sensitive for phase differences. This was also noted by [5] where stress range for principle stress is reduced due to out-of-phase loading. However calculations and experimentally received life cycles do not agree. There are several possible explanations to this behaviour. One more un-discussed issue is the S-N curves developed for uniaxial loading is being used for principal stress calculations with phase-differences. There should perhaps be a new set of curves made for principal stress calculations together with recommendations on maximal phase-difference. Phase-differences of ±20˚ and ±60˚ has been noted in reports by other authors. Principal stress method needs likely to be improved in EC 3 or perhaps being waived because of the existence of interaction method.

5.3.4 Modified Wöhler curve method

The Modified Wöhler curve method was used to predict the fatigue life for the tested specimens. The procedure for the modified Wöhler curve are showed in Section 4.1.3 and by using this procedure the predicted fatigue life for every specimen can be estimated which is showed in Table D3 in appendix D. To calibrate the modified Wöhler curve it was necessary to find the two best fitting S-N curves in EC 3, for shear it was curve 80 with the inverse slope of 5 and for the normal stress it was curve 80 with the slope 3, exactly the same curves were used in the EC 3 calculations. By using expression (5.13) the stress ratio can be estimated and with help of (5.14) the new slope value k can be calculated. To obtain the reference shear stress the expression given in (5.14) should be used and if this value is used in (5.16) the number of cycle to failure can be calculated. All the values for k, ρ_w, reference shear stress and the number of cycle to failure are summarised in Table D3 in appendix D. In the Figure 5.12 are the predicted cycle plotted versus the experimental cycle to failure.

$$\rho_w = \frac{\Delta\sigma_n}{\Delta\tau_n} \tag{5.13}$$

$$k(\rho_w) = 2\left[k(\rho_w = 1) - k(\rho_w = 0)\right] \times \rho_w + k(\rho_w = 0) \tag{5.14}$$

$$\Delta\tau_{A,\mathrm{Re}f}(\rho_w) = 2\left[\left(\frac{\sigma_A}{2} - \tau_A\right)\rho_w + \tau_A\right] \tag{5.15}$$

$$N_f = \left[\frac{\Delta\tau_{A,\mathrm{Re}f}(\rho_w)}{\Delta\tau_n}\right]^{k(\rho_w)} \times N_A \tag{5.16}$$

From the Figure 5.12 can it be seen that the Modified Wöhler curve give both conservative and non-conservative predictions. The loading conditions seem to have no affect on the results, out-of-phase loading cause equal damage as in-phase loading.

The greatest advantage with the result is the narrow scatter and the agreement with the experimental cycle to failure.

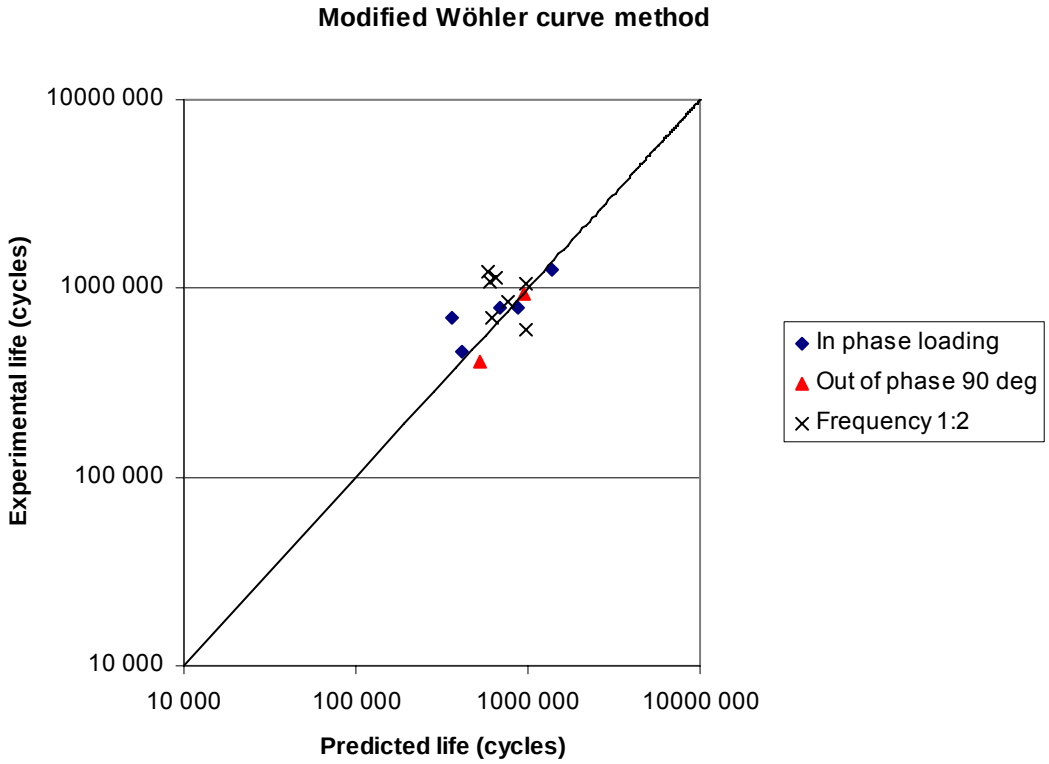

Figure 5.12 The predicted life plotted versus the experimental life.

5.3.5 Recommendations by IIW

Calculations with the International Institute of Welding recommendations have been done. The interactions formulas that are provided in the recommendations are similarly to the EC 3 formulas but with some difference. Both EC 3 and IIW recommend that the damage criterion based on the Palmgren- Miner should be used. The both design codes also provide that the principal stress method can be used, but in this method there is no difference between the codes and therefore are the calculations same as in Section 5.4.3. One of the differences between the codes is that the IIW make a distinction if the loading is in-phase or out-of-phase. If the shear stress and the normal stress are acting out-of phase then should sum of the fatigue damage not exceed 0.5. If the load is in-phase there should the sum of fatigue damage not exceed 1.0. In expression (5.17) is this damage criterion showed.

$$\sum D_d = \sum_1^i \frac{n_i}{N_i} \leq 0.5.....1.0 \qquad (5.17)$$

The number of cycles to failure N_i is calculated for shear and normal stress with expressions given in (5.18) and (5.19).

$$N = 2 \cdot 10^6 \cdot \left(\frac{C}{\Delta\sigma} \right)^m \tag{5.18}$$

$$N = 5 \cdot 10^6 \cdot \left(\frac{C}{\Delta\tau} \right)^m \tag{5.20}$$

C = The fatigue strength class

$\Delta\sigma, \Delta\tau$ = The stress ranges

m = The slope of the S-N curve

By using (5.18) and (5.19) in (5.17) with slope 5 and 3 will give the expression (5.21) for the n_i, the predicted number to failure in out-of-phase loading. For in-phase loading expression (5.22) should be used instead.

$$n_i = \frac{0.5 \cdot 5 \cdot 10^6 \cdot \left(\frac{C}{\Delta\sigma} \right)^3 \cdot 2 \cdot 10^6 \cdot \left(\frac{C}{\Delta\tau} \right)^5}{2 \cdot 10^6 \cdot \left(\frac{C}{\Delta\tau} \right)^5 + 5 \cdot 10^6 \cdot \left(\frac{C}{\Delta\sigma} \right)^3} \tag{5.21}$$

$$n_i = \frac{1.0 \cdot 5 \cdot 10^6 \cdot \left(\frac{C}{\Delta\sigma} \right)^3 \cdot 2 \cdot 10^6 \cdot \left(\frac{C}{\Delta\tau} \right)^5}{2 \cdot 10^6 \cdot \left(\frac{C}{\Delta\tau} \right)^5 + 5 \cdot 10^6 \cdot \left(\frac{C}{\Delta\sigma} \right)^3} \tag{5.22}$$

In the IIW the fatigue classes are the same as them in EC 3, for shear stresses 80 with the slope 5 and for normal stresses 80 with the slope 3. In the calculations, the partial coefficients have the value of 1.0. Out-of-phase loading and the loading with different frequency have been calculated with expression (5.21), the in-phase loading have been calculated with expression (5.22). It is important to mention that the curves provided in IIW have a standard deviation, as the EC 3 and this can affect the results from the calculations. All the results are summarised in appendix D Table D4 and in Figure 5.13 are the predicted cycle to failure plotted versus the experimental values.

It should be observed that in the presented calculations in this chapter are the recommendations based on IIW publication XIII-1539-96/XV-845-96 published 1996. There will be a new publications available soon which may differ from the one presented in this paper. When this study was done there has come an indication from International Institute of Welding that the calculation process and formulas will be audited.

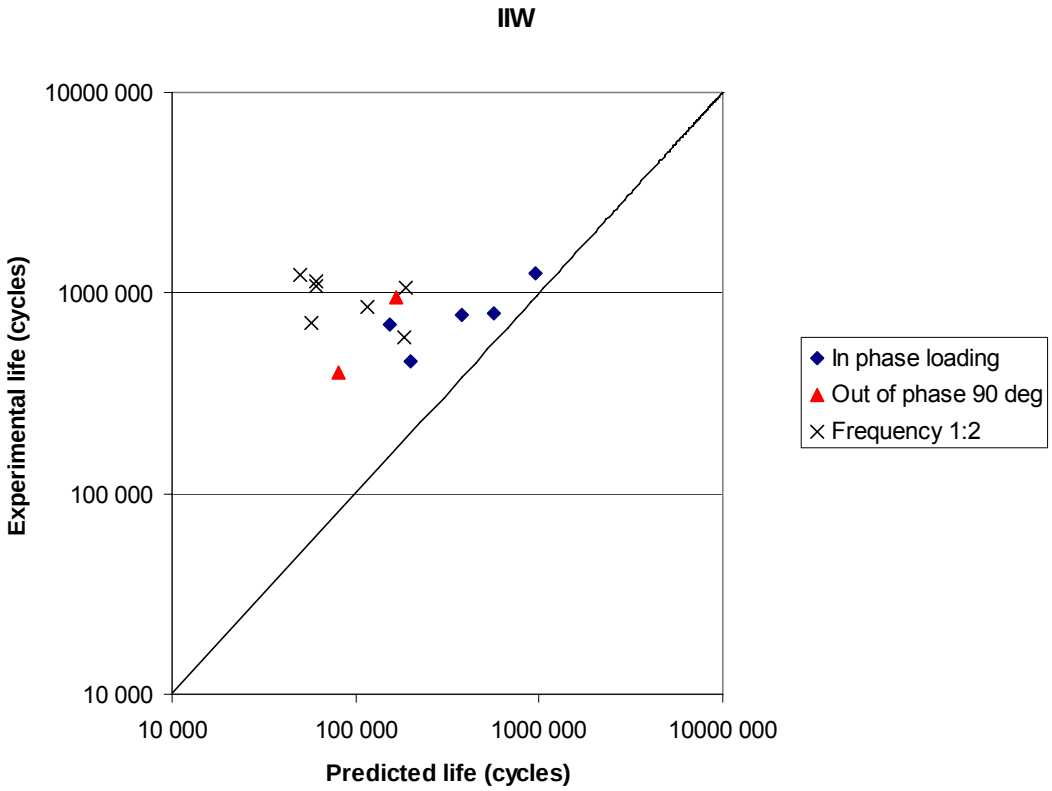

Figure 5.13 The predicted life plotted versus the experimental life.

6 Conclusions and summary

From the test calculations under Section 5.4 different conclusions may be held for different methods. There must be added that all calculations are made on one type of specimen. Fortunately the specimen was affected to various type of loading like in and out-of-phase loading but drawing the conclusion that the calculation method is accurate from just one test would be incorrect.

6.1 Conclusions from BSK 99

The BSK 99 interaction formula results in predictions that are conservative. The conservatism increases with choice of welding class. The welding classes in BSK 99 treat the welds smoothness and transition to parent metal which affects the conservatism by increase. The welding class WA generates the less conservative result closest to experimental real cycles to failure. There should be mentioned that the conservatism has a 60 % margin to failure and is rather course. The other welding classes causes even larger margin which seems to be the case overall. However there should be remembered that the result is for treated type of specimen and may be improved for other types. The method seems to be less affected by how loading acts on specimen. Out-of –phase loading generates predictions in same range as in-phase loading, at least in this particular case. To clearly verify the method a deep survey or access to earlier conclusion made by authors in beginning is needed. The method has some years behind and should therefore be accurately evaluated. On the other hand new knowledge may have come during time which may have effect the design of the formula.

6.2 Conclusions from interaction method from EC 3

The interaction method seems to work and give accurate predictions for booth, in and out-of –phase loading. The formula given by EC 3 recommends slope 3 for normal stresses and slope 5 for shear stresses. The recommendations will cause conservative predictions with quite large scatter as result. Such result will create less cost effective detailing but give some margin to failure as bonus. On the other hand test showed that slope 3 for booth normal and shear stress may be possible with the benefit of smaller scatter. Some results exceeded the limit were experimental real cycles was less than predicted cycles to failure. These values will be correlated to a better prediction when safety factors are put in to the calculations. There should be mentioned that this is a small scale experiment and may give different result for other type of specimens. However the method seems promising and indicates that it is suitable and simple to use in hand calculation.

6.3 Conclusions from principle stress method from EC 3

The principle stress method is quite simple and useful in predicting fatigue damage. There are studies made by [5] which indicate good agreement for in and out-of-phase loading on beam specimens. Calculations together with a limited set of experiment results made by archer [42] show a different result for out-of-phase loading. The calculations were based on recommendations given by [5] that FAT 80/3 could be used due to the lacking recommendations in EC 3. Such decision resulted in non-

conservative predictions for out-of-phase loading and frequency difference loading. In-phase loading was conservatively predicted with the same conditions. The received result differs from the recommendations given by [5]. Principle stress method seems to function for in-phase loading but shows lacks for out-of-phase loading. One explanation is the decrease in stress range in out-of-phase loading which has a large impact on the calculations. Because of the poor guidance in EC 3 which detail category should be used causes unnecessary interpretations of the design code. The method may be well applicable for multiaxial fatigue predictions with some development. The most important issue to know is that by using principle stress method and interaction method both accepted by EC 3 different predictions are received. This is a large disadvantage in a design code because it gives space to interpretations that may end up in errors. There should also be mentioned that this limited study needs to be increased to better answer whoever the method has lacks in general. At least a warning is in place for details affected to out-of-phase loading which in this study showed non-conservative predictions.

6.4 Conclusions from modified Wöhler curve method

The results from the calculations with the modified Wöhler seem to have a good agreement with the values from the tests. In Figure 5.12 are the obtained cycles to failure plotted versus the experimental cycles to failure. In the Figure 5.12 are the different loading conditions plotted separate, this to make it more easy to see the possible differences in the results. In this method it seems to be no difference if the loading is in-phase, out-of-phase or with different frequency, it is not easy to see if some loading is more harmful. The accuracy in the results is also satisfied and is mostly in the conservative zone. In Table D3 in appendix D there is a column called the safety factor and the meaning with this is how much of the fatigue life which is left until failure. From the column can it be seen that there is some values that are negative, they are in the non-conservative zone. The reason of this can have many causes, for example the used curves are from EC 3 and in these curves there are standard deviations that can affect the results. It can also depend on the calculation method but because of the few number of calculated test specimens it may be to early to draw any deeper conclusions about this. However it can be seen that the scatter band for the safety factor varies between -29.3 % and 48.2 % which is a very narrow area compared to some of the other calculations method presented in this report and which is evidence that the method can be used for predict the fatigue life independent of the loading conditions in this type of test specimen. One other conclusion from this method is that it is very important to use the right normal stress class. When the calculations were carried out it was noticed that if FAT 71 was chosen instead of FAT 80 the predicted cycle to failure differed to each other over 50 %. This is maybe one of the disadvantages with the method because mistakes will always be done in the choice of the FAT-classes and in this case it can end up in very non-conservative predictions.

6.5 Conclusions from recommendations by IIW

The recommendations from the IIW give a result which is in the conservative zone, for some of the specimens has a margin of 95.4 % to failure In the Figure 5.13 can it be seen that the in-phase loading gives the lowest fatigue life and this can be mostly explained with that the in-phase loading have been calculated with expression (5.22)

which allows 50 % more in the fatigue life than the out-of-phase loading. In this detail it was not necessary to reduce the fatigue life, the safety would have been enough even if the entire fatigue life should have been used. On the other hand it can be necessary to have a reserve in the fatigue life if some other welded details unlike this detail should be used. An example on this can be seen in Figure 4.23 in Section 4.2.1 there a test series performed by Dahle gives non-conservative results by using the IIW recommendations. The scatter band in all the results is between the values 23.7 % and 95.4 % which are significant larger than the modified Wöhler curve, EC 3 and the BSK 99. If only the in-phase loading are considered would the scatter band be much smaller and have a variation between 23.7 % - 77.9 % which is also larger than most of the other design codes. It is very easy to use this method, that is no trouble to do the calculations by hand and it is because of this the method have some advantages against other methods. This is probably one of the reason for the widely usage of this method.

As there has been mentioned under Section 5.4.5 all conclusions presented here are based on publication XIII-1539-96/XV-845-96 published 1996.

6.6 Conclusions from all the methods

In Figure 5.14 there is a summary overall test done in this paper. The results overall indicates of conservative predictions. This is the main conclusion due to the small limited test population that were considered. As there have been mentioned earlier Archer [42] included a wide loading scale with in and out-of-phase loading together with phase-difference loading. This gave a wide spectrum result for one type of specimen. To draw major conclusions from such a small investigation is difficult but it gave a hint how different formulas and methods manage to predict fatigue life. Together with the real experimental lifecycles methods were easy to compare and see if major divergence was received. In Appendix D are all the calculated results summarised.

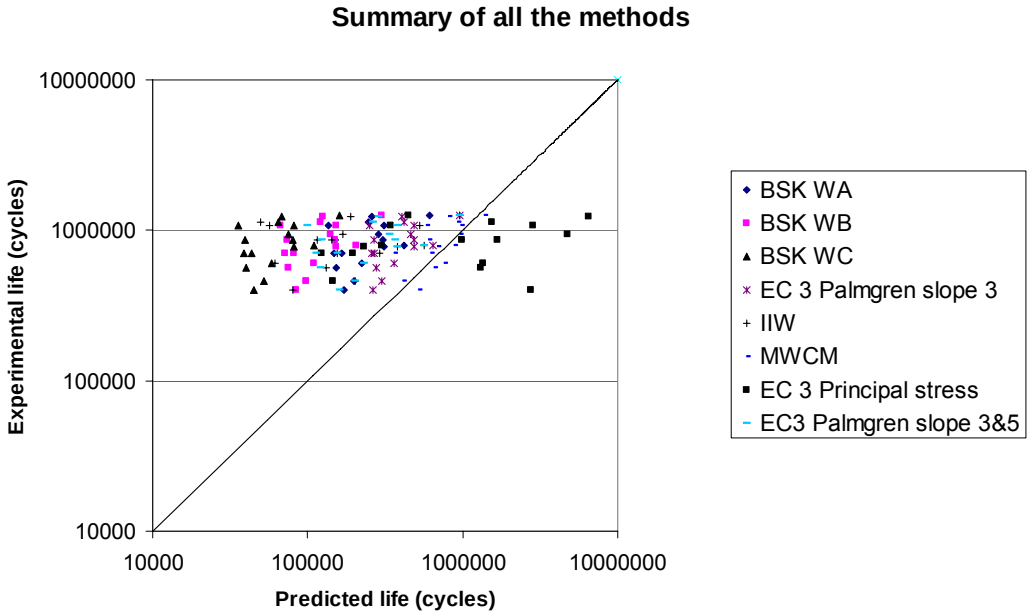

Figure 5.14 A summary of all the results.

6.7 Future research

From this survey and inventory of calculation methods the main conclusion is that most methods gives conservative predictions of fatigue life. The lack of this study is that it is rather limited regarding tested specimens. There are possibilities to improve future surveys by increasing the amount of tested types of specimens. Such study will give a wider documentation of how predictions correspond to experimental real life cycles. Methods that seem to be accurate may show non-conservative results and cause limitations due to fatigue life predictions. Other methods exist which are promising but, due to their complexity, not suitable for hand calculations. Critical plane method is one of these methods and should also be more deeply analysed and if possible compared with experimental result. It may be necessary to use computer analysis to rationalize calculations. The hot-spot method has shown interesting abilities in fatigue predictions. However the method requires FEM analysis, which also should be verified to experimental results. One more interesting method is the Modified Wöhler Curve method. The method needs however to be further tested and may also need improved guidelines for the used S-N curves. As it can be seen this subject gives room for further studies in several fields. Such investigations may bring a good contribution to solve the problem in accurate predictions for fatigue life. The subject may also require new experiments based on common details in civil engineering to bring more focus on problems in this area.

7 References

[1] Kussmaul K. F., McDiarmid D. L., Socie D. F. (1991): *Fatigue under biaxial and multiaxial loading.* Mechanical Engineers Publications Limited, Publication 10, London, United Kingdom, 1991, 480 pp.

[2] Maddox S. J. (2000): Fatigue design rules for welded structures. *Progress in Structural Engineering and Materials.* Vol 2, No. 1, Jan – Mar 2000, pp. 102 - 109.

[3] Yongming L. (2006): *Stochastic modelling of multiaxial fatigue and fracture.* Ph.D. Thesis. Graduate School of Vanderbilt University, Nashville, Tennessee, 2006, 187 pp.

[4] Niemi E. (1995): *Stress determination for fatigue analysis of welded components.* Abington Publishing, Abington hall, Abington, 1995, 69 pp.

[5] Maddox S. J. (2001): Interim fatigue design recommendations for fillet welded joints under complex loading. *Fatigue and fracture of engineering.* Vol 24, No. 5, May 2001, pp. 329 -337.

[6] Yousefi F., Witt M., Zenner H. (2001): Fatigue strength of welded joints under multiaxial loading. *Fatigue fracture engineering of material structures*. No.27, pp. 339 -355.

[7] Susmel L., Tovo R., (2004): On the use of nominal stresses to predict the fatigue strength of welded joints under biaxial loading. *Fatigue fracture engineering of material structures*, No.24, pp. 1005 -1024.

[8] Extracts from The European Convention for Constructional Steelwork (ESDEP). Chapter 3.4, 11.2.1, 11.2.2, 12.2, 12.8, 12.10 and 12:13.

[9] Hobbacher A. (1996): *Fatigue design of welded joints and components.* Abington Publishing, Abington hall, Abington, 1996, 127 pp.

[10] Socie D. F., Marquis G. B. (2000): *Multiaxial fatigue.* Society of Automotive Engineers, Warrendale, USA, Aug 2000, pp. 484.

[11] Morel F. (1999): A critical plane approach for life prediction of high cycle fatigue under multiaxial variable amplitude loading. *International Journal of Fatigue*, Vol. 22, 2000, pp. 101-119.

[12] Wang Y.-Y., Yao W.-X. (2003): Evaluation and comparison of several multiaxial fatigue criteria. *International Journal of Fatigue*, Vol. 26, 2004, pp. 17-25.

[13] You B.-R., Lee S.-B. (1995): A critical review on multiaxial fatigue assessments of metals. *International Journal of Fatigue.* Vol. 18, No. 4, 1996, pp. 235-244.

[14] Papadopoulos I. V., Davoli P., Gorla C., Filippini M., Bernasconi A. (1997): A comparative study of multiaxial high-cycle fatigue criteria for metals. *International Journal of Fatigue.* Vol.19, 1997, pp. 219-235.

[15] Papadopoulos I. V. (2001): Long life fatigue under multiaxial loading. *International Journal of Fatigue,* Vol. 23, 2001, pp. 839-849.

[16] Bäckström M. (2003): *Multiaxial fatigue life assessment of welds based on nominal and hot-spots stresses*. Ph.D. Thesis. VTT publications no. 502, Espoo, Finland, 2003, 97 pp. + app. 9 pp.

[17] Susmel L., Tovo R., Lazzarin P. (2004): The mean stress effect on high-cycle fatigue strength from a multiaxial point of view. *International Journal of Fatigue*, Vol. 27, 2005, pp. 928-943.

[18] Liu Y., Mahadevan S. (2005): Strain-based multiaxial fatigue damage modelling. *Fatigue and Fracture of Engineering Materials and Structures*, No. 28, 2005, pp. 1177-1189.

[19] Findley W. N. (1959): A theory for the effect of mean stress on fatigue of metals under combined torsion and axial load or bending. *Journal of Engineering for Industry.* Vol. 81, 1959, pp. 301-306.

[20] McDiarmid D. L. (1990); A general criterion for high cycle multiaxial fatigue failure. *Fatigue and Fracture of Engineering Materials and Structures*, Vol. 14, No. 4, 1991, pp. 429-453.

[21] Leese G. E., Socie D. (1989): *Multiaxial fatigue: Analysis and Experiments.* Society of Automotive Engineers. Warrendale, USA, 1989, 162 pp.

[22] Sonsino C. M., Macha E. (1999): Energy criteria of multiaxial fatigue failure. *Fatigue and Fracture of Engineering Materials and Structures*, No. 22, 1999, pp. 1053-1070.

[23] European standard (2003): *Eurocode 3: Design of steel structures part 1-9: Fatigue.* European committee for standardization.

[24] Susmel L., Tovo R. (2005): Local and structural multiaxial stress in welded joints under fatigue loading. *International Journal of Fatigue*, Vol. 28, 2006, pp. 564-575.

[25] Pineau A., Cailletaud G., Lindley T. C. (1996): *Multiaxial fatigue and design.* Mechanical Engineering Publications, London, England, (1996), 532 pp.

[26] Sonsino C. M., Kueppers M. (2001): Multiaxial fatigue of welded joints under constant and variable amplitude loadings. *Fatigue and Fracture of Engineering Materials and Structures*, No. 24, 2001, pp. 309-327.

[27] Sonsino C. M. (1994): Multiaxial fatigue of welded joints under in-phase and out-of-phase local strains and stresses. *International Journal of Fatigue*, Vol. 17, 1995, pp. 55-70.

[28] Bäckström M., Marquis G. (2001): A review of multiaxial fatigue of weldments: experimental results, design code and critical plane approaches. *Fatigue and Fracture of Engineering Materials and Structures*, No. 24, 2001, pp. 279-291.

[29] Papuga J, (2005): Mapping of fatigue damages –program shell of FE-calculation. *CTU in Prague* , 2005, pp. 115.

[30] Mohammad A.-E. (2006): *Utmattningskritiska brodetaljer i stål*. Department of Structural Engineering, Chalmers University of Technology, Publication no. 06:7, Göteborg, Sweden, 2006, 80 pp.

[31] Sonsino C. M., Dieterich K. (2004): Fatigue design with cast magnesium alloys under constant and variable amplitude loading. *International Journal of Fatigue*, Vol. 28, 2006, pp. 183-193.

[32] Kalluri S., Bonacuse P. J. (1999): *Multiaxial fatigue and deformation: Testing and prediction*. American Society for Testing and Materials, Philadelphia, USA, 2000, 441 pp.

[33] Anderson T. L. (1989): *Fracture Mechanics Fundamentals and Applications*. Taylor & Francis Group, Boca Raton, USA, 2005, 621 pp.

[34] Maddox S. J. (1969): *Fatigue strength of welded structures*. Abington Publishing, Cambridge, England, 1991, 198 pp.

[35] Eriksson Å., Lignell A-M., Olsson C., Spennare H. (2002): *Svets utvärdering med FEM.* Industri litteratur AB, Stockholm, Sweden, 2002.

[36] Bäckström M., Marquis G. (2004): Interaction equations for multiaxial fatigue assessment of welded structures. *Fatigue and Fracture of Engineering Materials and Structures*, No. 27, 2004, pp. 991-1003.

[37] Marquis G., Bäckström M., Siljander A. (1997): *Welded High-Strength Steel Structures.* EMAS, London, England, 1997, pp. 163-177.

[38] Sonsino C. M. (2007): Multiaxial fatigue of welded joints –recommendations for assessment in design codes. *Fraunhofer-institute for structural durability and systems reliability LBF*, Darmstadt. Germany.

[39] Lehtonen M. J. (1997): *Welded High-Strength Steel Structures.* EMAS, London, England, 1997, pp. 251-266.

[40] Susmel L., Lazzarin P. (2001): A bi-parametric Wöhler curve for high cycle multiaxial fatigue assesment. *Fatigue and Fracture of Engineering Materials and Structures*, No. 25, 2002, pp. 63-78.

[41] Niemi E.J, Marquis B.M. (2003): *Structural hot-spot stress method for fatigue analysis of welded components*. Metal structures-Design, Rotterdam, Millpress, 2003.

[42] Archer R. (1987): Fatigue of a welded steel attachment under combined direct stress and shear stress. Brighton, England, 1987.

Appendix A

Spec [nr]	Load Path	R_σ	R_τ	σ_{max}/τ_{max}	σ_{max} [MPa]	τ_{max} [MPa]	$\Delta\sigma$ [MPa]	$\Delta\tau$ [MPa]	$\Delta\sigma_{1,nom}$ [MPa]	N_f [cycles]	n predicted [cycles]
2	A	0.3	-	∞	355	0	266	0	266	45000	89962
1	A	0.1	-	∞	355	0	319	0	319	127000	52159
3	A	0.6	-	∞	355	0	149	0	149	274000	511852
5	A	0.7	-	∞	355	0	116	0	116	692000	1084749
4	A	0.7	-	∞	357	0	98	0	98	1110000	1798975
7	B	-	-1	0	7	163	7	327	331	40000	26413
8	B	-	-1	0	6	134	7	270	274	160000	46676
6	B	-	-1	0	7	76	6	151	154	627000	264125
16	C	-	0	0	13	221	23	218	230	520000	81788
11	D	-1	-1	3	207	70	405	139	448	44000	17613
12	D	-1	-1	2.3	178	78	356	155	414	122000	21670
9	D	-1	-1	0.9	100	110	198	221	341	274000	32532
10	D	-0.8	-1.2	2.3	134	59	244	130	300	1081000	55191
13	D	-0.8	-1.2	2.4	136	56	243	129	299	1467000	55806
15	E	0	0	2.2	351	158	348	160	410	11000	22131
14	E	0	-0.1	1.8	237	131	227	140	294	95000	57180
17	E	0	0	2.3	255	113	254	116	299	120000	57129
18	E	0	0	2.2	211	96	208	99	248	345000	99535
19	F	0	0	2.3	255	111	253	111	221	100000	132447
22	F	0	0	2.3	257	111	254	111	221	148000	132447
20	F	0	0	2.3	211	91	207	92	183	413000	233204
21	F	0	0	2.3	211	92	208	93	183	529000	232390

Fatigue test results, of SHS tube-to-plate as-welded geometry, test performed by Bäckström and are showed in [37], also the predicted cycles to failure according to BSK are showed.

Test [Nr]	Steel	R	$\Delta\sigma_a$ [Mpa]	$\Delta\tau_a$ [Mpa]	Crack Path/pos	N_f [cycles]
B14	350	-1	194.4	0	T	1540000
B15	350	-1	243	0	T	915000
B20	350	-1	315.9	0	T	300000
C4	350	-1	179.5	0	T/tw	455000
C5	350	-1	151.9	0	T/tw	478000
C6	350	-1	138.1	0	T/tw	887000
B16	350	-1	0	127.6	L	780000
B17	350	-1	0	183.5	L	140000
B18	350	-1	0	114.5	L	2220000
B19	350	-1	0	155.2	L	397000
B21	350	-1	0	153.9	L	97500
B22	350	-1	0	122.7	L	295500
B24	350	-1	0	152.2	L	343000
B25	350	-1	0	120.8	L	840000
B26	350	-1	0	110.9	L	1860000
B27	350	-1	0	145.6	L	304000
B28	350	-1	0	138.3	L	1050000
B29	350	-1	0	116.6	L	2144000
B30	350	-1	0	119.6	L	385000
B31	350	-1	0	145.2	L	870000
C1	350	-1	0	202.5	L	40000
C2	350	-1	0	196.2	L	51500
C3	350	-1	0	107.8	L	1670000
B11	350	-1	106.8	145.8	L	363000
B12	350	-1	125.3	160.4	L	285000
B13	350	-1	95	121.5	L	1490000
C7	350	-1	143.6	86.3	L	150000
C8	350	-1	150.4	103.6	L	137000
C9	350	-1	98.9	69	L	433000
C10	350	-1	83.9	110.5	T/tw	850000
C11	350	-1	106.3	138.1	L+T/tw	460000
C12	350	-1	145.2	165.7	L	120000
C13	350	-1	117.1	86.3	T/tw	760000
C14	350	-1	131.9	103.6	T/tw	180000
C15	350	-1	82.8	69	T/tw	815000
D16	350	-1	0	182.2	L	32000
D17	350	-1	0	143.5	L	62000
D19	350	-1	0	131.3	L	146000
D20	350	-1	0	132.3	L	360000
D21	350	-1	0	131.3	L	160000
D22	350	-1	106.3	184.1	T	930000
D23	350	-1	134.8	220.9	T	125000
D24	350	-1	70.9	137.7	L	2240000
D25	350	-1	138.7	138.1	L	210000
D26	350	-1	123.6	115.1	L	320000
D27	350	-1	122.4	101.3	L	660000
E32	350	-1	180	184.1	L	101500
E33	350	-1	126.5	138.1	T	842000
E34	350	-1	168.7	184.1	L	700000
E35	350	-1	135	147.3	L + T	133000
E36	350	-1	126.6	138.1	L + T	490000
E51	350	-1	135	138.1	T	772000
E52	350	-1	135	138.1	T	554000

Fatigue test results, of a welded box beam, performed by Dahle and the results are reported in [37]. The different cracks are: L- longitudinal cracks. T- transversal cracks. Tw- cracks running along transversal welds.

Test [Nr]	Steel	R	Δσa [Mpa]	Δτa [Mpa]	Crack Path/pos	Nf [cycles]	n predicted [cycles]
D22	350	-1	106.3	184.1	T	930000	474409
D23	350	-1	134.8	220.9	T	125000	269265
E33	350	-1	126.5	138.1	T	842000	886604
E51	350	-1	135	138.1	T	772000	843593
E52	350	-1	135	138.1	T	554000	843593
C10	350	-1	83.9	110.5	T/tw	850000	1230581
C11	350	-1	106.3	138.1	L+T/tw	460000	620139
C13	350	-1	117.1	86.3	T/tw	760000	1010015
C14	350	-1	131.9	103.6	T/tw	180000	662709
C15	350	-1	82.8	69	T/tw	815000	2510997

The used test results and the predicted life according to BSK.

Appendix B

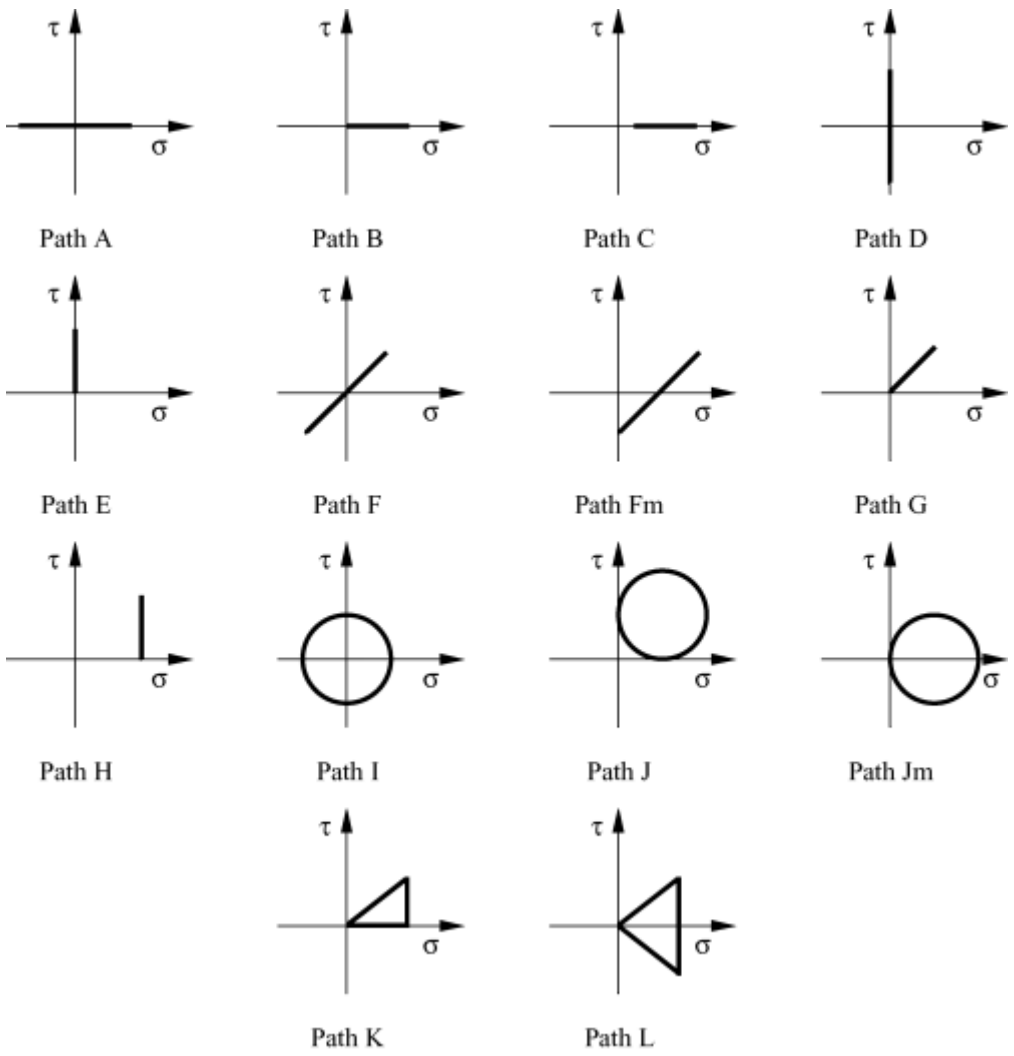

Figure B1 The different load paths in the tests [7].

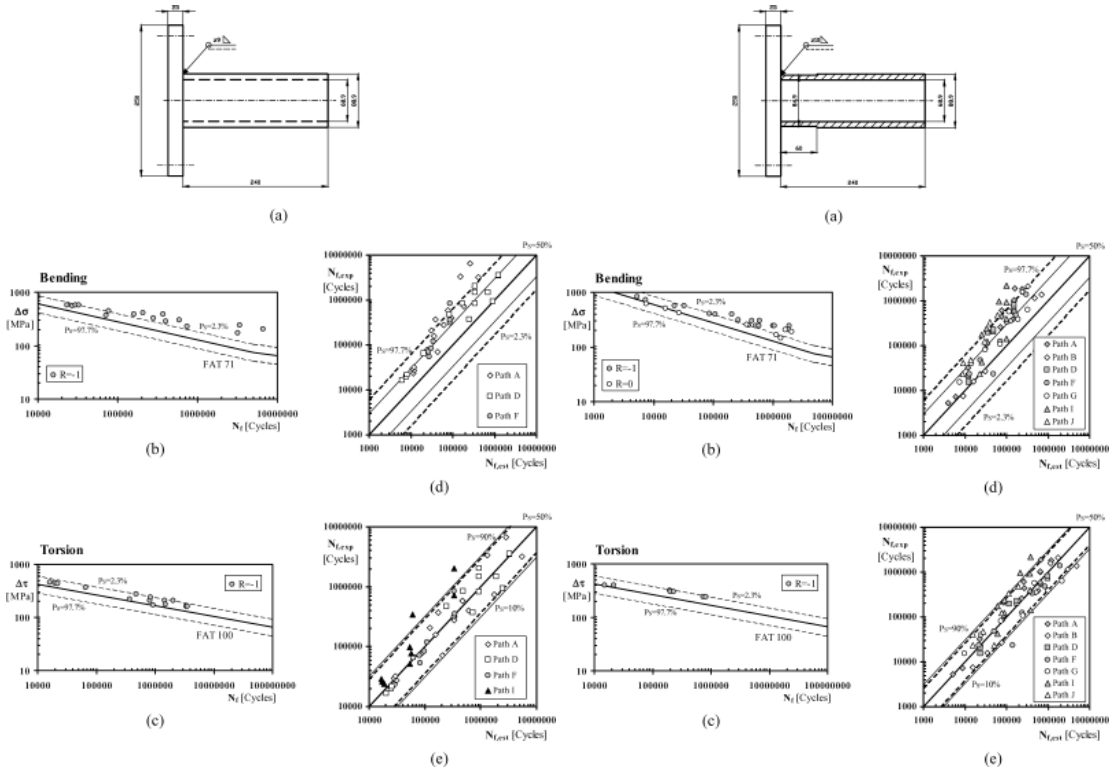

Figure B2 Tests performed by Sonsino (left) and Yousefi (right) [7].

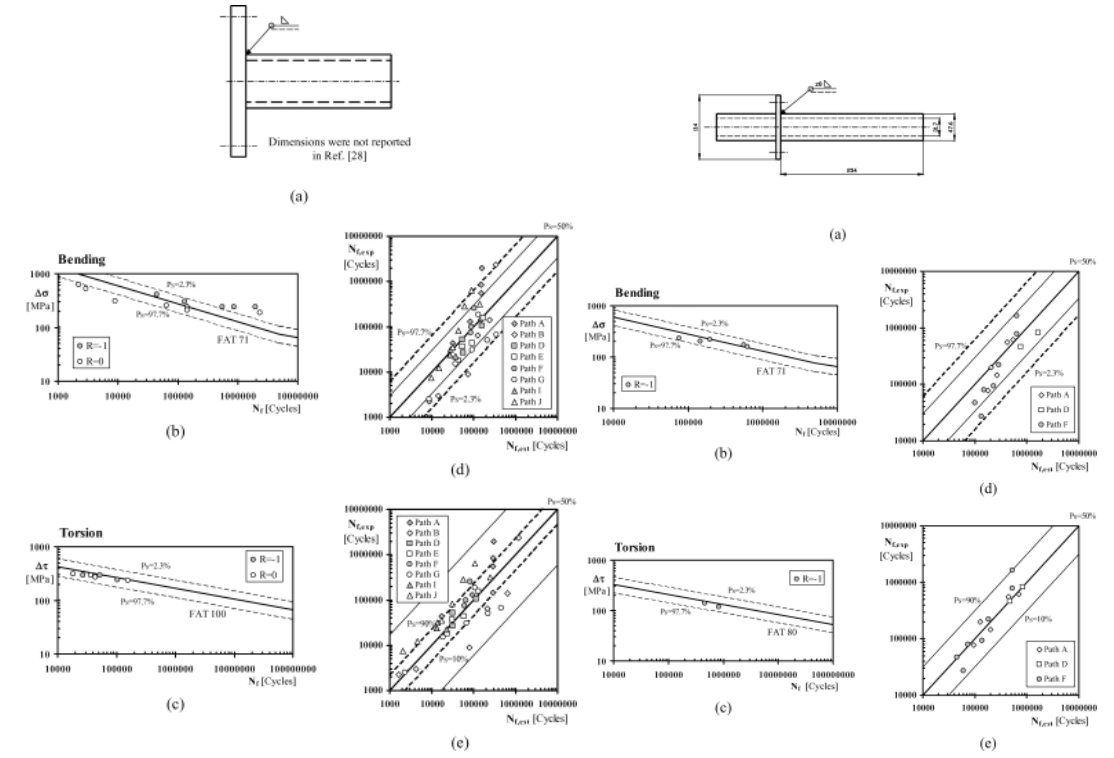

Figure B3 Tests performed by Amstutz (left) and Yung and Lawrence (right) [7].

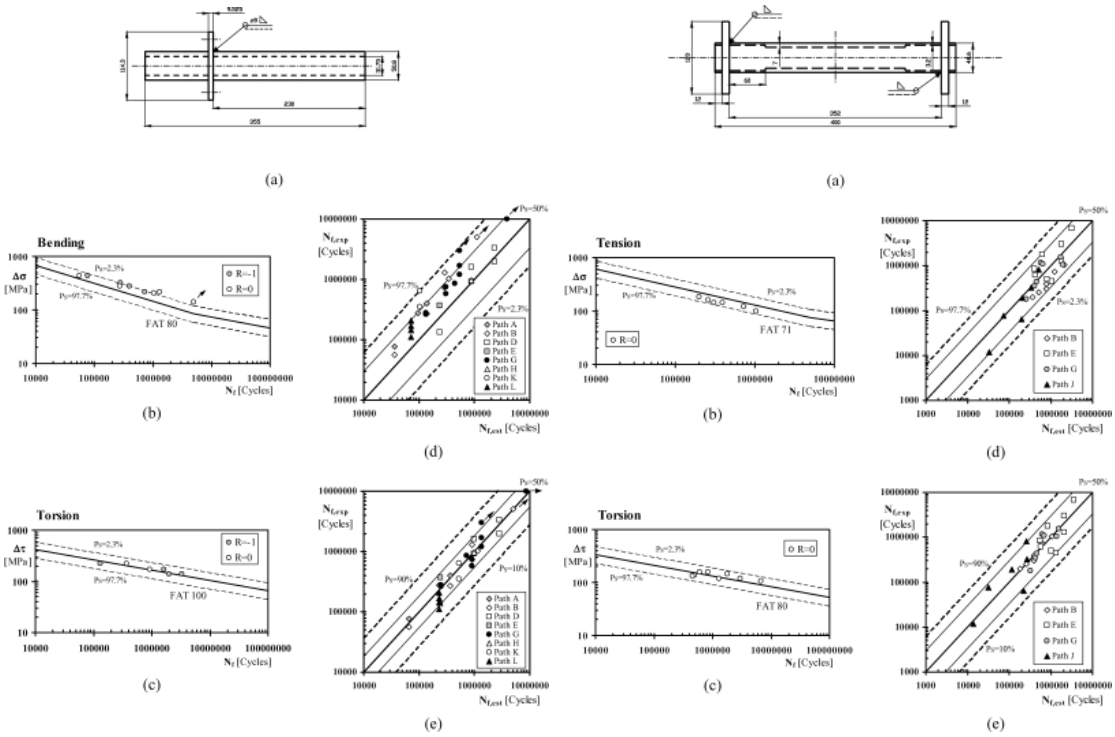

Figure B4 Tests performed by Siljander (left) and Razmjoo (right) [7].

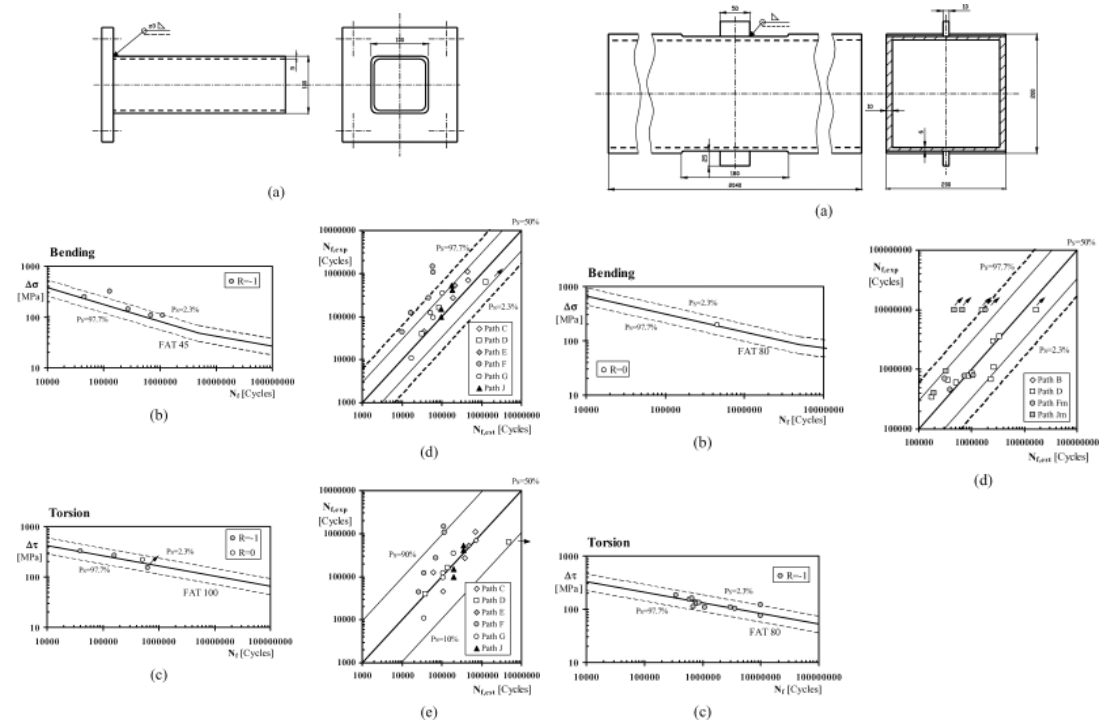

Figure B5 Tests performed by Bäckström (left) and Archer (right) [7].

Appendix C

Beam	Loading	Shear stress range, N/mm2	Direct stress range, N/mm2	R	Cycles to 20 mm crack
	Pure direct stress				
1			195	∞	453 000
	Pure shear stress				
2		103		0	3 560 000
3		135		0	766 000
4		109		0	2 980 000
5a		130		0	794 000
5b		131		0	864 000
6		111		0	685 000
7		108		0	1 080 000
8		120		0	10 000 000
9		75		0	10 000 000
10a		150		0	600 000
10b		161		0	662 000
11		186		0	347 000
	Shear & direct in phase				
12a		116	122	1	460 000
12b		124	127	1	698 000
13		101	102	1	783 000
14		81	81	1	1 247 000
15		91	94	1	793 000
	Shear & direct out of phase				
16		123	126	1	404 000
17		105	102	1	944 000
18		76	83	1	10 000 000
19		91	92	1	10 000 000
	1:2 Shear & direct Type 1				
20		101	102	1	1 068 000
21		138	106	1	704 000
	1:2 Shear & direct Type 2				
22		108	108	1	1 240 000
23		142	107	1	1 078 000
	1:2 Shear & direct Type 3				
24a		135	111	1	860 000
24b		113	100	1	1 136 000
25		115	109	1	600 000
	1:2 Shear & direct Type 4				
26		136	105	1	564 000
27		102	102	1	866 000

Table C1 Fatigue test results from Archer in [42].

Appendix D

Beam	Loading	Welding class WA C-class	Predicted cycles n_t	Safety f.	Welding class WB C-class	Predicted cycles n_t	Safety f.	Welding class WC C-class	Predicted cycles n_t	Safety f.
	Shear & direct in phase									
12a		76	199 364	56.7%	56	97 822	78.7%	50	52 312	88.6%
12b		76	166 883	76.1%	56	81 885	88.3%	50	43 789	93.7%
13		76	312 379	60.1%	56	153 275	80.4%	50	81 967	89.5%
14		76	610 398	51.1%	56	299 504	76.0%	50	160 166	87.2%
15		76	419 265	47.1%	56	205 720	74.1%	50	110 013	86.1%
	Shear & direct out of phase		Mean:	58.2%		Mean:	79.5%		Mean:	89.0%
16		76	170 960	57.7%	56	83 885	79.2%	50	44 859	88.9%
17		76	286 607	69.6%	56	140 629	85.1%	50	75 204	92.0%
	1:2 Shear & direct Type 1		Mean:	63.7%		Mean:	82.2%		Mean:	90.5%
20		76	312 379	70.8%	56	153 275	85.6%	50	81 967	92.3%
21		76	146 646	79.2%	56	71 955	89.8%	50	38 479	94.5%
	1:2 Shear & direct Type 2									
22		76	257 512	79.2%	56	126 353	89.8%	50	67 570	94.6%
23		76	135 942	87.4%	56	66 702	93.8%	50	35 671	96.7%
	1:2 Shear & direct Type 3									
24a		76	150 824	82.5%	56	74 005	91.4%	50	39 576	95.4%
24b		76	245 665	78.4%	56	120 540	89.4%	50	64 462	94.3%
25		76	222 198	63.0%	56	109 026	81.8%	50	58 304	90.3%
	1:2 Shear & direct Type 4									
26		76	152 798	72.9%	56	74 973	86.7%	50	40 094	92.9%
27		76	305 681	64.7%	56	149 988	82.7%	50	80 209	90.7%
			Mean:	75.3%		Mean:	87.9%		Mean:	93.5%

Table D1 The results by using BSK 99 for the three different welding classes

Beam	Loading	Classes τ	Classes σ	Palmgren Predicted cycles n_t (Slope 3)	Palmgren Safety f.	Palmgren Predicted cycles n_t (Slope 3&5)	Palmgren Safety f.	Principal stress Predicted cycles nt (Slope 3)	Principal stress Safety f.
	In phase								
12a		80	80	303 251	34.1%	200 878	56.3%	144 676	68.5%
12b		80	80	258 912	62.9%	154 472	77.9%	124 236	82.2%
13		80	80	489 599	37.5%	378 781	51.6%	232 150	70.4%
14		80	80	963 418	22.7%	951 451	23.7%	445 224	64.3%
15		80	80	646 401	18.5%	567 114	28.5%	303 407	61.7%
	Out of phase			Mean	35.1%	Mean:	47.6%	Mean:	69.4%
16		80	80	265 200	34.4%	160 018	60.4%	2743 484	-579.1%
17		80	80	461 504	51.1%	335 145	64.5%	4740 741	-402.2%
	1:2 Type 1			Mean	42.7%	Mean:	62.4%	Mean:	-490.6%
20		80	80	489 599	54.2%	378 781	64.5%	342 936	67.9%
21		80	80	268 127	61.9%	113 637	83.9%	194 380	72.4%
	1:2 Type 2								
22		80	80	406 442	67.2%	288 001	76.8%	6503 074	-424.4%
23		80	80	250 469	76.8%	99 940	90.7%	2861 046	-165.4%
	1:2 Type 3								
24a		80	80	267 502	68.9%	122 284	85.8%	993 884	-15.6%
24b		80	80	419 174	63.1%	263 999	76.8%	1555 042	-36.9%
25		80	80	363 649	39.4%	230 746	61.5%	1358 863	-126.5%
	1:2 Type 4								
26		80	80	278 785	50.6%	121 510	78.5%	1315 032	-133.2%
27		80	80	482 469	44.3%	367 508	57.6%	1667 413	-92.5%
				Mean:	58.5%	Mean:	75.1%	Mean:	-94.9%

Table D2 The results by using the EC 3

Beam	Loading	Ratio ρ_w	Classes according to EC 3 τ	σ	Slopes k_τ	k_σ	k calibrated	τ_{ref} MPa	Predicted cycles n_t	Safety f.
	Shear & direct in phase									
12a		1.1	80	80	5	3	2.9	66.4	410 437	10.8%
12b		1.0	80	80	5	3	3.0	68.8	361 895	48.2%
13		1.0	80	80	5	3	3.0	70.1	691 012	11.7%
14		1.0	80	80	5	3	3.0	71.0	1 378 732	-10.6%
15		1.0	80	80	5	3	2.9	68.1	878 001	-10.7%
	Shear & direct out of phase								Mean:	9.9%
16		1.0	80	80	5	3	3.0	68.8	522 455	-29.3%
17		1.0	80	80	5	3	3.1	73.5	949 262	-0.6%
	1:2 Shear & direct Type 1								Mean:	-14.9%
20		1.0	80	80	5	3	3.0	70.1	969 308	9.2%
21		0.8	80	80	5	3	3.5	91.6	623 104	11.5%
	1:2 Shear & direct Type 2									
22		1.0	80	80	5	3	3.0	71.0	812 884	34.4%
23		0.8	80	80	5	3	3.5	92.9	581 854	46.0%
	1:2 Shear & direct Type 3									
24a		0.8	80	80	5	3	3.4	86.8	598 354	30.4%
24b		0.9	80	80	5	3	3.2	81.2	931 776	18.0%
25		0.9	80	80	5	3	3.1	75.6	759 150	-26.5%
	1:2 Shear & direct Type 4									
26		0.8	80	80	5	3	3.5	91.3	649 850	-15.2%
27		1.0	80	80	5	3	3.0	71.0	964 938	-11.4%
									Mean:	10.7%

Figure D3 Results obtained by using the modified Wöhler curve method.

Beam	Loading	Classes τ	σ	Out of phase Predicted cycles n_t	In phase Predicted cycles n_t	Safety f.
	Shear & direct in phase					
12a		80	80		200 878	56.3%
12b		80	80		154 472	77.9%
13		80	80		378 781	51.6%
14		80	80		951 451	23.7%
15		80	80		567 114	28.5%
	Shear & direct out of phase				Mean	47.6%
16		80	80	80 009		80.2%
17		80	80	167 572		82.2%
	1:2 Shear & direct Type 1				Mean	81.2%
20		80	80	189 390		82.3%
21		80	80	56 818		91.9%
	1:2 Shear & direct Type 2					
22		80	80	144 001		88.4%
23		80	80	49 970		95.4%
	1:2 Shear & direct Type 3					
24a		80	80	61 142		92.9%
24b		80	80	131 999		88.4%
25		80	80	115 373		80.8%
	1:2 Shear & direct Type 4					
26		80	80	60 755		89.2%
27		80	80	183 754		78.8%
					Mean	87.6%

Figure D4 Results obtained by using recommendations from IIW.

Beam	Loading	Experimental life	MWCM n_t	BSK 99 WA n_t	BSK 99 WB n_t	BSK 99 WC n_t	Palmgren EC3 Slope 3 n_t	Palmgren EC3 Slope 3&5 n_t	EC 3 Pr. Stress n_t	IIW n_t
	In phase									
12a		460 000	410 437	199 364	97 822	52 312	303 251	200 878	144 676	200 878
12b		698 000	361 895	166 883	81 885	43 789	258 912	154 472	124 236	154 472
13		783 000	691 012	312 379	153 275	81 967	489 599	378 781	232 150	378 781
14		1 247 000	1 378 732	610 398	299 504	160 166	963 418	951 451	445 224	951 451
15		793 000	878 001	419 265	205 720	110 013	646 401	567 114	303 407	567 114
	Out of phase									
16		404 000	522 455	170 960	83 885	44 859	265 200	160 018	2743 484	80 009
17		944 000	949 262	286 607	140 629	75 204	461 504	335 145	4740 741	167 572
	1:2 Type 1									
20		1 068 000	969 308	312 379	153 275	81 967	489 599	378 781	342 936	189 390
21		704 000	623 104	146 646	71 955	38 479	268 127	113 637	194 380	56 818
	1:2 Type 2									
22		1 240 000	812 884	257 512	126 353	67 570	406 442	288 001	6503 074	144 001
23		1 078 000	581 854	135 942	66 702	35 671	250 469	99 940	2861 046	49 970
	1:2 Type 3									
24a		860 000	598 354	150 824	74 005	39 576	267 502	122 284	993 884	61 142
24b		1 136 000	931 776	245 665	120 540	64 462	419 174	263 999	1555 042	131 999
25		600 000	759 150	222 198	109 026	58 304	363 649	230 746	1358 863	115 373
	1:2 Type 4									
26		564 000	649 850	152 798	74 973	40 094	278 785	121 510	1315 032	60 755
27		866 000	964 938	305 681	149 988	80 209	482 469	367 508	1667 413	183 754

The result from the calculations.